EFFECT OF GEL STRENGTH ON DRUG RELEASE FROM SWELLABLE MATRICES THROUGH POLYMER EROSION

By

Lan Xiao

A dissertation submitted in partial fulfillment of

the requirements for the degree of

Doctor of Philosophy

(Pharmaceutical Sciences)

at the

UNIVERSITY OF WISCONSIN-MADISON

2007

A dissertation entitled

EFFECT OF GEL STRENGTH ON DRUG RELEASE

FROM SWELLABLE MATRICES THROUGH

POLYMER EROSION

submitted to the Graduate School of the
University of Wisconsin-Madison
in partial fulfillment of the requirements for the
degree of Doctor of Philosophy

by

LAN XIAO

Date of Final Oral Examination: January 16, 2007

Month & Year Degree to be awarded: **December** **May** 2007 **August**

****

Approval Signatures of Dissertation Committee

Joseph L. Robinson

Ralph M Albrecht

Signature, Dean of Graduate School

EFFECT OF GEL STRENGTH ON DRUG RELEASE FROM SWELLABLE MATRICES THROUGH POLYMER EROSION

Lan Xiao

Under the Supervision of Professor Joseph R. Robinson

at the University of Wisconsin-Madison

Swellable matrix tablets have been used extensively in oral controlled drug delivery systems. Upon contact with aqueous medium, water diffuses into the matrix and the glassy polymer begins to undergo a glassy-to-gel transition to form a viscous mucilaginous gel layer; a diffusional barrier that retards further ingress of water and acts as a rate-controlling barrier to drug release. Gel strength has been argued as a key attribute that influences the resultant drug dissolution. Yet, no systemic work has been done to correlate the gel strength and drug release and no tool is available for routine tests of gel strength. Therefore, the focus of this thesis is to study how gel strength affects drug release from swellable hydrophilic matrices through influencing polymer erosion. Hydroxypropyl methylcellulose (HPMC) was the model polymer used in this study.

We first developed a method of using Texture Analyzer to characterize polymer gel strength. Using the above method, the effects of some formulation related variables, such as polymer viscosity/molecular weight and concentration, and excipient types (lactose and Starch 1500) on the strength of both homogeneous HPMC gels and HPMC swelling tablets were studied. Gel strength increased with both polymer molecular weight and concentration; and Starch 1500 was found to be a gel-strength enhancing agent, while lactose had no effect. Texture Analyzer was also used to delineate the structure of swollen HPMC tablets. Profiles of gel strength, gel layer thickness and polymer concentration in

the gel layer were obtained and the latter two results were found to be in agreement with previous ones obtained using more sophisticated techniques in the literature.

A mathematical model was constructed and validated to correlate gel strength and polymer erosion, and was used to study the effect of polymer molecular weight, excipient type and/or content on polymer erosion. HPMC erosion rate decreased with molecular weight, quantitatively in agreement with the model prediction. Addition of Starch 1500 decreased the erosion of HPMC matrix, while lactose had no effect. A case study of drug release from Depakote ER® tablets in different medium demonstrated the direct correlation of gel strength and drug release through polymer erosion.

APPROVED:

Joseph R. Robinson, Professor

Co-advisor Lian Yu, Professor

Date: 16 Jan 2007

In memory of my advisor, Professor Joseph R. Robinson

ACKNOWLEDGEMENTS

A journey is easier when you travel together. Interdependence is certainly more valuable than independence. This thesis is the result of five years of work whereby I have been accompanied and supported by many people. It is a pleasant aspect that I have now the opportunity to express my gratitude for all of them.

My overwhelming thanks go to my major advisor, Professor Joseph R. Robinson, for his patience, guidance and fatherly love. I could not have imagined having a better advisor and mentor for my Ph.D. His sharp scientific vision, get-to-the-point working style, remarkable scientific knowledge, and integral view on research and his mission for providing 'only high-quality work and not less', has made a deep impression on me. He is an exceptional role model for me in both scientific career and personal life. His forever optimistic attitude to life always encourages me whenever I face difficulties in life. It is my great sorrow that Dr. Robinson can not physically see me finishing the journey of my Ph.D. study, but I know he can see it from the heaven and he will never fade away in my memory.

I would definitely say a big "thank-you" to Dr. Tzuchi Robert Ju, my co-advisor, at Abbott Laboratories. He is an expert in polymer sciences and he is the first person encouraged me to initiate this thesis topic and guided me through the thesis, with whom I had many productive scientific discussions. He kept an eye on the progress of my work and always was available when I needed his advises, resources and help. He also took effort in reading and providing me with valuable comments on earlier versions of this thesis.

I also sincerely thank my current advisor, Dr. Lian Yu, who was so kind to take me and help me finishing my degree by checking my thesis writing and giving me precious suggestions and comments. Many thanks shall go to the other members of my Ph.D. committee: Drs Ralph Albrecht, Ronald Burnette, Darin Furgeson, Glen Kwon, and Richard Peterson, who monitored my work and provided me with many valuable suggestions and great love and support especially after Dr. Robinson's leave. In addition, I am grateful to our Dean, Jeanette Roberts, and all the faculty members in the Pharmaceutical Sciences and the School of Pharmacy for their help and financial support.

I shall extend my gratitude to Abbott Laboratories for providing me the opportunities to use their facilities and many people at Abbott for the convenience, the valuable suggestions and the friendship they provided: Dennis Lee, Kenneth Gleason, Cristina Fisher, Claudia Davila, Michelle Long, Yihong Qiu, Eric Schmidt, Mark Kontny and Ping Tong.

I would also like to thank fellow graduate students during my graduate studies, specifically, my labmates: Adam Alani, Yogeeta Narkar and Deepa Rao. They are like part of my family. The road to my graduate degree has been long and winding and their friendship and encouragements made this long journey much joyable to me. Especially, their thoughtfulness and daily help gave me great support during the hardship of my pregnancy. Also, I would like to give me special thanks to Linda Frei, who was always there when I needed help in my Ph.D. program.

Last but certainly not least, my special thanks go to my husband, Weiguo Cheng, for his unconditional love, his patience, and support during the Ph.D. period. Thanks for the loving and happy family he provided which gave me the courage and strength to face all the difficulties in my life. I am also very grateful to my dear parents, Peisheng Yang

and Jufen Feng, for their endless love and support. And our lovely baby son, Joseph Cheng, definitely deserves a thank-you note for the great joy he brought to my life.

TABLE OF CONTENTS

CHAPTER I INTRODUCTION **1**

REFERENCES 5

CHAPTER II PROBING GEL STRENGTH IN HOMOGENEOUS HPMC GEL SYSTEMS USING TEXTURE ANALYZER **8**

ABSTRACT 8

INTRODUCTION 9

MATERIALS AND METHODS 12

Materials *12*

Sample Preparation *13*

Texture Analyzer Measurements *14*

RESULTS AND DISCUSSION 15

1. Model Construction and Validation of Texture Analyzer Profile *15*

1.1. Model Construction 15

1.2. Model Validation and Test Parameters Optimization 17

2. Applications *21*

2.1. Polymer Concentration and Molecular Weight Dependence of Gel Strength 21

2.2. Effect of Excipients on HPMC Gel Strength 21

2.3. Ionic Strength Effect 24

CONCLUSIONS 25

REFERENCES 27

CHAPTER III CHARACTERIZING SWELLING BEHAVIOR OF HPMC MATRIX TABLETS USING TEXTURE ANALYZER **46**

ABSTRACT 46

INTRODUCTION 47

MATERIALS AND METHODS 51

Materials *51*

Sample Preparation *51*

One-dimensional Swelling Experiment *52*

Texture Analyzer Profiling *52*

RESULTS AND DISCUSSION 53

1. Theory *53*

2. Applications *54*

2.1. Characterization of Pure HPMC Tablets Swelling at Fixed Hydration Time 54

2.2. Evolution of Pure HPMC Tablets Swelling 57

2.3. Effect of Polymer Viscosity Grade on the Swelling of HPMC Tablets 62

2.4. Effect of Polymer Concentration and Excipient Type on the Swelling of HPMC K15M Tablets64

CONCLUSIONS 66

REFERENCES 68

CHAPTER IV CONSTRUCTION AND VALIDATION OF MATHEMATICAL MODEL CORRELATING GEL STRENGTH AND POLYMER EROSION 85

ABSTRACT 85

INTRODUCTION 86

MATERIALS AND METHODS 94

Materials *94*

Sample Preparation *94*

One-dimensional In Vitro Dissolution Study *95*

HPLC Assays *96*

Evaporative Light Scattering Detection (ELSD) *96*

RESULTS AND DISCUSSION 97

1. Mathematical Model Construction *97*

2. Model Validation *102*

2.1. Effect of HPMC Viscosity Grade on HPMC Dissolution 102

2.2. Effect of Excipient Type and Content on HPMC Dissolution 105

CONCLUSIONS 109

REFERENCES 110

CHAPTER V UNDERSTANDING THE EFFECT OF SDS-HPMC INTERACTION ON DRUG RELEASE FROM DEPAKOTE® ER TABLETS 130

ABSTRACT 130

INTRODUCTION 131

MATERIALS AND METHODS 135

Materials *135*

Sample Preparation *135*

Cloud Point Measurement *136*
Solubility Test *137*
One-dimensional Swelling Experiments *137*
Texture Analyzer Measurements *137*
In Vitro Dissolution Tests and Assays *138*
RESULTS AND DISCUSSION 139
1. Interaction between Active Ingredient and HPMC *139*
Cloud Point Measurement 139
Gel Strength Measurement 140
2. Interaction between Active Ingredient and SDS *141*
3. Interaction between SDS and HPMC *142*
Effect of SDS Concentration on HPMC Gel Strength in Homogeneous Gel Systems 142
Effect of SDS on HPMC Homogeneous Gel Strength at Different Ionic Strength 143
Effect of SDS on Gel Strength of HPMC and Depakote® ER Swelling Tablets 144
4. Drug and HPMC Dissolution *145*
CONCLUSIONS 148
REFERENCES 149

CHAPTER VI SUGGESTED FUTURE STUDIES 172

REFERENCE 175

Figures and Tables

Figure I-1 Schematic representation of a hydrophilic matrix in the swelling medium 7

Figure II-1 Schematic representation of the two-stage mechanism model for a TA test 31

Figure II-2 Schematic representation of a typical force-displacement profile in the homogeneous gel at low speed range (<1mm/sec) 32

Figure II-3 The effect of probe size on the force-displacement curves for 10% w/w HPMC K15M gel. 33

Figure II-4 The effect of probe radius on (a) slope from compression region, k_c; and (b) slope from shear region, k_s 34

Figure II-5 The effect of probe speed on force-displacement curves in the range of 0.02 mm/sec to 1.0 mm/sec. 35

Figure II-6 The effect of probe speed on gel strength in the range of 0.02 mm/sec to 1.0 mm/sec 36

Figure II-7 The effect of probe speed on force-distance curve in high speed range (5.0 mm/sec to 20 mm/sec). 37

Figure II-8 The effect of probe size on force-displacement curves at high speed (10 mm/sec). 38

Figure II-9 Effect of probe speed on peak force. 39

Figure II-10 Polymer concentration dependence of gel strength 40

Figure II-11 Force distance profile comparison of HPMC K15M with different excipients. 41

Figure II-12 Effect of starch 1500 on HPMC gel strength. 42

Figure II-13 Effect of SDS on HPMC gel strength at different ratios 43

Figure II-14 Ionic strength effect on gel strength 44

Figure II-15 A schematic representation of the gel structure change as a function of ionic strength 45

Figure III-1 The force-distance profile of HPMC K15M matrix tablets at two hours swelling 74

Figure III-2 The representative semi-log gel strength profile of HPMC K15M matrix at two hours swelling. 75

Figure III-3 The representative polymer concentration profile in swelling matrix of HPMC K15M at two hours.....76
Figure III-4 The force-distance profiles of HPMC K15M matrices with varying time of swelling.....77
Figure III-5 The gel strength profiles of HPMC K15M matrices with varying time of swelling.....78
Figure III-6 Dynamic changes in gel layer and swollen glassy layer thickness for HPMC K15M matrices as a function of time.....79
Figure III-7 The effect of viscosity grade on the polymer concentration profiles of swelling table at 2 hour hydration.....80
Figure III-8 The effect of viscosity grade of HPMC on the gel layer thickness as a function of time.....81
Figure III-9 Dynamic changes in (a) gel layer and (b) swollen glassy layer thickness of HPMC K15M matrices with and without different excipients versus time.....82
Figure III-10 The gel strength profile of HPMC K15M matrices containing different excipients at varying time of swelling.....83
Figure III-11 Disintegration experiment of HPMC K15M tablet with different excipients in 0.25M phosphate buffer after 30 mins.....84
Figure IV-1 The schematic illustration of evaporative light scattering detector (ELSD).....117
Figure IV-2 A typical chromatogram of HPMC K15M detected by SEC-HPLC-ELSD.....118
Figure IV-3 The standard curve of peak area of ELSD and the concentration of HPMC K15M.....119
Figure IV-4 One dimensional dissolution kinetics of HPMC with four viscosity grades.....120
Figure IV-5 The effect of HPMC molecular weight on the disentanglement concentration.....121
Figure IV-6 The effect of molecular weight on HPMC dissolution rate.....122
Figure IV-7 Effect of lactose on HPMC K15M release.....123
Figure IV-8 Lactose effect on HPMC K4M erosion.....124

Figure IV-9 Effect of SDS on the release of HPMC K15M at different K15M:SDS ratios. 125
Figure IV-10 The effect of Starch-1500 on the dissolution of HPMC K15M. 126
Figure IV-11 Effect of Starch 1500 on the disentanglement concentration of HPMC K15M..... 127
Figure IV-12 The correlation of HPMC K15M release rate with the calculated polymer disentanglement concentration of K15M at different ratios of HPMC/Starch-1500. 128
Figure IV-13 The effect of HPMC/Starch 1500 ratio on the dissolution rate of HPMC K15M..... 129
Figure V-1 Chemical structure of divalproex sodium..... 154
Figure V-2 Mean in vivo absorption versus in vitro release profiles of divalproex sodium extended release formulations B, F and G based on initial in vitro test method 155
Figure V-3 Mean *in vivo* absorption versus in vitro release profiles of Formulations B, F and G based on predictive *in vitro* test method 156
Figure V-4 The transmittance profiles of 0.5% w/w HPMC K15M in the solution of 0.05M phosphate buffer with or without sodium valproate. 157
Figure V-5 Effect of divalproex sodium on the strength of HPMC K15M homogeneous gels with and without 75M SDS 158
Figure V-6 Effect of pH or SDS on drug release from Depakote® ER tablets. 159
Figure V-7 Effect of SDS concentration on HPMC K15M gel strength. 160
Figure V-8 Schematic representation of the model proposed for the interaction between HPMC and SDS. 161
Figure V-9 Equilibrium SDS concentration vs. the total SDS concentration 162
Figure V-10 Effect of SDS on HPMC gel strength at different ionic strength 163
Figure V-11 Effect of 75mM SDS on the strength of HPMC swelling compacts.. 164
Figure V-12 Effect of 75mM SDS on the strength of Depakote ER swelling tablets.. 165
Figure V-13 HPMC and drug release comparison in 0.05M PBS, pH 5.5 medium.166
Figure V-14 HPMC and drug release comparison in 0.05M PBS + 75mM SDS, pH 5.5 medium. 167

Figure V-15 One-dimensional HPMC and drug release c omparison in (a) 0.05M PBS without and (b) with 75mM SDS, pH 5.5 168

Figure V-16 Visual observation of Depakote® ER tablet dissolution in PBS buffer with and without 75mM SDS 169

Figure V-17 Effect of ionic strength on drug and HPMC release in 0.05M PBS + 75mM SDS, pH 5.5 medium. 170

Figure V-18 Effect of ionic strength on drug and HPMC release in 0.05M PBS, pH 5.5 medium. 171

Table III-1 Estimate of the average water diffusion constant at HPMC gel layer and its dependence on the viscosity grade. 73

Table IV-1 The parameters used for the calculation of disentanglement concentration of HPMC.....115

Table IV-2 The parameters used for the calculation of disentanglement concentration of HPMC K15M with the presence of Starch 1500.....116

Table V-1 Formulations of controlled-release hydrophilic matrix tablets of divalproex sodium 151

Table V-2 Solubility data of valproic acid at different conditions 152

Table V-3 SDS micelle concentration at different salt concentration. 153

CHAPTER I Introduction

Drug delivery systems (DDS) have become an integral part of the development of new medicines. The majority of oral DDS are matrix-based systems. Swellable matrices are monolithic systems prepared by compression of a powdered mixture of a hydrophilic polymer and a drug. This type of swellable matrix can be more specifically called a "swellable-soluble" or " swellable-erodible" matrix (Colombo 1993). Upon contact with aqueous solution, water molecules diffuse into the matrix. When enough water has entered into the matrix, the glass transition temperature (T_g) of the polymer drops to the level of the system temperature. Subsequently, polymer chains undergo a glass-to-gel transition to form a viscous mucilaginous gel layer (rubbery polymer) (Melia 1991), which retards further ingress of water and drug transport via its viscous resistant force.

During drug delivery, the gel layer is exposed to continuous changes in its structure and thickness. It begins when the polymer becomes hydrated and swells, where polymer chains are strongly entangled. Moving away from this swelling position, the gel layer becomes progressively hydrated and the polymer concentration continuously decreases to a critical value where the polymer chains disentangle and dissolve or erode. As a result of simultaneous polymer swelling and erosion, two fronts that separate different matrix states exist: swelling front (S) and eroding front (E) (Figure I-1). A swelling front can be identified as the boundary separating the gel region from the glassy region and an eroding front separates the gel region from the swelling medium. The relative movement of these two fronts determines the gel layer thickness, which is the distance between these two fronts. In the early stage, gel layer thickness increases due to polymer swelling. The successive polymer dissolution counteracts this increase in

thickness, producing a diminution of the gel layer thickness. Finally, the matrix disappears as the glassy core depletes.

It is well recognized that drug release from swellable-soluble polymer matrix is typically described in terms of two simultaneously operating mechanisms. These are drug diffusion through the gel layer and erosion of outer gel layer (Korsmeyer 1983; Peppas 1985; Melia 1991; Shah 1993; Wan 1993). The relative contribution of these two mechanisms depends on the relative rates of drug diffusion and polymer erosion. When drug diffusion is much faster than polymer erosion, diffusion is the predominant drug release mechanism. If drug diffusion rate is much slower than polymer erosion rate, such as in the case of a matrix with insoluble active agents, polymer erosion predominates in the drug release. More often, with soluble drugs, an appropriate combination of diffusion and erosion mechanisms determines the release kinetics and the contributions of these two mechanisms to the overall release are considered additive (Durig 2002). It may be desirable to design a polymer matrix which allows one to control the overall release of drug via the appropriate choice of polymer and/or excipients, utilizing the different contribution by polymer erosion to produce the desired overall drug release.

Due to its importance on drug release from swellable-soluble matrix tablets, the understanding of polymer dissolution has gained much interest to researchers recently. Polymer chain dissolution from the matrix surface is believed to involve two distinguishable processes. The first step involves the disentanglement of individual polymer chains at the matrix surface, which depends on the rate of hydration. This occurs at a critical polymer concentration, defined as the polymer disentanglement concentration, $C_{p,dis}$ (Harland 1988; Bonferoni 1992). The second step involves the transport of dissolved

chains from the surface across a diffusion layer, adjacent to the matrix, to the bulk solution (Ju 1995; Reynolds 1998).

Mathematical modeling has been extensively used to understand the polymer dissolution and its contribution to the drug release (Tu 1977; Harland 1988; Devotta 1994; Narasimhan 1997; Siepmann 1999; Siepmann 2002). These models can be classified into two broad categories: 1) use of phenomenology and models with Fickian equations (Harland 1988; Siepmann 1999). The phenomenological models identified a polymer 'dissolution rate' as a key parameter. However, they failed to quantitatively predict this rate from the molecular properties of the polymer and the solvent as treated this rate as a model parameter. 2) analysis using anomalous transport models for solvent transport and scaling laws for chain disentanglement (de Gennes 1979; Peppas 1994). This approach of using molecular theories appeared to yield useful insight into the understanding of the physics of the polymer dissolution. However, quantitative correlation between polymer dissolution and gel properties that can be routinely characterized has not been adequately addressed. Rheological properties of gels have been proposed to be related to the polymer dissolution since both of them are sensitive to inter-chain interactions and entanglements, while some authors have suggested the relevance of gel strength to the resistance of polymer dissolution (Van Aerde 1988; Herman 1989a; Herman 1989b). However, no definitive conclusion was drawn and no systemic study was done to correlate the gel strength and drug release through polymer erosion partly due to the lack of a proper tool for routine tests of gel strength.

Therefore, the **aim of our study** is to develop a gel strength characterization tool and investigate how gel strength affects drug release from swellable matrices through polymer erosion. We expect the results from this study to provide us a tool to screen

polymers and excipients in terms of gel strength, a quantitative correlation between gel strength and polymer erosion, a new insight of correlating gel strength and drug release and to improve formulation development efficiency by the choice of gel-strength modulating excipients/polymers.

Based on the aim, the ultimate **objectives** of this study are fourfold:

First, we intend to develop a characterization tool for routine tests of gel strength using Texture Analyzer (TA). Specifically, a mathematical model for better interpretation of gel strength measured using TA will be constructed and validated by varying commonly used experimental conditions, such as probe speed and probe size. The optimal test conditions will also be determined.

Second, the above method, if validated, will then be used to probe the effect of some formulation related variables, such as polymer concentration, polymer grade (molecular weight), different excipient types and/or contents, on gel strength in both homogeneous HPMC gels and HPMC swelling tablets.

Third, the mathematical model(s) correlating gel strength with polymer dissolution from hydrophilic matrices will be constructed and validated; and the effect of formulation related variables on polymer erosion through gel strength will be examined.

Fourth, a case study will be conducted to show the correlation between gel strength and drug release.

REFERENCES

Bonferoni M. C., Caramella C., Sangalli M. E., Conte U., Hernandez R. M. and Pedraz J. L. (1992). "Rheological behaviour of hydrophilic polymers and drug release from erodible matrixes." Journal of Controlled Release **18**: 205-212.

Colombo P. (1993). "Swelling-controlled release in hydrogel matrices for oral route." Advanced Drug Delivery Reviews **11**(1-2): 37-57.

de Gennes P. G. (1979). Scaling Concepts in Polymer Physics. Ithaca, NY, Cornell University Press.

Devotta I., Ambeskar V. D., Mandhare A. B. and Mashelkar R. A. (1994). "The life time of a dissolving polymeric particle." Chem Eng Sci **49**(5): 645-654.

Durig T. and Fassihi R. (2002). "Guar-based monolithic matrix systems: effect of ionizable and non-ionizable substances and excipients on gel dynamics and release kinetics." Journal of Controlled Release **80**: 45-56.

Harland R. S., Gazzaniga A., Sangalli M. E., Colombo P. and Peppas N. A. (1988). "Drug/polymer matrix swelling and dissolution." Pharmaceutical Research **5**: 488-494.

Herman J. and Remon J. P. (1989a). "Modified starches as hydrophilic matrices for controlled oral delivery: II. *In vitro* drug release evaluation of thermally modified starches." International Journal of Pharmaceutics **56**: 65-70.

Herman J ., Remon J . P. and De W ilder J. (1989b). "Modified starches as hy drophilic matrices for controlled oral delivery: I. Production and characterization of thermally modified starches." International Journal of Pharmaceutics **56**: 51-63.

Ju R. T. C., Nixon P. R. and Patel M. V. (1995). "Drug release from hydrophilic matrixes 1. New scaling laws for predicting polymer and drug release based on the polymer disentanglement concentration and the diffusion layer." Journal of Pharmaceutical Sciences **84**(12): 1455-1463.

Korsmeyer R. W., Gurny R., Doelker E., Buri P. and Peppas N. A. (1983). "Mechanisms of solute release from porous hydrophilic polymers." International Journal of Pharmaceutics **15**: 25-35.

Melia C. D. (1991). "Hydrophilic matrix sustained release systems based on polysaccharide carriers." Critical Reviews in Therapeutic Drug Carrier Systems **8**(4): 395-421.

Narasimhan B. and Peppas N. A. (1997). "Molecular analysis of drug delivery systems controlled by dissolution of the polymer carrier." Journal of Pharmaceutical Sciences **86**: 297-304.

Peppas N. A. (1985). "Analysis of Fickian and non-Fickian drug release from polymers." Pharm. Acta. Helv. **60**: 110-111.

Peppas N. A., Wu J. C. and Von Meerwall E. D. (1994). "Mathematical modeling and experimental characterization of polymer dissolution." Macromolecules **27**: 5626-5638.

Reynolds T. D., Gehrke S. H., Hussain A. S. and Shenouda L. S. (1998). "Polymer Erosion and Drug Release Characterization of Hydroxypropyl Methylcellulose Matrices." Journal of Pharmaceutical Sciences **87**(9): 1115-1122.

Shah N., Zhang G., Apelian V., Zeng F., Infeld M. H. and Malick A. W. (1993). "Predication of drug release from hydroxypropyl methylcellulose (HPMC) matrices: effect of polymer concentration." Pharmaceutical Research **10**(11): 1693-1695.

Siepmann J., Podual K., Sriwongjanya M. and Peppas N. A. (1999). "A new model describing the swelling and drug release kinetics from hydroxypropyl methylcellulose tablets." Journal of Pharmaceutical Sciences **88**: 65-72.

Siepmann J., Streubel A. and Peppas N. A. (2002). "Understanding and predicting drug delivery from hydrophilic matrix tablets using the "Sequential Layer" model." Pharmaceutical Research **19**(3): 306-314.

Tu Y.-O. and Ouano A. C. (1977). "Model for the kinematics of polymer dissolution." IBM J Res Develop **21**(2): 131-142.

Van Aerde P. and Remon J. P. (1988). "*In vitro* evaluation of modified starches as matrices for sustained release dosage forms." International Journal of Pharmaceutics **45**: 145-152.

Wan L. S. C., Heng P. W. S. and Wong L. F. (1993). "Relationship between swelling and drug release in a hydrophilic matrix." Drug Development a nd Industrial Pharmacy **19**(10): 1201-1210.

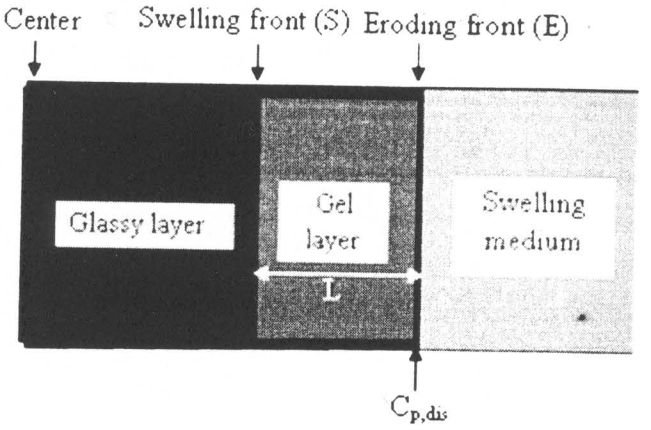

Figure I-1 Schematic representation of a hydrophilic matrix in the swelling medium. The space defined by the double lines represents the undissolved matrix. Two fronts are indicated in the schematic as swelling front (S), the interface between the glassy layer and the gel layer, and eroding front (E), the interface between the gel layer and swelling medium. L is the gel layer thickness. $C_{p,dis}$ is the polymer concentration at eroding front.

CHAPTER II Probing Gel Strength in Homogeneous HPMC Gel Systems Using Texture Analyzer

ABSTRACT

Purpose. Properties of polymeric gels have a great impact on drug release behaviors in hydrophilic matrix dosage forms. The purpose of this study was to develop a method of using Texture Analyzer to characterize polymeric gel strength. ***Methods.*** Texture Analyzer was employed to measure the strength of hydroxypropyl methyl cellulose (HPMC) homogeneous gel systems at different HPMC concentrations and grades (molecular weight), additives (lactose, Avicel, Starch 1500 and SDS) and ionic strength. ***Results.*** We proposed a two-stage mechanism for Texture Analyzer force-distance profiles collected from a homogeneous gel system and constructed mathematical models describing the two stages: compression and shearing of gels during the test procedure. The gel strength (G) was defined as a modulus measuring the viscosity of the gel and has the unit of force/area, $G = 2\pi\eta\dot{\gamma}$, where $\dot{\gamma}$ is the shear rate and η is the viscosity of the gel. Probe size and probe speed effects were studied to validate the model and the optimal test conditions were identified. Effects of polymer concentration, molecular weight, different additives and ionic strength on gel strength were also explored. A power-law relationship between gel strength and polymer concentration was observed for HPMC gels and this relationship is independent of molecular weight. The value of the exponent (3.8) is consistent with the results from viscosity study of concentrated polymer solutions in good solvent, supporting the validity of the mathematical model. The addition of lactose did not affect the strength of HPMC gel, while Avicel increased the gel strength slightly. Both Starch 1500 and SDS enhanced the strength of HPMC K15M gels at different

HPMC/excipient ratios. We also found that gel strength increased with ionic strength, reached a maximum, and then decreased afterward. Further, the penetration force-distance curves showed different patterns when different probe speeds were applied. ***Conclusions.*** Fundamental understanding of Texture Analyzer data gained through the model we developed demonstrated that Texture Analyzer is a proper tool to characterize polymeric gels.

Key Words: Texture Analyzer; gel strength; HPMC; swellable hydrophilic matrix.

INTRODUCTION

Different approaches have been employed to characterize the strength of polymeric gels; however, definition of gel strength differs among various methods and researchers. The viscoelastic parameters of gels as measured by rheological techniques were commonly used to represent the gel strength and were related to drug release through polymer erosion in the case of matrices based on xanthan gum, locust bean gum mixtures, and Na carboxymethylcellulose (Mannion 1991; Bonferoni 1995). Nevertheless, the rheology method is limited to homogeneous gel samples and not applicable to swelling tablets, which exhibit heterogeneous swelling from the periphery to the center of the tablets. To assess the gel strength of hydrated tablets, a penetration method (Tang 1994; Veith 2004) using a penetrometer or an Instron universal testing machine was used. The penetration force, a resistance force encountered by the penetration of a probe, or the total work of penetration at a selected penetration depth of fully hydrated tablets, was expressed as a measure of gel strength in this method. However, the penetration force or work of penetration is subjected to change when a different penetration depth was used for the same gel sample (Herman 1989a; Herman 1989b; Jamzad 2005).

Recently, Texture Analyzer (TA) has received attention for characterization of pharmaceutical gels (Ferrari 1994; Jones 1996; Yang 1998; Ferrari 2001; Jones 2002). The use of Texture Analyzer dated back to 1963 in the food industry as a tool to characterize food properties by simulating the masticating action of the human mouth (Friedman 1963; Szczesniak 1963; Pons 1996). In this technique, an analytical probe is connected to a force transducer within the analyzer that measures the force of resistance encountered by the probe during depressing into the sample under examination. From the resultant force-distance plot, the mechanical resistance of the sample to the penetration of the probe, referred to as the gel strength, is derived as the ratio between the penetrating force and the displacement of the probe inside the sample (Ferrari 1994; Ferrari 2001). Several parameters can also be derived, such as hardness (force required to attain a given deformation), compressibility/spreadability (the work required to deform the product during the first compression cycle of the probe), and adhesiveness (the work necessary to overcome the attractive forces between the contacting surfaces of sample and probe) (Pons 1996). These parameters have found utility in the development of pharmaceutical semi-solid systems (Jones 1997; Jones 1999).

As a penetration method in nature, the Texture Analyzer can accommodate a wide range of sample types, such as liquid, gel, capsules, powders, swelling tablets and so on, which rheometers can not achieve. In contrast to alternative penetration methods like penetrometer and consistometer measurements, which simply base on the determination of the penetration distance at a distinct force, Texture Analyzer also provides information on gel structure, as complete force-distance diagrams are recorded during the penetration process. On the other hand, by expressing gel strength as the ratio between penetrating

force and the displacement, Texture Analyzer reduces the variability of measurement compared to other penetration methods.

More importantly, Texture Analyzer was found to be capable of delineating the structure of a swelling tablet (Yang 1998). The gel layer thickness dynamics of swelling tablet were measured using this method and found to be consistent with the results obtained by more sophisticated methods. Moreover, in our study, we will show that polymer concentration profiles across the gel layer can be determined by properly interpreting the force-distance profile. The structure of a swelling tablet is very crucial to understand the drug release mechanism (Lee 1980; Harland 1988), therefore, there were many efforts carried on in this area. The optical microscopy based on the refractive index change at the interface of polymer gel and glassy core has been used to measure the structure of a swelling tablet (Papadimitriou 1993; Colombo 1995; Kim 1997). However, due to the lack of sufficient amount of water, the microscopy could not differentiate structure beyond that interface. Several non-invasive imaging techniques have been adapted to probe swelling tablets, including ^{1}H NMR imaging (Rajabi-Siahboomi 1994), confocal laser scanning microscopy (Cutts 1996), cryogenic scanning electron microscopy (Melia 1994) and light scattering imaging (Gao 1996). These techniques were capable of identifying gradients of polymer concentration and water mobility across the entire gel region. However, despite their high accuracy and precision, they are sophisticated and often time consuming and difficult to set up or operate. On the other hand, because of its short analysis time and user-friendliness, Texture Analyzer has proved to be a relatively convenient method to characterize swelling systems with comparable accuracy (Yang 1998). Yet, the characterization of swelling tablets using Texture Analyzer is not the focus of this chapter and will be presented in Chapter III.

Even though Texture Analyzer shows great potential for characterizing polymeric gels, more work is needed. First, no fundamental understanding of Texture Analyzer data, i.e., rigorous theoretical basis between force and distance, is available. Secondly, it has been difficult to cross-compare available Texture Analyzer data, as different experimental conditions, such as probe size and probe speed, have been used and these parameters have profound impact on results. Lastly, most of the information gathered so far has been limited to only force-displacement profiles, and as we will demonstrate in this chapter, further data analysis is warranted. Therefore, the aims of this study are multiple. First, we intended to develop a mathematical model for better interpretation of gel properties as measured by Texture Analyzer. Secondly, we would validate the above model by varying commonly used experimental conditions such as probe speed and probe size. The model, if validated, will then be used to extract intrinsic properties of gels and the swelling behavior of hydrophilic polymer tablets can be better characterized accordingly. The model gel system used in this study is hydroxypropylmethylcellulose (HPMC), a hydrophilic polymer commonly used in oral controlled release dosage forms.

MATERIALS AND METHODS

Materials

METHOCEL®, commercially available hydroxypropylmethyl cellulose (HPMC), with viscosity grades of K15M (M_n=134,000, 15 096 cP in 2% w/w solutions at 20 ^{0}C), K4M (M_n=96,000, 4870 cP in 2% w/w solutions at 20 ^{0}C) and K100LV (M_n=29,000, 92 cP in 2% w/w solutions at 20 ^{0}C) were from Dow Chemical Company without further purification. Spray dried lactose monohydrate, microcrystalline cellulose (Avicel®

PH102) and Starch 1500® were obtained from Fast-Flo, FMC Biopolymer and Colorcon, respectively. Sodium dodecyl sulfate (SDS) was from BDH laboratory supplies. Potassium phosphate monobasic was from EMD Chemicals Inc. and sodium hydroxide was from J.T. Baker Inc.

Sample Preparation

Three viscosity grades HPMC K15M, K4M and K100LV hydrogels at concentrations from 5% to 17% (w/w) were prepared. Precisely weighed HPMC powders (2.0 g to 6.8 g) were initially dispersed into appropriate amount of 80-90 ^{0}C deionized water under strong agitation to form homogeneous dispersion. The total weight of dispersion was 40.0 g. The dispersion was then cooled to room temperature under mild agitation until a homogenous gel formed. All samples were stored at 4 ^{0}C refrigerator for at least 24 h and equilibrate under room temperature before analyses and were covered with Para film to prevent water evaporation during storage. All gel samples were prepared in 50 ml Pyrox® beakers with 3.7cm in diameter.

HPMC K15M gels with different ionic strength were also prepared. The preparation procedure was same as above, except that potassium phosphate buffer solution (pH 6.8) was used instead of deionized water.

The gels of binary mixture of HPMC and excipients (lactose, Avicel, SDS or Starch 1500) at different concentrations were prepared as follows: precisely weighed excipient powders were initially dissolved or dispersed into appropriate amount of 80-90 ^{0}C deionized water and HPMC K15M powders were further added into the corresponding excipient solution or dispersion at 80-90 ^{0}C under strong agitation to form homogeneous dispersion. The total weight of the dispersion was also 40.0g. HPMC/excipient ratios

were 15:1, 15:2 and 15:3 for HPMC/SDS, 1:1, 1:2 and 2:1 for HPMC/Starch and 1:1 (w/w) for HPMC/lactose and HPMC/Avicel.

Texture Analyzer Measurements

TA.XT Plus Texture Analyzer (Texture Technologies Corp., Stable Micro Systems, Algonquin, IL, U.S.A.) instrument is a microprocessor-controlled texture analysis system that measures the profiles of stress-strain behavior for sample under test. It consists of an analyzer and a personal computer equipped with Texture Exponent 32 software that automates data acquisition and analysis. The motion of the probe is controlled by a stepping motor that records the displacement up to the accuracy of 1μm.

During the test, a sample was positioned in the center of the testing platform. A flat-tipped, round steel probe of different sizes (2 to 5 mm in diameter) and 30mm in length was used. The probe traveled at fixed speed until a critical force of 0.04 g was detected (threshold v alue f or t riggering the T exture Ana lyzer). At t his point t he data acquisition started and the probe proceeded downward through the samples at a pre-determined speed. The motion of the probe continued until the measured strain reached a predetermined limit, where the probe was automatically withdrawn at 0.2 mm/sec and stopped when the probe returned to its start position. Data were collected at a rate of 10 points per second by Texture Expert^{TM} software. For each sample, three replicates were run at different positions of the sample; average values were calculated and plotted in the force-distance profile.

RESULTS AND DISCUSSION

1. Model Construction and Validation of Texture Analyzer Profile

1.1. Model Construction

We proposed a two-stage mechanism for a typical Texture Analyzer force-distance profile obtained from a homogeneous gel system. The first stage starts with the initial contact of the probe and ends when the probe begins to penetrate inside the gel, as shown in Figure II-1 (a). During this stage, gel undergoes compression by the probe and displaced gel is pushed away from the probe toward the container wall. We hypothesize that compression force is the dominant force in this stage. The second stage starts when the probe begins to penetrate inside the gel and the moving of the probe exerts shear on the gel, as shown in Figure II-1 (b). We hypothesize that shear force is the dominant force in the second stage.

In Figure II-1(a), compression force, F_c, exerted by the probe causes displacement of the gel by a distance of L. For small compressive strains, it is known that the load is linearly related to displacement (L) as $L/F_c = 3/(8Er_p)$ for a flat, cylindrical punch in contact with an incompressible elastic half-space with an elastic modulus E. This equation assumes a rigid, frictionless punch engaged in adhesionless contact with a thick layer (Shull 2002). Following this notion, the compression force can be expressed as

$$F_c = \frac{8}{3} E r_p L \quad (L<L_t) \qquad \text{Equation II-1}$$

where r_p is the radius of probe, E is the Young's modulus of the gel, and L_t is the length of indentation prior to probe penetration. After maximum compression deformation (L_t) is reached, the probe penetrates inside the gel and shearing force (F_s) on the gel starts

becoming dominant over compression. The probe displacement, L, can be approximated as the penetration depth of probe ($L>>L_t$ for L_t is quite small). Note unlike conventional rheological experiments where shear force is caused by rotating plates, shear force (F_s) measured in Texture Analyzer is in a direction parallel to the probe motion and can be expressed as

$$F_s = 2\pi r_p L \eta \dot{\gamma} \qquad \text{Equation II-2}$$

where $\dot{\gamma}$ is the shear rate and η is the viscosity of the gel. Equation II-2 is valid only under a constant deformation and this condition is met in this study because the probe moves at a constant speed. Generally, a power-law relationship between viscosity and shear rate exists, as described by the Ostwald equation (Alvarez-Lorenzo 2001)

$$\eta = k \dot{\gamma}^{n-1} \qquad \text{Equation II-3}$$

where the indices of k and n represent the consistency and fluidity of the sample, respectively. For a shear-thinning system, n falls between 0 and 1 and is greater than 1 for a shear-thickening system. Combining Equation II-2 and II-3 leads to

$$F_s = 2\pi k r_p \dot{\gamma}^n L \qquad \text{Equation II-4}$$

From Equation II-4 above, we define gel strength, G, in the similarity of definition of young's modulus in Equation II-1, as

$$G = 2\pi\eta \dot{\gamma} = 2\pi k \dot{\gamma} \qquad \text{Equation II-5}$$

which is a modulus measuring the viscosity of the gel and has the unit of force/area.

Experimentally, these two stages can be recognized as two straight lines in a typical force-displacement profile obtained from a homogenous gel system, as shown in Figure II-2. The slope in the compression region, k_c, can be derived from Equation II-1 as

$$k_c = \frac{8}{3} r_p E$$ Equation II-6

which is expected to be proportional to probe radius. The Young's modulus, E, becomes

$$E = \frac{3}{8} \frac{k_c}{r_p}$$ Equation II-7

Furthermore, the slope in the shear-dominant region, k_s, can be derived from Equation II-4 as

$$k_s = 2\pi k r_p \dot{\gamma}^n$$ Equation II-8

Because shear rate ($\dot{\gamma}$) is proportional to probe speed (p_s), the slope in the shear region can be also expressed as

$$k_s = 2\pi k k' r_p p_s^{\ n}$$ Equation II-9

where k' is the proportional constant between shear rate and probe speed. Therefore, k_s, is proportional to the probe radius (r_p) and p_s^n. The gel strength (G) can be derived as the ratio of k_s to the radius of the probe based on Equation II-5 and II-8

$$G = k_s / r_p = 2\pi k k' p_s^n$$ Equation II-10

Based on Equations II-6 and II-8, k_c and k_s are proportional to probe radius. Based on Equation II-10, a power-law relationship between the gel strength and probe speed at fixed probe size is expected. To validate the model, we studied the effects of probe size and probe speed on gel strength.

1.2. Model Validation and Test Parameters Optimization

1.2.1. Effect of Probe Size.

Figure II-3 shows the force-distance profiles for a 10% w/w HPMC K15M gel measured using different probe diameters (2 mm, 3 mm, 4 mm and 5 mm) at a test speed of 0.1 mm/sec. As expected, increasing probe size significantly increased both compression and shear forces. The slopes in the compression and the shear regions were derived and plotted as a function of probe radius and shown in Figure II-4, linearity with probe radius was confirmed for both slopes, in agreement with the model predictions (Equation II-6 and II-8).

As we can see from Figure II-3, the compression region became more and more apparent as probe size increased and the entire force-distance profile deviated from linear pattern progressively. This is because compression or Young's modulus of the gel is much higher than the gel strength in the shear region. Therefore, in order to minimize the compression region and to aid extraction of gel strength in the shear region, 2 mm probe was selected as the optimal probe size for subsequent experiments.

1.2.2. Effect of Probe Speed.

Based on Equation II-10, a power-law relationship between gel strength and probe speed at a constant probe size is expected. This was verified using HPMC K15M gels at concentrations 10% and 5% (w/w). The probe speed was varied in the range of 0.02 mm/sec to 1.0 mm/sec. The force-distance profiles are shown in Figure II-5. The gel strength was derived and using linear regression, power-law relationships ($G = 4.87 p_s^{0.41}$ for 10% w/w gel and $G = 0.32 p_s^{0.55}$ for 5% w/w gel) were obtained and depicted in Figure II-6. Agreement between model predications and experimental data supports again the validity of the model. The values of exponent n are less than 1, suggesting shear-thinning behavior of HPMC gels. This is also consistent with the finding from rheology studies in

other groups (Kawaguchi 1999). Furthermore, the value of *n* increases with a decrease in polymer concentration, which is reasonable, as a more dilute gel (5% w/w) would approach the behavior of Newtonian liquids with n =1. For homogeneous gel systems, a wide range of probe speeds can be used. Our preliminary studies on swelling tablets found the optimal probe speed to be in the range of 0.05 to 0.2 mm/sec. Probe speed higher than 0.2 mm/sec might cause the swollen gel to collapse; on the other hand, probe speed lower than 0.05 mm/sec would decrease the sensitivity of measurement. Thus, the probe speed was fixed at 0.1 mm/sec in subsequent experiments.

1.2.3. Effect of Probe Speed in the High Range

Interestingly, at higher probe speed (above 2 mm/sec), the force-distance profile pattern is different from those in the low speed region. As shown in Figure II-7, the force increased sharply with displacement, reached a peak and then dropped. This behavior has been observed by Nakamura *et al.* who studied the effect of compression velocity on the strength and the structure of gellan gels (Nakamura 2001). They varied the probe speed from 0.005 to 1000 mm/min, and found that similar load-compression curve shown in Figure II-7. They also observed from the photograph of the gel that the gel was broken in the probe speed from 1 to 1000 mm/min. In their study, the probe size is larger than that of gel sample so that the probe will not penetrate inside the sample in all processes of compression. The probe is much smaller than gel sample in our study. Despite the discrepancy of relative size of probe to gel sample in these two studies, we believe the gels underwent the similar fracture under such fast compression. We visually observed that the force started to drop before the probe penetrated inside the gel; therefore, the relative size of probe to gel sample will not make much difference since only compression happens in this stage. This was further verified by varying probe size and similar facture behavior was

found as shown in Figure II-8. Similar patterns of penetration force-displacement were also observed by Ferrari *et al.* (Ferrari 1994) in different polymeric systems. They found that for 6% (w/w) HPMC gel system, the force profile was similar to the curve shown in Figure II-2 when the speed was 0.02 mm/sec and κ-carrageenan gels showed fracture behavior under compression with curves similar to those shown in Figure II-7. The authors further attributed these different behaviors to rheological properties obtained by rheometer and concluded that when a break was observed in the force-distance profile, a yield point was also observed in the rheological study. Their conclusions may not be applicable in our system since we observed the patterns for all systems by simply changing the probe speed. We believe that when probe speed is slow, the deformation of the gel can be relaxed by the collective diffusion of gel network, and gel fracture does not happen, thus a typical force-distance profile similar to Figure II-2 will be obtained; when the probe speed is high, it causes rather rapid rate of gel compression, which can not be relaxed by the collective diffusion of gel network, and the gel fracture takes place, thus a fracture peak force is observed in the force-distance profile as shown in Figure II-7.

To further understand the gel facture behavior under compression, the force and distance at peak point versus probe speed were plotted and shown in Figure II-9, and they both linearly increased with the probe speed, consistent with the previous results (Nakamura 2001), which further confirmed that HPMC gel underwent similar structure change (gel fracture) as gellan gels in Nakamura and Tokita's study.

2. Applications

2.1. Polymer Concentration and Molecular Weight Dependence of Gel Strength

It is well known that polymer concentration and molecular weight modulate gel strength through polymer chain entanglement. Their effects were studied using three different viscosity grades of HPMC (K15M, K4M and K100LV) at various concentrations (5% to 17% w/w). As shown in Figure II-10, gel strength increased with polymer concentration for all three viscosity grades. Furthermore, a single power-law relationship (n=3.8) between gel strength and the polymer c oncentration was obtained using linear regression analysis. Interestingly, the 3.8 power-law relationship was also found between the viscosity and concentration of a concentrated polymer solution in a good solvent by polymer s cientists (Rubinstein 20 03). T his in dicates true s olution behavior of H PMC hydrogels and is consistent with the finding that no yield points were observed in both G' and G'' curves of HPMC hydrogels using a dynamic rheometer (Ferrari 1994; Talukdar 1996). Those agreements further validate the utility of gel strength measured by Texture Analyzer for the characterization of polymeric gels.

From Figure II-10 we also see that the gel strength increases with molecular weight at same p olymer concentration, this is in agreement w ith the current understanding o f polymer physics. It was found that the concentration where polymer chains start to entangle is polymer molecular weight related. Higher molecular weight leads to lower entanglement concentration, therefore results in higher gel strength at same concentration.

2.2. Effect of Excipients on HPMC Gel Strength

Excipient type is one of the most important formulation variables in the pharmaceutical industry. It was suggested that unlike in conventional dosage forms

inclusion of excipients in hydrophilic controlled-release tablets should not be regarded as neutral or simple additives as their various physico-chemical properties may have significant implications on water penetration, kinetics of matrix hydration, polymer erosion, and hence mechanism of drug release (Williams III 2002; Jamzad 2005). However, very little work was done to investigate the influence of excipient type on polymeric gel properties in the matrix.

Spray-dried lactose (SDL), microcrystalline cellulose (MCC) and partially pregelatinized starch are three commonly used excipients in the manufacture of solid dosage forms. Small soluble SDL is used as diluent/filler, swellable, insoluble excipient (MCC) is used as disintegrant. Partially pregelatinized maize starches are normally used as binder, disintegrant and filler in immediate release tablet formulations. However, the use of partially pregelatinized starches in combination with other polymers, such as HPMC, in sustained release tablets has not been fully examined (Cunningham 1999; Levina 2004). Most native starches consist of two polymers of glucose, partially water-soluble branched amylopectin and water soluble linear amylose. Partially pregelatinized starch contains soluble (gelatinized) and insoluble fractions. The specific grade used in our study, Starch 1500®, contains 5% of free amylose and 15% of free amylopectin. Recently, the influence of Starch 1500, in comparison to two other commonly used excipients, microcrystalline cellulose (MCC) and lactose, on drug release from HPMC 2208 has been studied by Levina and Rajabi-Siahboomi(Levina 2004). The study showed that for both soluble and slightly water-soluble drugs, chlorpheniramine maleate and theophylline, addition of Starch 1500 retarded drug releases compared to MCC or lactose (Levina 2004). To uncover the causes of different release behaviors of HPMC tablets by lactose and Starch 1500, their effects on HPMC gel strength were studied.

The effect of lactose on HPMC K15M gel strength was shown in Figure II-11(a). Lactose did not show any effect on the strength of HPMC gel. Lactose is a small soluble molecule, behaves similarly to water molecule in the solution, and does not cause more entanglements of polymer chains, so the gel strength did not increase with the addition of lactose. This is very important for us to understand the effect of lactose on the drug release, as we will show in following chapters.

The effect of Avicel on HPMC 15M gel strength was shown in Figure II-11(b). It seemed that addition of 6% w/w Avicel into 6% w/w HPMC hydrogel increased the gel strength slightly. This is probably due to the increase in actual concentration of HPMC by addition of Avicel particles, because after subtraction of this space filling effect, the effect of Avicel on HPMC gel strength was very minimal indicating no or very weak interaction between avicel particle and HPMC chains.

The effect of starch on HPMC K15M gel strength was shown in Figure II-12 (a). The addition of starch increased the gel strength significantly and higher starch content increased the gel strength to a greater extent. Interestingly, if we define an effective polymer concentration (EPC) as the following equation: EPC = concentration of HPMC + 0.85*concentration of Starch, we found that the gel strength of three ratios of binary mixture of HPMC and starch fell into one master curve when plotted as effective polymer concentration (Figure II-12 (b)).

SDS is another interesting additive that has been used as a drug solubilizer in either formulation or dissolution medium. It was found that the addition of SDS retards the release of chlorpheniramine from HPMC tablets and a good *in vitro-in vivo* correlation was obtained when SDS was used in the dissolution medium of Felodipine ER® tablets (Daly 1984; Abrahamsson 1994). The interaction between HPMC and SDS in the solution

has been studied previously (Nilsson 1995). It was found that SDS could increase HPMC viscosity by adsorbing to HPMC chains and forming clusters when SDS concentration exceeds critical adsorption concentration, however, very little work was done to study the interaction between SDS and HPMC in gel state. The effect of SDS on gel strength of HPMC was shown in Figure II-13. The addition of SDS increased the HPMC K15M gel strength at all the concentrations studied; and the higher ratio of SDS to HPMC increased the gel strength to a greater extent, in agreement with previous study in solution.

Neither SDS nor starch could form gel itself, however, they increased the strength of HPMC gel. We believe it is because both SDS and starch increase the entanglement of HPMC chains due to their specific interaction with HPMC. For Starch 1500, the soluble amylose molecules in partially pregeltilized starch might have synergistic interactions with HPMC. For SDS, same as in solution, it might adsorb onto HPMC chains to form micelles providing more entanglement points.

2.3. Ionic Strength Effect

Ionic strength has been used as a tool to test drug release behavior of hydrophilic matrix systems under stress conditions. Ionic strength exerted significant effects on theophylline release from Lasma® tablets (Po 1990). The drug release rate of theophylline decreases with an increase of ionic strength initially and then increases at ionic strength above 0.5M. Interestingly, K. Mitchell *et al.* studied the effect of ionic strength on the disintegration times of HPMC matrices (Mitchell 1990), and found that the disintegration time decreased to a minimum before rising as the ionic strength increased. It has been suggested that gel strength can affect drug dissolution from hydrophilic

matrices (Van Aerde 1988; Herman 1989a; Herman 1989b). To confirm the hypothesis, effect of ionic strength over the range of 0 to 0.8 M on HPMC gel strength was studied and shown in Figure II-14. At low ionic strengths, an increase in ionic strength did not significantly affect gel strength. As ionic strength continued to increase, an increase in gel strength was observed until a maximum was reached. Afterward, gel strength declined with further increase in ionic strength and finally no gel was formed. These mirror images of ionic strength effect on theophylline release, HPMC matrix disintegration and gel strength confirmed that ionic strength could affect drug release through modulating gel strength. While studies on drug release are warranted to confirm the hypothesis, it is reasonable to assume that gel strength measurement by Texture Analyzer can become a convenient tool for assessing the performance of hydrophilic matrices.

The ionic strength effect on gel strength could be partially explained by Hegg in 1982 as shown in Figure II-15 (Hegg 1982). According to this model, as ionic strength increases, the gel structure changes from homogeneous network to network with polymer aggregates. HPMC has both hydrophilic and hydrophobic segments, when ionic strength increases, the polarity of solvent increases, which promotes the aggregation of hydrophobic groups. We observed the same phenomenon and found that when ionic strength increases, the HPMC hydrogel was changing from transparent to opaque to turbid, and finally phase separation happened.

CONCLUSIONS

A two-stage mechanism for a typical Texture Analyzer force-distance profile collected from a homogeneous gel system was proposed. Based on this two-stage mechanism, a mathematic model for gel strength measurement using Texture Analyzer was constructed and validated for the first time. Through our model, the intrinsic gel

property that is independent of test conditions such as probe size can be determined. Optimal test conditions for gel strength measurements were also identified and applied to study model HPMC gel systems. A power-law relationship between gel strength and polymer concentration was observed for HPMC gels with all the viscosity grades studied and the exponent was found to be 3.8. The effect of four different excipients on the gel strength was studied. Among them, lactose did not have any effect, Avicel slightly increased the gel strength mainly due to space-filling effect, while both SDS and Starch 1500 increased the strength of HPMC gel significantly at all the HPMC/excipient ratios studied because both SDS and Starch 1500 are believed to increase the entanglement of HPMC chains. It was found that gel strength increased with ionic strength to a maximum and then started to drop. The understanding of fundamental information about Texture Analyzer data can provide us an opportunity to better characterize the swelling behavior of hydrophilic matrix and explore more valuable information for drug release, such as gel layer thickness and polymer concentration across the gel layer.

REFERENCES

Abrahamsson B., Johansson D., Torstensson A. and Wingstrand K. (1994). "Evaluation of solubilizers in the drug release testing of hydrophilic matrix extended-release tablets of felodipine." Pharmaceutical Research **11**(8): 1093-1097.

Alvarez-Lorenzo C., Duro R., Gomez-Amoza J. L., Martinez-Pacheco R., Souto C. and Concheiro A. (2001). "Influence of polymer structure on the rheological behavior of hydroxypropylmethylcellulose-sodium carboxymethyl cellulose dispersions." Colloid and Polymer Science **279**(11): 1045-1057.

Bonferoni M. C., Rossi S., Ferrari F., Bertoni M. and Caramella C. (1995). "Influence of medium on dissolution-erosion behaviour of Na carboxymethylcellulose and on viscoelastic properties of gels." International Journal of Pharmaceutics **117**: 41-48.

Colombo P., Bettini R., Massimo G., Catellani P. L., Santi P. and Peppas N. A. (1995). "Drug diffusion front movement is important in drug release control from swellable matrix tablets." Journal of Pharmaceutical Sciences **84**(8): 991-997.

Cunningham C . R. (1999). " Maize s tarch a nd super-disintegrants indirect c ompression formulation." Pharm. Manufac. Rev. **December**: 22-24.

Cutts L. S., Hibberd S., Adler J., Davis M. C. and Melia C. D. (1996). "Characterizing drug release processes within controlled release dosage form using the confocal laser scanning microscope." Journal of Controlled Release **42**(2): 115-124.

Daly P. B., Davis S. S. and Kennerley J. W. (1984). "The effect of anionic surfactants on the release of chlorpheniramine from a polymer matrix tablet." International Journal of Pharmaceutics **18**: 201-205.

Ferrari F., Bertoni M., Caramella C. and La Manna A. (1994). "Description and validation of an apparatus for gel strength measurements." International Journal of Pharmaceutics **109**(2): 115-124.

Ferrari F., Rossi S., Bonferoni M. C. and Caramella C. (2001). "Rheological and mechanical properties of pharmaceutical gels. Part I: Non-medicated systems." Bollettino Chimico Farmaceutica **140**(5): 329-336.

Friedman H. H., Whitney J. E. and Szczesniak A. S. (1963). "The texturometer: a new instrument for objective texture measurement." Journal of Food Science **28**(390-396).

Gao P. and Meury R. H. (1996). "Swelling of hydroxypropylmethylcellulose matrix tablets. 1. Characterization of swelling using a novel optical imaging method." Journal of Pharmaceutical Sciences **85**: 725-731.

Harland R. S., Gazzaniga A., Sangalli M. E., Colombo P. and Peppas N. A. (1988). "Drug/polymer matrix swelling and dissolution." Pharmaceutical Research **5**: 488-494.

Hegg P. O. (1982). "Conditions for the formation of heat-induced gels of some globular food proteins." Journal of Food Science **47**(4): 1241-1244.

Herman J. and Remon J. P. (1989a). "Modified starches as hydrophilic matrices for controlled oral delivery: II. In vitro drug release evaluation of thermally modified starches." International Journal of Pharmaceutics **56**: 65-70.

Herman J., Remon J. P. and De Wilder J. (1989b). "Modified starches as hydrophilic matrices for controlled oral delivery: I. Production and characterization of thermally modified starches." International Journal of Pharmaceutics **56**: 51-63.

Jamzad S., Tutunji L. and Fassihi R. (2005). "Analysis of macromolecular changes and drug release from hydrophilic matrix systems." International Journal of Pharmaceutics **292**(1-2): 75-85.

Jones D. S., Irwin C. R., Woolfson A. D., Djokic J. and Adams V. (1999). "Physicochemical characterization and preliminary in vivo efficacy of bioadhesive, semisolid formulations containing flurbiprofen for the treatment of gingivitis." Journal of Pharmaceutical Sciences **88**(6): 592-598.

Jones D. S., Lawlor M. S. and Woolfson A. D. (2002). "Examination of the flow rheological and textural properties of polymer gels composed of poly(methylvinylether-co-maleic anhydride) and poly(vinylpyrrolidone): rheological and mathematical interpretation of textural parameters." Journal of Pharmaceutical Sciences **91**(9): 2090-2101.

Jones D. S., Woolfson A. D. and Brown A. F. (1997). "Textural, viscoelastic, and mucoadhesive properties of gels composed of cellulose polymers." International Journal of Pharmaceutics **151**: 223-233.

Jones D. S., Woolfson A. D. and Djokic J. (1996). "Texture profile analysis of bioadhesive polymeric semisolids: mechanical characterization and investigation between formulation components." Journal of Applied Polymer Science **61**(12): 2229-2234.

Kawaguchi M., Shimomoto K., Shibata A. and Kato T. (1999). "Effect of anisotropy on viscous fingering patterns of polymer solutions in linear Hele-Shaw cells." Chaos:An Interdisciplinary Journal of Nonlinear Science **9**(2): 323-328.

Kim H. and Fassihi R. (1997). "Application of a binary polymer system in drug release rate m odulation. 1. Characterization of r elease mechanism." J ournal of P harmaceutical Sciences **86**(3): 316-322.

Lee P. I. (1980). "Diffusional release of a solute from a polymeric matrix. Approximate analytical solutions." J. Membrane Sci. **7**: 255-275.

Levina M. and Rajabi-Siahboomi A. R. (2004). "The influence of excipients on drug release from hydroxypropyl methycellulose matrices." Journal of Pharmaceutical Sciences **93**: 2746-2754.

Mannion R. O., Melia C. D., Mitchell J. R., Harding S. E. and Green A. P. (1991). "Effect of xanthan/locust bean gum synergy on ibuprofen release from hydrophilic matrix tablets." Journal of Pharm. Pharmacol. **43**: 78.

Melia C. D., Hodsdon A. C., Davis M. C. and Mitchell J. R. (1994). "Polymer concentration profiles o f the s urface gel layer of x anthan, a lginate a nd H PMC m atrix systems." Proceedings of the International Symposium on Controlled Release of Bioactive Materials. **21th**: 724-725.

Mitchell K., Ford J. L., Armstrong D. J., Elliott P. N. C., Rostron C. and Hogan J. E. (1990). "The influence of additives on the cloud point, disintegration and dissolution of hydroxypropyl methyl cellulose gels and matrix tablets." International Journal of Pharmaceutics **66**(1-3): 233-242.

Nakamura K., Shinoda E. and Tokita M. (2001). "The influence of compression velocity on strength and structure for gellan gels." Food Hydrocolloids **15**: 247-252.

Nilsson S. (1995). "Interactions between water-soluble cellulose derivatives and surfactants. 1. The HPMC/SDS/Water system." Macromolecules **28**: 7837-7844.

Papadimitriou E., Buckton G. and Efentakis M. (1993). "Probing the mechanism of swelling of hydroxypropylmethylcelloluse matrices." International Journal of Pharmaceutics **98**: 57-62.

Po A. L. W., Wong L. P. and Gilligan C. A. (1990). "Characterization of commercially available theophylline sustained- or controlled-release systems: *in-vitro* drug release profiles." International Journal of Pharmaceutics **66**(1-3): 111-130.

Pons M. and Fiszman S. M. (1996). "Instrumental texture profile analysis with particular reference to gelled systems." Journal of Texture Studies **27**: 597-624.

Rajabi-Siahboomi A. R., Bowtell R. W., Mansfield P., Henderson A., Davis M. C. and Melia C. D. (1994). "Structure and behavior in hydrophilic matrix sustained release dosage forms: 2. NMR imaging studies of dimensional changes in the gel layer and core of HPMC matrices undergoing hydration." Journal of Controlled Release **31**: 121-128.

Rubinstein M. and Colby R. H., Eds. (2003). Polymer Physics, Oxford University Press.

Shull K. R. (2002). "Contact mechanics and the adhesion of soft solids." Materials Science and Engineering: R: Reports **R36**(1): 1-45.

Szczesniak A. S. (1963). "Classification of Textural Characteristics." Journal of Food Science **28**: 385-389.

Talukdar M. M., Vinckier I., Moldenaers P. and Kinget R. (1996). "Rheological characterization of xanthan gum and hydroxypropyl methyl cellulose with respect to controlled-release drug delivery." Journal of Pharmaceutical Sciences **85**(5): 537-540.

Tang Q. N., McCarthy O. J. and Munro P. A. (1994). "Oscillatory rheological comparison of the gelling characteristics of egg-white, whey-protein concentrates, whey-protein isolate, and beta-lactoglobulin." J. Agric. Food Chem. **42**: 2126-2130.

Van Aerde P. and Remon J. P. (1988). "In vitro evaluation of modified starches as matrices for sustained release dosage forms." International Journal of Pharmaceutics **45**: 145-152.

Veith P. D. and Reynolds E. C. (2004). "Production of a high gel strength whey protein concentrate from cheese whey." J. Dairy Sci. **87**: 831-840.

Williams I II R. O., R eynolds T . D., C abelka T . D ., Sykora M . A. and Mahaguna V. (2002). "Investigation of excipient type and level on drug release from controlled release tablets containing HPMC." Pharmaceutical Development and Technology **7**(2): 181-193.

Yang L., Johnson B. and Fassihi R. (1998). "Determination of continuous changes in the gel layer thickness of poly(ethylene oxide) and HPMC tablets undergoing hydration: a texture analysis study." Pharmaceutical Research **15**(12): 1902-1906.

(a)

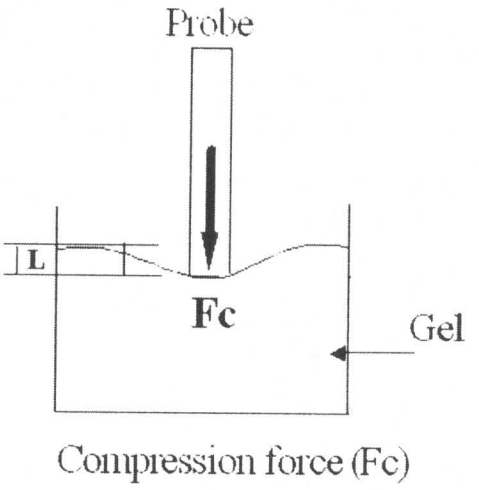

(b)

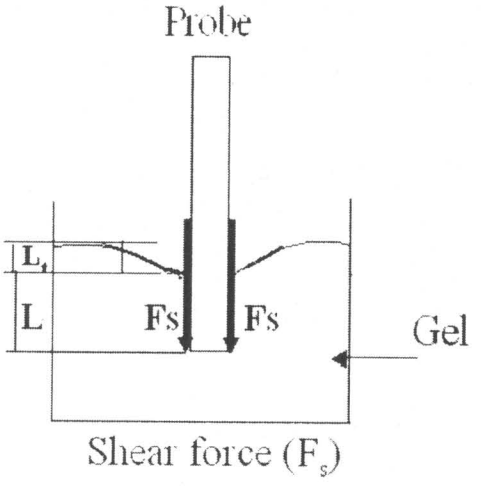

Figure II-1 Schematic representation of the two-stage mechanism model for a TA test: (a) stage of compression (before probe penetrates the gel); and (b) stage of shear (after probe penetrates the gel).

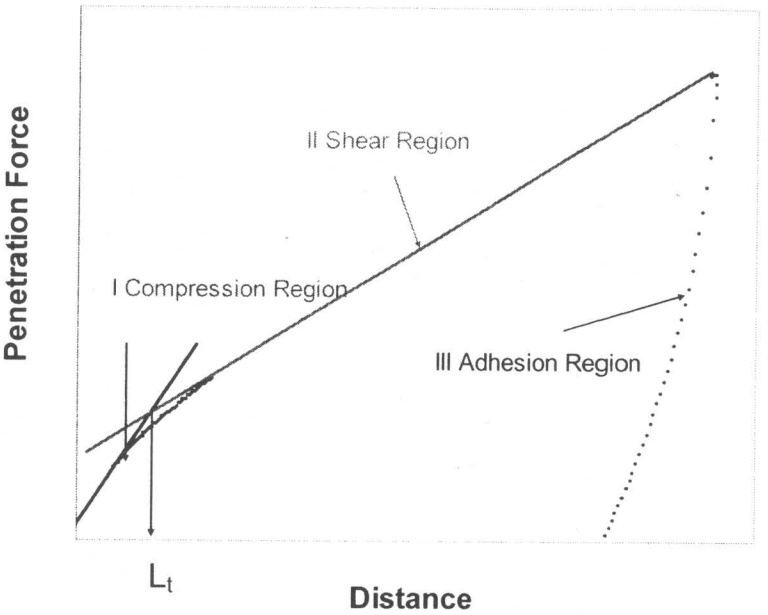

Figure II-2 Schematic representation of a typical force-displacement profile in the homogeneous gel at low speed range (<1mm/sec). L_t is the length of indentation prior to probe penetration. Compression region and shear region are shown in the profile as two straight lines, expressed as I and II, respectively. Region III is adhesive region which is not within the scope of our study.

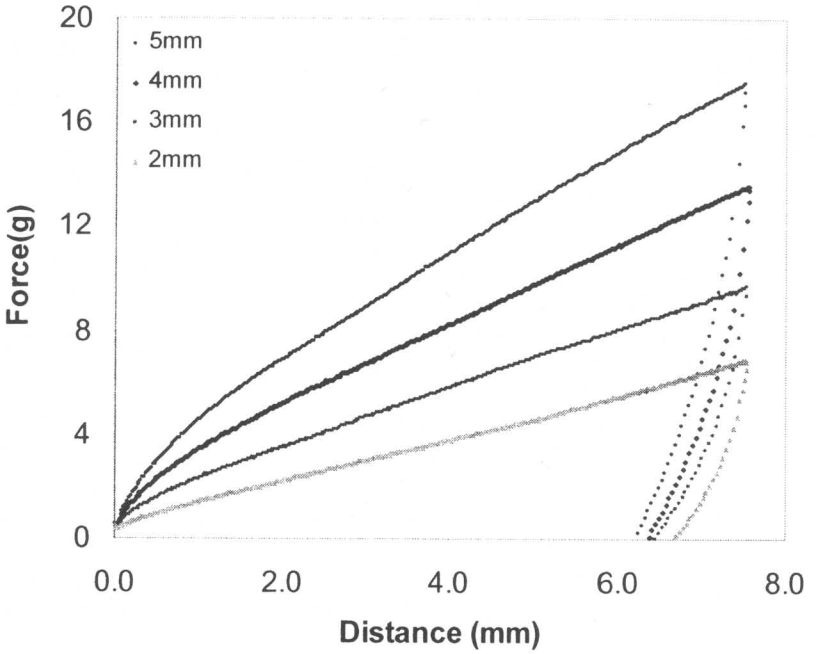

Figure II-3 The effect of probe size on the force-displacement curves for 10% w/w HPMC K15M gel: 2 mm (green), 3 mm (red), 4 mm (blue) and 5 mm (black). The probe speed used was 0.1 mm/sec.

(a)

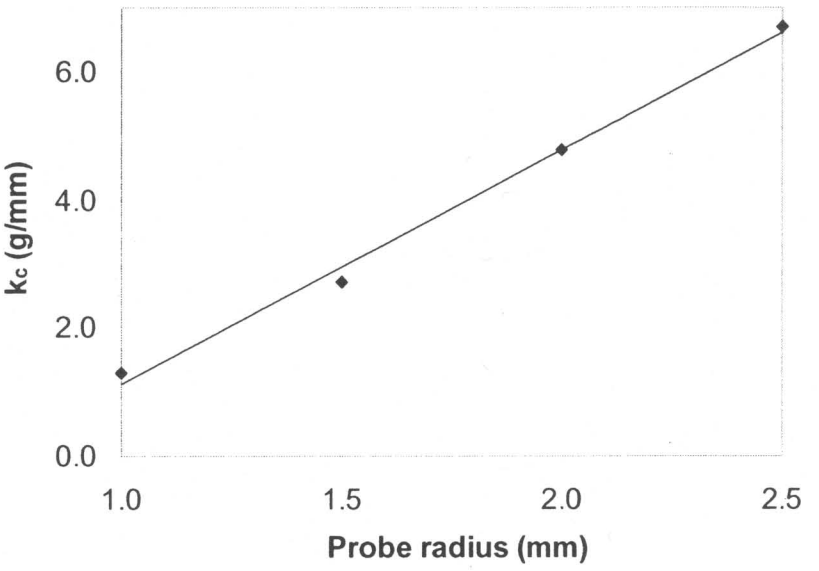

(b)

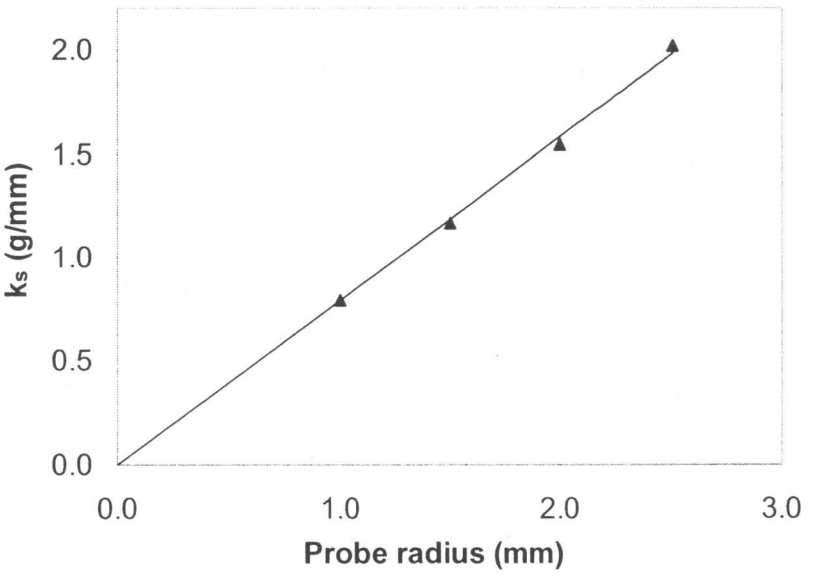

Figure II-4 The effect of probe radius on (a) slope from compression region, k_c; and (b) slope from shear region, k_s. The probes used were 2mm, 3mm, 4mm and 5mm in diameter. The probe speed was 0.1mm/sec and gel sample was 10% w/w HPMC K15M for all measurements.

(a)

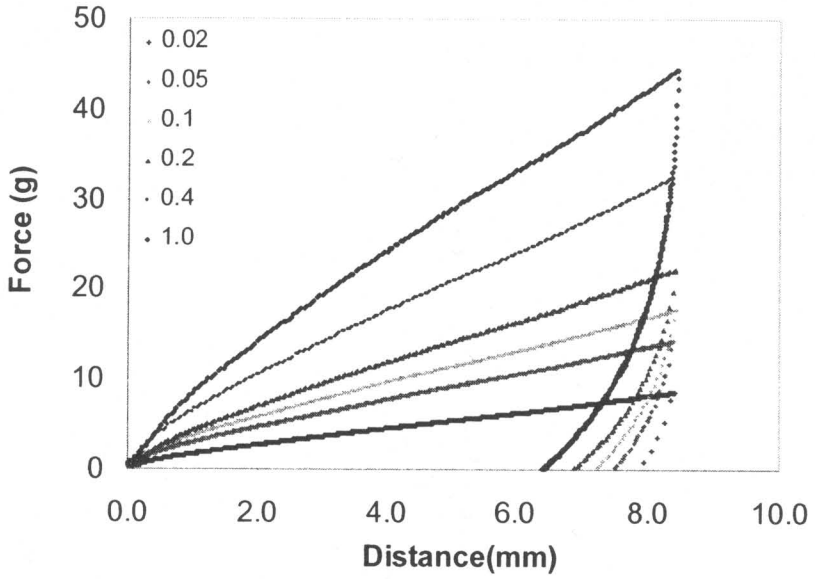

(b)

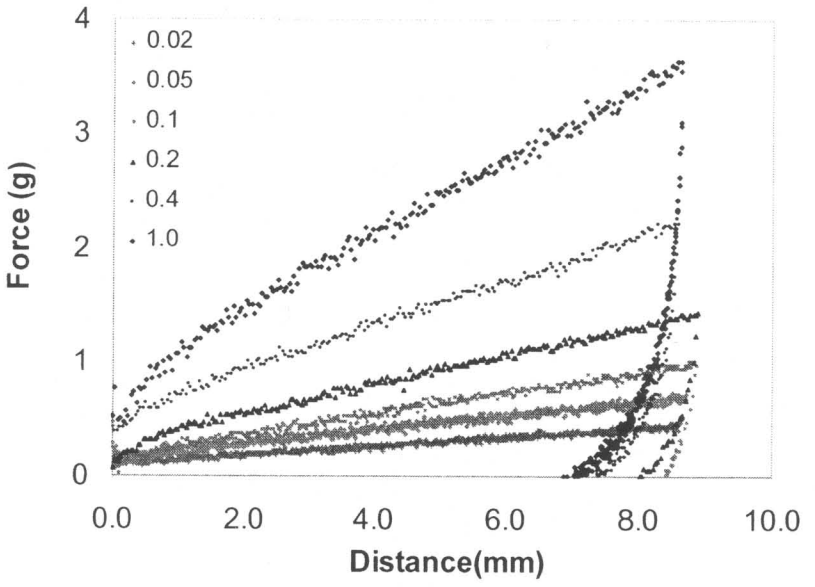

Figure II-5 The effect of probe speed on force-displacement curves in the range of 0.02 mm/sec to 1.0 mm/sec for (a) 10% (w/w) and (b) 5% (w/w) HPMC K15M. The probe size is 4mm in diameter for all measurements.

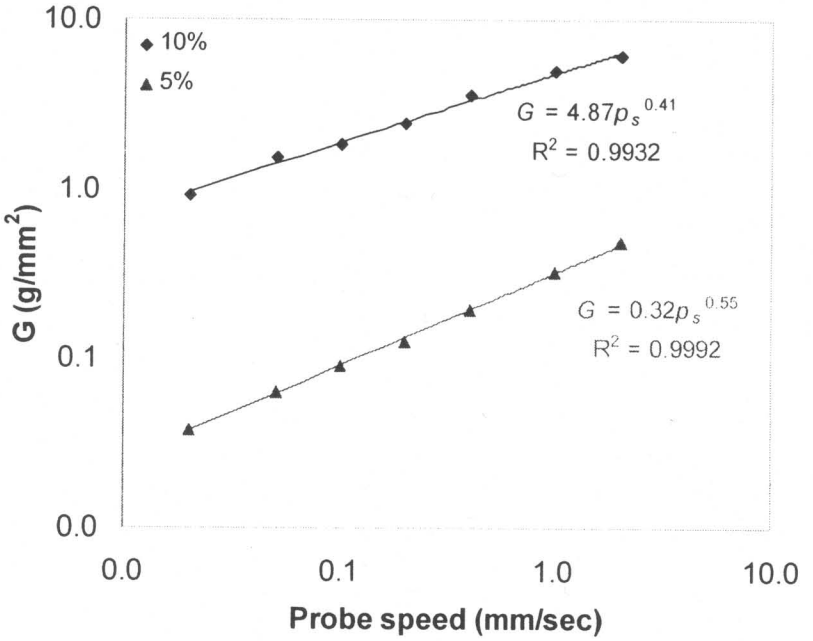

Figure II-6 The effect of probe speed on gel strength in the range of 0.02 mm/sec to 1.0 mm/sec. The probe size used was 4mm in diameter and the gel samples were 5% and 10% (w/w) HPMC K15M.

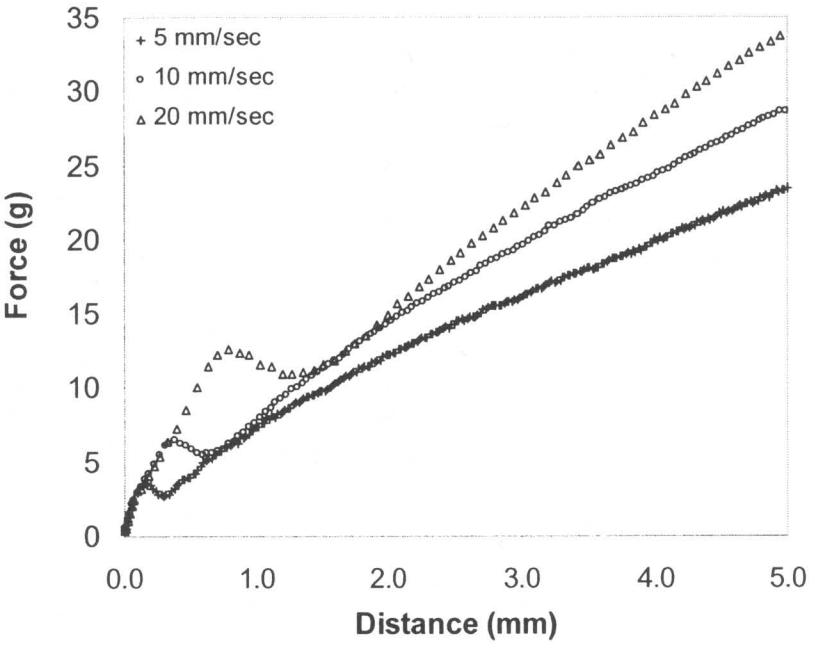

Figure II-7 The effect of probe speed on force-distance curve in high speed range (5.0 mm/sec to 20 mm/sec). The probe size is 4 mm in diameter and the gel sample is 10% (w/w) HPMC K15M.

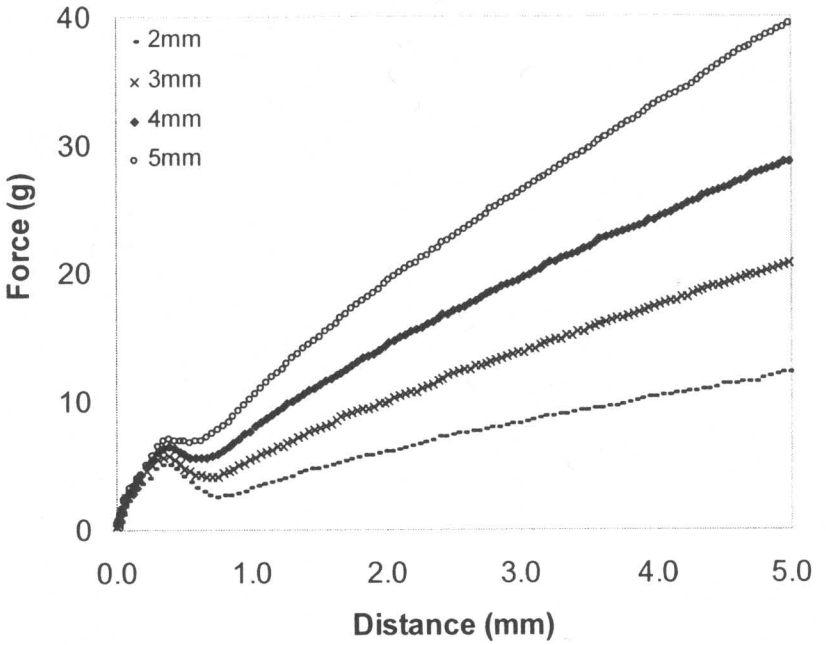

Figure II-8 The effect of probe size on force-displacement curves at high speed (10 mm/sec). The probe size was 2 mm, 3 mm, 4 mm and 5 mm in diameter and the gel sample is 10% (w/w) HPMC K15M.

(a)

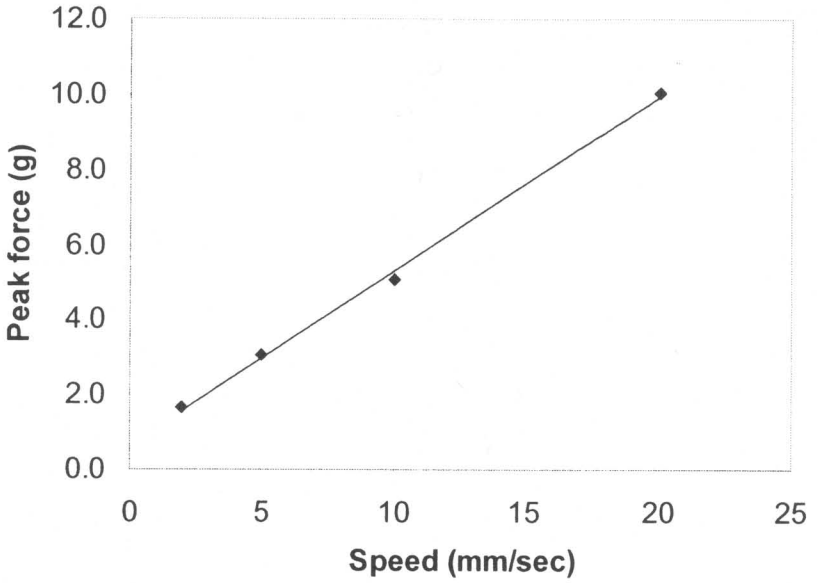

(b)

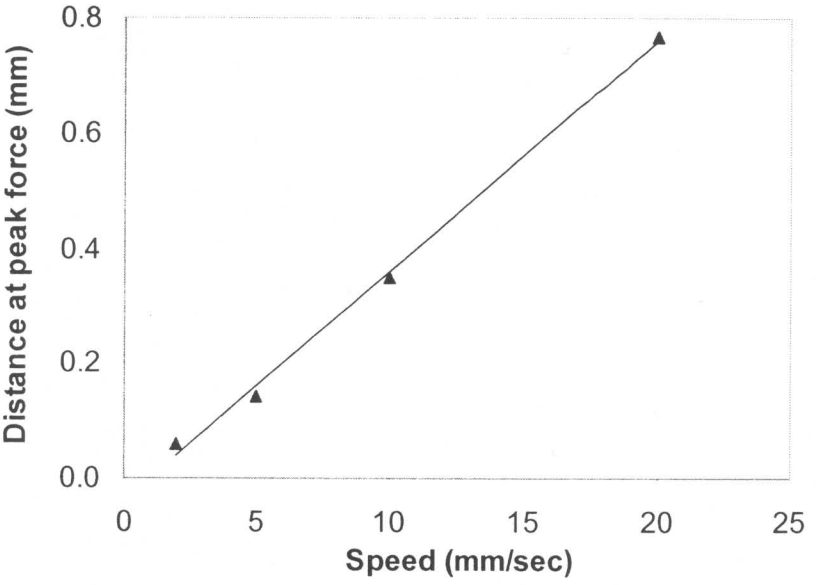

Figure II-9 Effect of probe speed on peak force (a) and distance at peak force (b) in high speed range (2.0 mm/sec to 20 mm/sec). The probe size is 4mm in diameter and the gel sample is 10% (w/w) HPMC K15M.

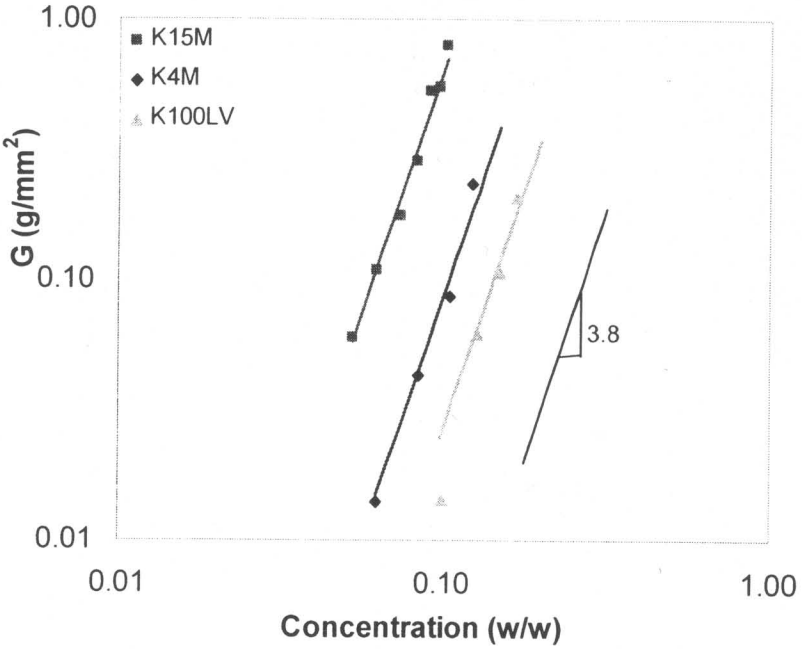

Figure II-10 Polymer concentration dependence of gel strength for HPMC as a function of molecular weight reflected as viscosity grade (K15M, K4M and K100LV) in log-log scale. The probe speed was 0.1 mm/sec and probe size was 2 mm for all the measurements.

(a)

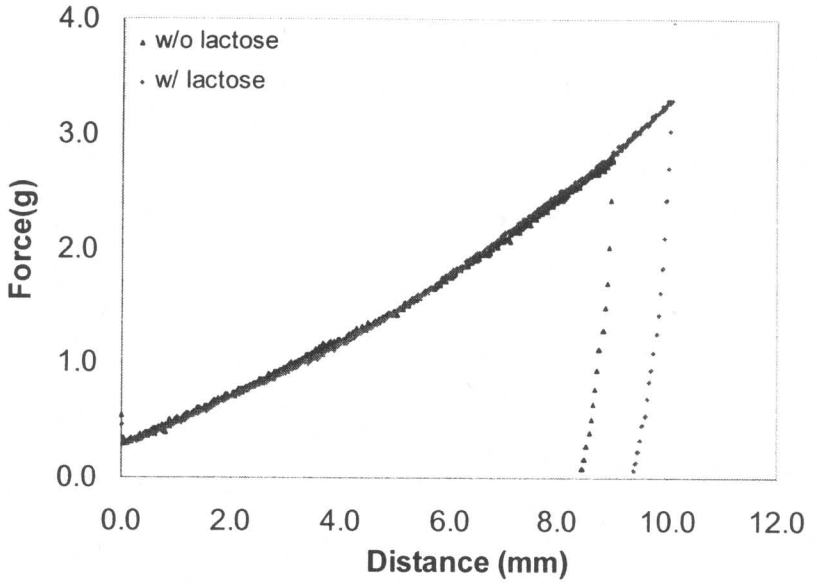

(b)

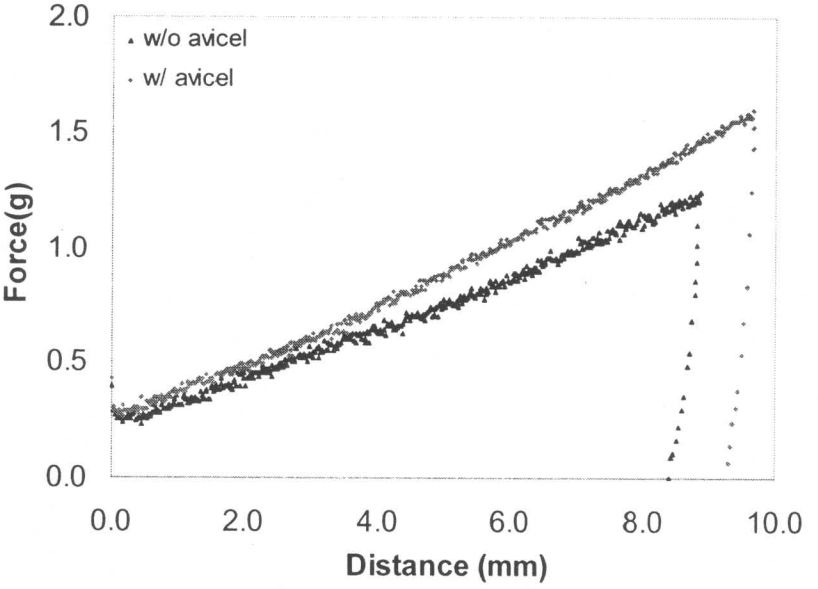

Figure II-11 Force distance profile comparison of HPMC K15M with different excipients (a) lactose (8%:8%) and (b) Avicel (6%:6%) w/w.

(a)

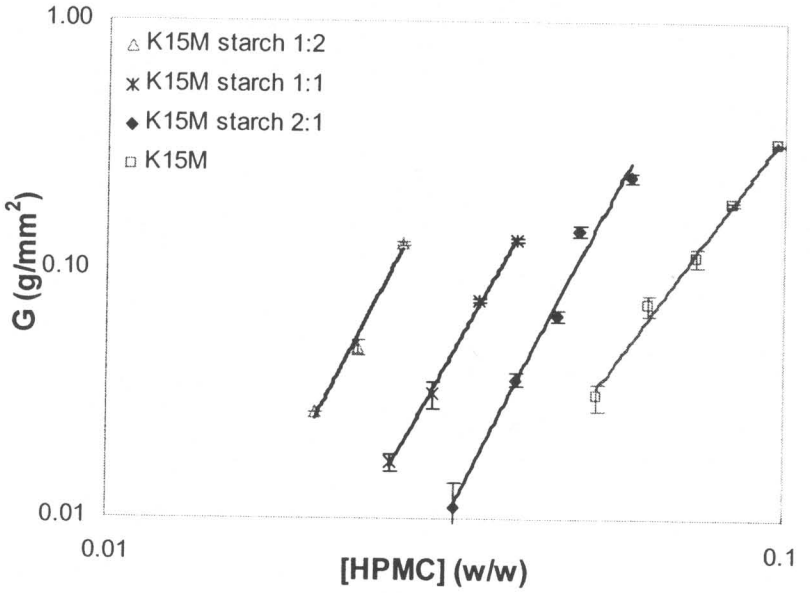

(b)

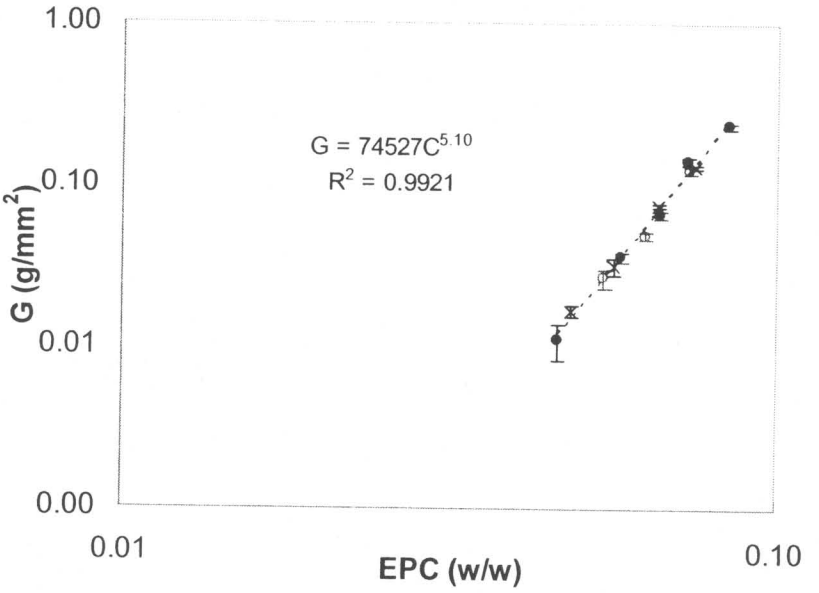

Figure II-12 Effect of Starch 1500 on HPMC gel strength.

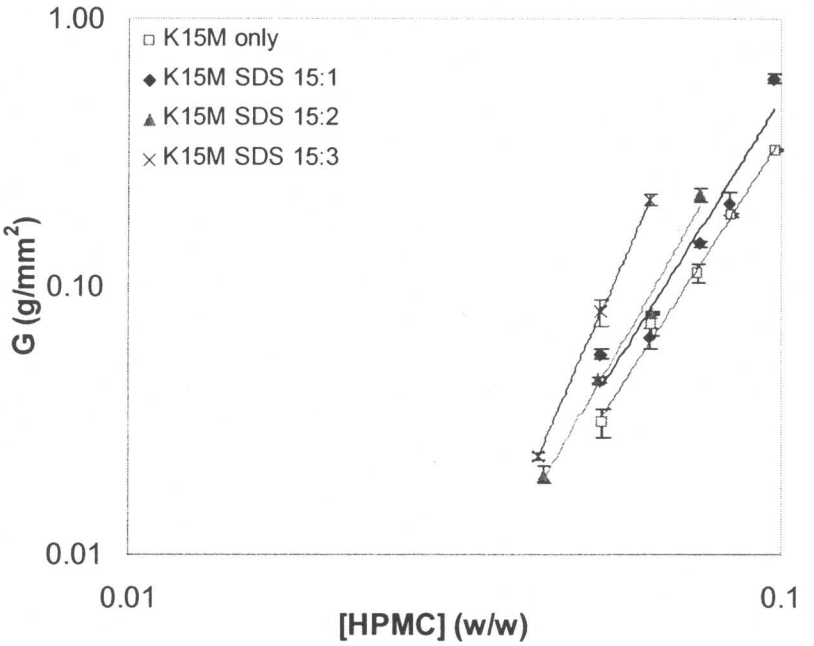

Figure II-13 Effect of SDS on HPMC gel strength at different ratios

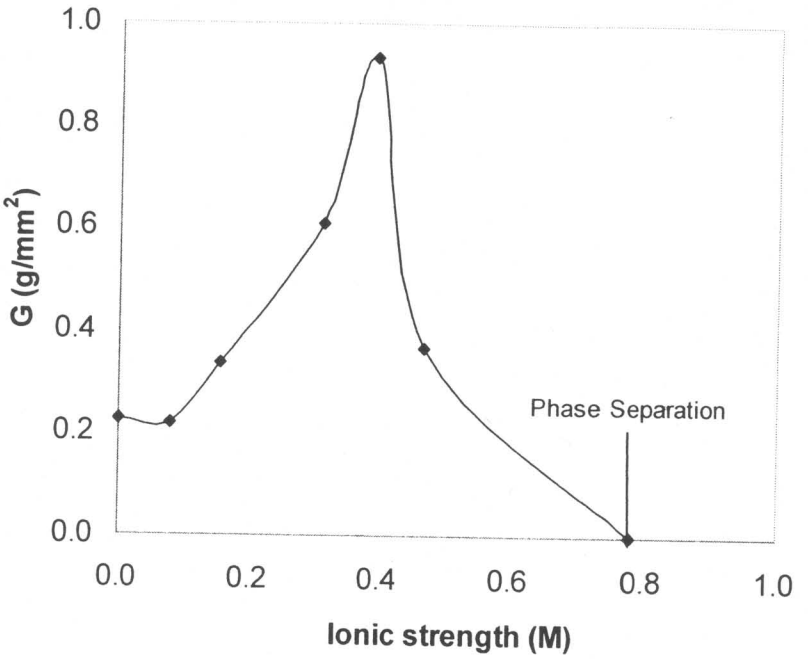

Figure II-14 Ionic strength effect on gel strength. The experiment was done on 8% w/w HPMC K15M gel sample with 2 mm probe and 0.1 mm/sec probe speed.

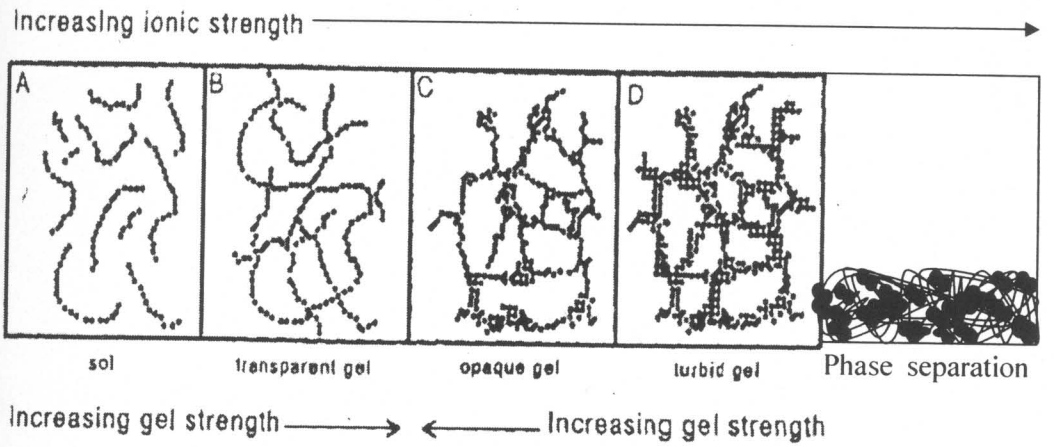

Figure II-15 A schematic representation of the gel structure change as a function of ionic strength

CHAPTER III Characterizing Swelling Behavior of HPMC Matrix Tablets Using Texture Analyzer

ABSTRACT

Purpose. The purpose of this study was using Texture Analyzer to delineate the structure of hydrating HPMC tablets, to determine the profiles of gel strength, gel layer thickness, swollen glassy layer thickness and polymer concentration across the gel layer and to study the effects of polymer viscosity grades and excipients on the swelling of HPMC tablets. ***Methods.*** Texture Analyzer was employed to measure the gel strength across the gel layer at different swelling times. ***Results.*** The profiles of force-distance, gel strength, gel layer, swollen glassy layer thickness and polymer concentration across the gel layer at different swelling times were determined and the results were comparable to those obtained using other techniques such as NMR imaging, Cryogenic-SEM and light scattering imaging. The gel layer thickness increased linearly with the square root of swelling time indicating diffusion-controlled mechanism. The gel layer thickness of high viscosity grade HPMC developed faster. Addition of Starch 1500 to HPMC matrices significantly enhanced strength of swelling gels without changing the thickness of gel layer while lactose has no impact on either gel strength or gel layer thickness. ***Conclusions.*** Texture Analyzer was demonstrated to be a convenient and accurate characterization tool for swelling hydrophilic matrices. Detailed structure and dynamics of swelling matrices were determined. Gel strength rather than gel layer thickness might be responsible for excipient effects on drug release from HPMC matrices.

Key Words: Texture Analyzer; gel strength; gel layer thickness; HPMC; swelling tablets

INTRODUCTION

Hydrophilic matrices are widely used as oral extended-release dosage forms, which are often termed as swellable matrix tablets. Upon contact with aqueous media, polymers in the dosage form hydrate to form a viscous mucilaginous gel layer (Melia 1991), a diffusional barrier that retards further ingress of water and acts as a rate-controlling barrier to drug release. The tablet core remains dry when water molecules have not penetrated yet, and serves as a reservoir of drug and of polymer that replenishes the surface gel layer as it dissolves or is eroded. As water molecules diffuse inward, polymers in the dry core hydrate and swell and drug molecules dissolve and diffuse through the gel layer. It is well recognized that drug release from hydrophilic matrices occurs via a combination of diffusion through the gel layer and erosion of the outer gel surface (Narasimhan 1997; Siepmann 1999a). Correspondingly, drug release is controlled by the properties of the gel layer, the solubility of the drug, and the degree of mechanical attrition to which the dosage form is subjected (Melia 1991). Therefore, gaining insight into swelling behavior of hydrophilic matrices, especially the structure of a swelling tablet, gel layer thickness, gel strength and polymer concentration across the gel layer is critical for understanding drug release mechanisms and predicting drug release behaviors.

The gel layer thickness has been considered as one of the key parameters affecting drug release from the swelling-controlled matrix system. Continuous increase in gel thickness of the rate-controlling polymer will lead to declining release rates irrespective of the system geometry, while it is argued that maintenance of constant gel layer thickness might produce zero-order release kinetics from a planar surface (Lee 1980; Harland 1988). It has also been demonstrated that the profile of gel layer thickness versus time consists of three stages: 1) initial increase due to polymer swelling; 2) maintenance of constant gel-

layer thickness between the swelling and dissolution fronts, often referred to as front synchronization; 3) reduction in gel-layer thickness as the glassy core is depleted (Peppas 1994).

Studies using cryogenic scanning electron microscopy (Cryo-SEM)(Melia 1994) and other techniques (Gao 1996a; Rajabi-Siahboomi 1996) have shown that a polymer/water concentration profile exists in the gel layer. Such concentration gradients in the gel layer are very important for understanding the drug release mechanism, because it was well recognized that the both water and drug diffusion constants were polymer/water concentration dependent following a Fujita-type (Fujita 1961) exponential relationship according to the free volume theory of diffusion. Such relationship between diffusion and water concentration was often used in mathematical modeling of drug release from a swelling tablet (Siepmann 1999b; Siepmann 2002). Therefore, knowing the polymer concentration profile in the gel layer will provide more insights to the understanding and modeling of drug release from a polymeric matrix.

Gel strength was also proposed to affect the drug release mainly by regulating the dissolution of polymeric matrix at the interface between the gel and the dissolution medium(Bonferoni 1992). A good agreement was shown between the strength of HPMC gels and their erosion rates (Bonferoni 1995).

The investigation of matrix swelling behavior generally involves the determination of front movement during the dissolution process, from which gel layer thickness and core dimensional changes are calculated. Optical microscopy has been widely used to detect the movement of water advancing front based on the significant change in the refractive index at the interface of polymer gel and glassy core (Tu 1977; Colombo 1993; Papadimitriou 1993; Kim 1997). However, int ermediate regions and polymeric domains t hat do not

contain sufficient amount of water to affect the optical properties may not be distinguishable by this method. Another drawback of this method is that they did not provide any composition information across the gel layer.

Cutts *et al.* (Cutts 1996) developed a non-invasive method using the confocal laser scanning microscope (CLSM). A dye was added into the swelling solution, and this solution marker fluoresces strongly in the presence of hydrated HPMC and cellulose, and the bright areas of the image therefore represent the gel layer. This method enabled the authors to obtain a time series of images and dynamic gel layer thickness evolution with time for HPMC tablets.

Gao *et al.* (Gao 1995a; Gao 1996a) developed an optical image analysis method based on light scattering to examine the dynamic swelling behavior of HPMC-based matrix tablets. They found that the intensity of light scattered from HPMC gels depends on polymer concentration. A mathematical model was derived to describe the relationship between the scattered light intensity and HPMC concentration by assuming the turbidity of the gel is an exponential function of polymer concentration. This method was able to not only determine the gel layer thickness, but also semi-quantitatively estimate the HPMC concentration profile across the gel layer. However, when HPMC concentration is higher than 50%, the results given were no longer reliable.

Nuclear magnetic resonance imaging (NMRI) has been used to study the formation of the gel layer in hydrated tablets (Rajabi-Siahboomi 1994). In order to obtain quantitative information from NMR imaging, Fyfe and Blazek (Fyfe 1997; Fyfe 2000) first studied how NMR relaxation parameters and self-diffusion were affected by the polymer concentration using equilibrium HPMC-water mixtures. Then the HPMC

concentration across the gel layer at each time in swelling process was determined indirectly from its effect on the relaxation parameters of the water.

All of the above techniques are sophisticated, often time consuming and difficult to perform, despite their high accuracy and precision. Furthermore, no single technique is capable of extracting all the critical information from a swelling matrix. For example, no information about gel strength (an important parameter in drug release) can be obtained from any of the techniques above. As a consequence, developing a technique that is user-friendly, reliable, and capable of characterizing swelling behavior of a hydrophilic matrix on a routine basis is highly desirable to formulation scientists.

Recently, a laboratory scale Texture Analyzer (TA) has been investigated to study the swelling process of poly (ethylene oxide) and HPMC tablets undergoing hydration by Libo Yang and other researchers (Yang 1998). The force necessary for penetration of a cylindrical probe into the swelling tablet is measured precisely. The slope of the force-distance profile was used as a qualitative indication of gel strength and polymer concentration profile within the swollen region by assuming a linear relationship between gel strength and polymer concentration. Based on the approximation of force-distance slope to infinity, the interface between glassy core and rubbery gel was determined. The gel layer thickness was obtained by calculating the difference between the maximum penetration distance of the swollen and the dry tablets at different stages of hydration. Their method might be useful to determine the gel layer thickness, but not accurate enough to determine the polymer concentration profile across the gel layer because of the power-law instead of linear relationship between gel strength and polymer concentration, as shown in Chapter II.

The work in Chapter II provided a rigorous theoretical basis and mathematical models for the interpretation of TA data in homogenous gel systems. Based on that, a new approach to characterize the swelling behavior of hydrophilic matrix tablets using TA was developed in this chapter. As a result, gel layer thickness, swollen glassy layer thickness, gel strength and polymer concentration profiles across the gel layer could be delineated. The effects of polymer viscosity grade and excipient type on the swelling of dry tablets were also studied. Hydroxypropyl methylcellulose (HPMC), a commonly used hydrophilic polymer in oral controlled dosage forms, is the model polymer used in this study.

MATERIALS AND METHODS

Materials

METHOCEL®, commercially available hydroxypropylmethyl cellulose (HPMC) with four viscosity grades, K100M, K15M, K4M and K100LV were the same as those used in Chapter II. Spray dried lactose monohydrate and Starch® 1500 were obtained from Fast-Flo and Colorcon, respectively. 0.05 M phosphate buffer (pH 6.8) was used in swelling experiments

Sample Preparation

The tablets containing 100% hydroxypropylmethylcellulose (Methocel™, K15M, Dow Chemical Company) were prepared using a reciprocating tabletting machine (model EKO, Korsch, Berlin, Germany), equipped with a flat-faced punch of 1.0 cm diameter, in order to manufacture tablets weighing 0.3 g with a thickness of 4.0 mm. The tablets containing 40% HPMC K15M and 60% (w/w) lactose monohydrate (Fast-Flo®) or 40% HPMC 15M and 60% (w/w) Starch® 1500 (Colorcon) were prepared by first mixing the

ingredients in a blender and then compressing the mixtures using the same machine under the same conditions.

One-dimensional Swelling Experiment

One planar base of the tablet was covered with organic coating (14.0 g Eudragit® RS in the mixture of 50 mL acetone and 50 mL isopropanol) impermeable to water in order to prevent deformation during the determination of the glass/gel interface, and the tablet was subsequently glued to the bottom of a glass vial with the same diameter as that of the tablet to provide one dimensional swelling. The samples prepared in this manner were then placed in 0.05 M phosphate buffer (pH=6.8) at room temperature. The swelling tablets were carefully taken out at predetermined time intervals for texture analysis.

Texture Analyzer Profiling

The TA.XT Plus Texture Analyzer (Texture Technologies Corp., Stable Micro Systems, Algonquin, IL, U.S.A.) instrument is a microprocessor-controlled texture analysis system that measures the profiles of stress-strain behavior for samples under test. It consists of an analyzer and a personal computer equipped with Texture Exponent 32 software that automates data acquisition and analysis. The motion of the probe is controlled by a stepping motor that records the displacement up to the accuracy of 1μm.

During the test, a sample was positioned in the center of the testing platform. A flat-tipped, round steel probe of 2mm in diameter and 30mm in length was used in this study. The probe traveled at fixed speed (0.2mm/sec) until the surface of the matrix was detected at 0.04 g of force (threshold value for triggering the Texture Analyzer). At this point the data acquisition started and the probe proceeded downward and through the samples at a pre-determined speed of 0.1mm/sec. The motion of the probe continued until

the measured force reached a predetermined limit where the probe was automatically withdrawn at 0.2mm/sec and test stopped when the probe returned to its start position. The predetermined force was established in such a manner that it could differentiate the swollen glassy polymer from the dry core. This force was optimally determined to be 6000 gram. Data were collected at a rate of 10 points per second by Texture Expert™ software for further analysis. Three tablets were run at each swelling time point.

RESULTS AND DISCUSSION

1. Theory

Our previous work on homogeneous gels showed that accumulated shear force is the dominant force after the probe penetrates inside the gel, which is expressed as.

$$F_s = Gr_p L \qquad \text{Equation III-1}$$

here, F_s is the shear force experienced by the probe in a direction parallel to the probe penetration, r_p is the radius of the probe, G is the gel strength which is the slope of force over distance when 2mm probe is used, and L is the penetration depth of the probe. For swelling tablets, the presence of a polymer concentration gradient within the tablet is expected to render a corresponding gel strength gradient. We assume the x-axis is the direction of the probe movement and the origin of x=0 is at the gel-solution interface. For a swelling matrix where gel strength G varies with position, $G(x)$, the force measured by Texture Analyzer, $F(x)$, can be expressed as:

$$F(x) \approx F_s(x) = r_p \int_0^x G(x)dx \qquad \text{Equation III-2}$$

where x is the penetration depth of the probe. As such, gel strength at any position x can be derived from the force-distance profile by taking the first derivative as

$$\frac{dF(x)}{dx} = r_p G(x) \qquad \text{Equation III-3}$$

In addition, a power-law relationship between gel strength and polymer concentration ($G = kC_p^{\ n}$) was established. Therefore, polymer concentration in the gel layer can be related to gel strength as:

$$C_p = 10^{\frac{1}{n}(\log G - \log K)} \qquad \text{Equation III-4}$$

Both k and n are constants that can be determined from homogeneous gel systems.

2. Applications

2.1. Characterization of Pure HPMC Tablets Swelling at Fixed Hydration Time

2.1a. Force-distance Profile of HPMC K15M Tablets at Two Hours Hydration

Figure III-1 shows a typical force-distance profile of tablets containing 100% HPMC K15M at two hours hydration in 0.05 M phosphate buffer. As shown in the figure, the resistance force encountered by the probe is a strong function of the traveled distance. Low resistance was recorded near the periphery of the matrix (i.e., low initial force detected) and the force monotonically increased as the probe approached toward the tablet core. Similar profiles were also reported for HPMC tablets undergoing hydration elsewhere (Yang 1998; Durig 2002). As indicated by NMR studies (Rajabi-Siahboomi 1996), the polymer concentration is negligible at the outer edge of the swelling tablet and reaches its maximum at the glassy front. Thus, outer regions were characterized by low gel strength and low resistance to penetration, while inner and less hydrated regions have denser gels requiring greater forces for penetration.

2.1b. Gel Strength Profile and Structure of Swelling Tablets Determination

The corresponding gel strength profile at two hours was derived from a force-distance profile using Equation III-3 and shown in Figure III-2 (a). To reduce the noise, especially at low gel strength region, the gel strength data was further treated by averaging five points in Figure III-2 (a) and plotted in Figure III-2 (b) with same trend but less noise. The spatial resolution was 50μm after the treatment of averaging. Three distinct regions are observed. Previously, a three-layer structure was reported by Melia *et al.* (Melia 1992), which are gel layer, swollen glassy layer and dry glassy core. Later, a four-layer structure was proposed by Ju *et al.* (Ju 1995a). In addition to the three layers reported by Melia, a polymer diffusion layer was proposed between gel layer and bulk solution. Polymer diffusion layer is a highly hydrated layer and thus does not present a major barrier for probe penetration. We do not expect it will be detected by the probe penetration using Texture Analyzer. The gel layer exhibits adequate gel strength and its presence is represented by the first monotonic increase of gel strength in the profile. The region next to the gel layer is the swollen glassy layer, which is partially hydrated and is represented as the second region of the gel strength profile. The innermost region is the dry glassy core, an anhydrate region, represented by the plateau after the swollen glassy layer.

We recognized that so far most models dealing with polymer swelling assumed a two-layer structure (gel layer and glassy layer) and a glassy-rubbery interface as the boundary beyond which solvent molecules did not penetrate further into the inner part of the matrix. However, Ueberreiter (Ueberreiter 1968) pointed out that solvent concentration did not decrease to zero beyond the glassy-rubbery interface. A glassy polymer contains a great number of channels and holes of molecular dimensions and the first penetrating solvent molecules filled the voids so that the subsequent glassy-rubbery

transition was achieved. Ueberreiter's proposal was consistent with the porosity of 0.1 found for tablets made of HPMC(Ju 1995b). It was also demonstrated by Rutherford backscattering spectrometry (Hui 1987) that the water penetration front preceded the phase transition front during the swelling process of polymer. A swollen glassy layer was thus suggested by Ueberreiter as part of the structure and later adopted by Ju *et al.* (Ju 1995a) and supported by Melia *et al.* in HPMC matrices using scanning electron microscopy (Melia 1992). This partially hydrated layer is clearly shown in Figure III-2.

2.1c. Polymer Concentration Profile

We previously identified a power-law relationship between gel strength measured by Texture Analyzer and polymer concentration (C_p). Based on Equation III-5, polymer concentration across the swelling tablet was calculated and shown in Figure III-3. A linear polymer concentration gradient was observed within the gel layer. Such linearity relationship was assumed in many models dealing with polymer swelling and drug release to simplify the mathematical treatment (Lee 1987; Harland 1988) and also verified by numerical calculations (Narasimhan 1996). Our data, for the first time, supports this pseudo-steady state assumption. The polymer concentration at the gel/swollen glassy interface was estimated as approximately 0.4 w/w, which is in good agreement with the results from slicing and weighing method(Melia 1994), light scattering imaging(Gao 1996a), and NMR imaging(Melia 1994; Gao 1996a; Fyfe 1997; Baumgartner 2005). We are encouraged by the agreement and it further validates the model we developed and demonstrates that Texture Analyzer can be a proper tool obtaining polymer concentration profiles across the gel. It is worthwhile to point out that this polymer concentration at gel/glass transition is much lower than the theoretical prediction based on free volume theory and the results from thermodynamic experiment (Hancock 1994). This difference

indicates that the system does not reach the thermodynamic equilibrium at the gel/glass interface; therefore more water content was needed for the gel/glass transition to take place. In addition, the initial gel concentration (x=0) is around 10% w/w that represents the concentration limit detectable by TA. In our method, one relationship between gel strength and polymer concentration has to be assumed and this relationship can be established by measuring the gel strength of homogenous gel at different concentrations. For most HPMC gels, because the homogenous gel at high polymer concentration could not be practically prepared, the power-law relationship between gel strength and polymer concentration was established in low concentrations and extrapolated to high concentrations. The agreement of polymer concentration at the gel/glass interface between our study and the studies using other techniques demonstrated the validity of this assumption.

2.2. Evolution of Pure HPMC Tablets Swelling

2.2a. Force-distance Profiles

Force distance profile at different hydration stages were depicted in Figure III-4 (1.0, 2.0, 4.0, 6.0, 8.0, 12.0 and 18.0 hours). The gradient of the force-distance curves specifically in the region below 200 grams progressively decreased with the time of hydration, showing the evolution of swelling gel. As expected, prolonged swelling time resulted in longer penetration distance. However, detailed structural information of swelling tablets cannot be extracted from the force-distance profile directly.

2.2b. Gel Strength Profiles

Gel strength profiles at different hydration stages were shown in Figure III-5 (1.0, 2.0, 4.0, 6.0, 8.0, 12.0 and 18.0 hours). Similar pattern of profile was observed at all

hydration times. The transition, however, between gel layer and swollen glassy layer became smoother and smoother. The gel strength at transition decreased with time of hydration. The reason is not clear and might be also due to that the polymer chains were not at thermodynamic equilibrium state at transition points. The same phenomenon was observed in polymer concentration profile and data is not shown here.

2.2c. Evolution of Matrix Structure: Gel Layer and Swollen Glassy Layer Thickness.

Information regarding the detailed and time-dependent structure of a gelled matrix is key to understand swelling and therefore drug release kinetics. As shown in Figure III-2 , a swollen matrix is identified as consisting of three regions: the gel layer, the swollen glassy layer and the dry glassy core. Thickness for the gel layer and swollen glassy layer are defined here by the outer surface of the swelling tablet, the gel/swollen glassy layer interface and water penetration front (swollen glassy/dry glassy core interface). Figure III-6(a) shows the increase in gel layer thickness versus time for tablets containing 100% HPMC K15M. Two distinct gel growth phases can be readily identified. An initial, rapid growth in gel thickness occurs at early times ($t \leq 4$ hours), followed by continuous but relatively slow advancement. Our experimental observation of the two-phase gel layer growth agrees with the theoretical work in three-dimensional swelling experiments of polymer matrices of radially symmetric geometries by Ju *et al.* (Ju 1995b). In their work, a third stage with an acceleration of gel growth that results from the merging of the water penetration fronts in the center of the tablets was also proposed. In our one-dimensional swelling experiments, however, this third stage was not observed due to the slower swelling rate and limited time window investigated. The similar profile and the lack of front synchronization over the time period studied has also been found by other researchers using NMR microscopy(Baumgartner 2005), optical microscopy (Pham 1994;

Baumgartner 2005) and optical imaging method (Pham 1994; Gao 1996b; Yang 1998). It is well known that the growth of hydrophilic polymer gel depends on the swelling rate at the water penetration front and erosion rate at the outer surface of the gel. However, gel erosion often lags behind since the polymer concentration has to reach a threshold value before erosion or disentanglement occurs, which results in a rapid buildup in gel layer thickness during the initial swelling period. On the other hand, as the rate of solvent penetration is slowed down sufficiently by the increasing diffusional distance while polymer chain disentanglement progresses steadily, the rate of gel layer thickness buildup slows down as shown in Figure III-6. The continuous buildup of gel layer thickness as reported in Figure III-6 suggests the polymer chain disentanglement in HPMC K15M is quite slow.

Many mathematic models were proposed to predict the gel layer thickness profile during the tablet swelling, and most of them have to be solved numerically. Lee and Peppas (Lee 1987) proposed a model that gave an analytical solution of gel layer thickness as a function of time.

$$\delta \approx \sqrt{\frac{2(1+C_p^*)(1-C_p^*-C_{p,eq})D_w t}{C_p^*}} \qquad \text{Equation III-5}$$

where δ is the gel layer thickness, D_w is the water diffusion constant. C_p^* and $C_{p,eq}$ are the polymer concentration at the interfaces of gel/glass and gel/solvent, respectively.

In their model, two major assumptions were used. First, pseudo-steady state assumption, which assumes that polymer concentration gradient across the gel layer is linear; second, a constant diffusion coefficient of water was assumed, which means the water diffusion coefficient does not depend on the polymer concentration. The first

assumption seemed to be valid based on our result shown in Figure III-3. But the second assumption is questionable since the water diffusion coefficient was found to be dependent on the polymer concentration (Fujita 1961; Katzhendler, I. 1997). Many models were later developed using polymer concentration dependent diffusion coefficient (Siepmann 1999a; Siepmann 2000; Siepmann 2001; Siepmann 2002), but the differential equations could not be solved analytically. In order to avoid complex numerical calculations while still gain some insight into polymer swelling in molecular level, we propose to use an average diffusion constant.

Fujita-type (Fujita 1961) exponential relationship between water diffusion constant and polymer concentration was assumed according to the free volume theory of diffusion:

$$D_w = D_{w,eq} \exp\left[-k_w\left(1-\frac{C_w}{C_{w,eq}}\right)\right] \qquad \text{Equation III-6}$$

where k_w is constant characterizing this concentration-dependence of water diffusion in polymer. $D_{w,eq}$ and $C_{w,eq}$ are the water diffusion constant and concentration at the interface of gel/solvent, respectively. As shown in Figure III-3, a linear relationship between polymer/water concentration and the distance from the gel/solvent interface can be assumed, so

$$C_w(x) = C_{w,eq} + \frac{C_w^* - C_{w,eq}}{\delta} x \qquad \text{Equation III-7}$$

where C_w^* is the water concentration at gel/glass interface. Therefore, the average diffusion constant of water in gel layer is

$$\langle D_w \rangle = \frac{\int D_w(x) x dx}{\int x dx} \qquad \text{Equation III-8}$$

where x is the coordinate in one dimensional swelling originating at the interface of gel/solvent. The integration results are the following:

$$\langle D_w \rangle = \frac{2D_{w,eq}}{\beta^2}\left[1-(\beta+1)\exp(-\beta)\right] \qquad \text{Equation III-9}$$

where

$$\beta = k_w\left(1-\frac{C_w^*}{C_{w,eq}}\right) \qquad \text{Equation III-10}$$

As we can see, the average diffusion constant is independent on gel thickness or the swelling time, so the diffusion constant used in Equation III-5 can be replaced by the average diffusion constant.

Based on Equation III-5, the gel layer thickness was linear to the square root of time, which is verified by our swelling data of HPMC K15M tablets shown in Figure III-6(b). From the slope in the figure we can calculate the average diffusion constant of water in HPMC gel and water concentration at gel/solvent interface was obtained from the literature (Ju 1995a). The k_w for different HPMC was also obtained from literature (Katzhendler, Ifat 2000). The result was shown in Table III-1.

Swollen glassy layer thickness tells about the rate of solvent front penetration into the polymer, which is important to understand swelling kinetics. However, this information is not readily available due to the lack of proper techniques to detect the water penetration front. The interface between the glassy core and rubbery gel in

pharmaceutical matrices have been detected either by optical method, which relies on the different optical characteristics of the swollen gel and glassy polymer or alternatively, NRM techniques which measures the magnetic resonance signal intensity of H^1 due to the presence of water at the phase transition front. However, these techniques are not able to detect the interface between the swollen glassy layer and dry core due to the detection limits. In previous Texture Analyzer work, the author demonstrated that they were able to detect the interface between the swollen glassy layer and dry core where the slope of force-distance profile went to infinity. In the present work, the swollen glassy/dry glassy core interface could be detected by the accurate measurement of the variations in the gel strength. As a result, the swollen glassy layer thickness was extracted from gel strength profile as shown in Figure III-2 and the time revolution of swollen glass layer thickness was shown in Figure III-6(a). It was found that the swollen glassy layer thickness growth monotonically with time and is greater than the gel layer thickness within the experimental time scale. This agrees with the theoretical prediction by Ju *et al.* (Ju 1995c). In Ju's model, a decline of swollen glassy layer thickness was predicted when the matrix is completely hydrated, which was not observed due to the presence of dry core within the time window we investigated.

2.3. Effect of Polymer Viscosity Grade on the Swelling of HPMC Tablets

Four different viscosity grades HPMC, K100M, K15M, K4M and K100LV were studied. The structure of the swelling tablets detected by Texture Analyzer was quite similar. The polymer concentration profile at 2 hour hydration for four viscosity grades was shown in Figure III-7. The gel/glass transition was clear for all four grades. One interesting part is that polymer concentration at transition point decreased with polymer molecular weight. This seems to be in contradiction with the fact that the glass transition

temperature of a certain polymer is independent on the molecular weight beyond a certain molecular weight. However, as we discussed above, it is unlikely that a swelling system reaches the thermodynamic equilibrium especially for a fast swelling HPMC tablet. The relaxation of HPMC with smaller molecular weight is faster than those with higher molecular weight, so less water content is needed for the gel/glass transition to take place, resulting higher polymer content at gel/glass interface.

The gel layer thickness as a function of time was plotted in Figure III-8 (a). Four viscosity grades followed very similar trend, while gel layer thickness of high molecular weight developed faster than that of small molecular weight. This is in good agreement with previous results (Wan 1993). We further found that the gel layer thickness linearly increased with the square root of time as shown in Figure III-8 (b), indicating diffusion-controlled swelling mechanism. From the slopes, we calculated the average diffusion constants ($<D_w>$) and water diffusion constants at gel/solvent interface ($D_{w,eq}$) based on Equation III-5 and III-9, and the results were shown in Table III-1, where HPMC concentration at gel/glass interface was obtained from Texture Analyzer data, and the water concentration at gel/solvent interface was obtained from the literature (Ju 1995a). The k_w for different HPMC was also obtained from literature (Katzhendler, Ifat 2000). From Table III-1 we can see that average water diffusion constant in HPMC gel layer is higher for high viscosity grade, and corresponding water diffusion constant at gel/solvent interface was also higher. This is because the polymer concentration at the interfaces of both gel/solvent ($C_{p,eq}$) and gel/glass (C_p^*) of high viscosity grade were lower. Based on Equation III-6 we can calculate the water diffusion constant at given concentration, and the results were also shown in Table III-1. The water diffusion constant at given HPMC concentration is independent on the viscosity grade, in agreement with previous results

(Gao 1995a; Gao 1995b). It is reasonable since the size of water molecule is much smaller than the mesh size of HPMC for all grades investigated here; the steric restriction on water imposed by polymer through a sieving mechanism would be minimal.

2.4. Effect of Polymer Concentration and Excipient Type on the Swelling of HPMC K15M Tablets

Several formulation variables have been known critical to drug release, including polymer concentration, polymer molecular weight and excipient type. In this study, we investigated the effect of polymer concentration and two commonly used excipients, lactose and pregelatinized starch, on HPMC gel strength and gel layer thickness.

Figure III-9 (a) shows the gel layer thickness dynamics of three different tablets, pure HPMC K15M, HPMC K15M (40%) with Starch 1500 (60%) or lactose (60%). Neither polymer concentration nor addition of lactose or starch altered the gel layer thicknesses of HPMC K15M within the time window investigated. The effect of polymer concentration on gel layer thickness agrees well with the results from Gao's work (Gao 1996b). Gao *et al*. used a semi-quantitative optical imaging method to monitor the swelling of five HPMC matrices with different HPMC/lactose ratio from 20/77 to 80/17. They found the gel layer thickness profiles of all five formulations in the concentration series are close to each other, except that a small difference is observed for the 20/77 formulation at t >3 h. The swollen glassy layer thickness dynamics of three different tablets is shown in Figure III-9 (b). No significant difference between tablets of pure HPMC K15M and 40% HPMC K15M with 60% lactose was observed. Yet, the swollen glassy layer thickness of HPMC tablets containing 60% starch was shorter. The reason for

this difference is unclear and it might be caused by different porosity in different formulations.

Gel strength profiles from above three different tablets are shown in Figure III-10 at three hydration times (2hr, 8hr and 18hr). At the same hydration time, the gel with Starch 1500 was significantly stronger than that with lactose, and the strength of pure HPMC K15M gel was in between. As hydration time increased, the strength difference was enlarged. These data are in good agreement with the data obtained from homogenous gel systems present in Chapter II. Lactose did not affect the strength of HPMC gel, while Starch 1500 enhanced it significantly. The stronger gel of HPMC tablets containing Starch 1500 is due to the gel-enhancing properties of Starch 1500. The weaker gel of HPMC tablets containing lactose compared to that of pure HPMC is caused by 60% lower HPMC concentration.

Based on gel layer thickness and gel strength data, a possible explanation to why Starch 1500 retarded drug release c omparing to lactose was due to the gel-enhancing properties of the former excipient. This was further confirmed by the disintegration experiment in phosphate buffer with 0.25M ionic strength. As shown in Figure III-11 the tablet containing 60% lactose and 40% HPMC K15M was disintegrated at 30 mins, while no disintegration happened for the tablets containing 60% Starch 1500 and 40% HPMC K15M after two hours. It is suggested that gel strength rather than gel layer thickness is responsible for Starch 1500's performance of extended drug release compared to lactose.

CONCLUSIONS

In conclusion, the present study has demonstrated the great potential of using Texture Analyzer for a comprehensive characterization of the swelling behavior of

hydrophilic polymeric matrices by accurately determining the structure of swelling tablets, gel layer thickness, gel strength and polymer concentration profile across the gel layer. This method provides the advantage that different information can be obtained using one instrument and the results appear to be comparable to other techniques such as NMR imaging, Cryogenic-SEM and light scattering imaging in the investigation of polymer matrix swelling behavior. Based on Texture Analyzer data, it was found that the gel layer thickness of high viscosity grade HPMC developed faster due to the faster water diffusion in the gel layer. Addition of starch and lactose did not affect the gel layer thickness dynamics significantly, while starch increased the gel strength of swelling tablet compared to lactose. Therefore, it was postulated that gel strength instead of gel layer thickness was responsible for excipient performance on extended drug release. However, no work has been done to correlate the gel strength and drug release due to the lack of proper tool; and the development of Texture Analyzer as a routine gel strength characterization tool can facilitate the study in this field. Therefore, the application of Texture Analyzer on the routine bases might be of great value to scientists involved in formulation design and dosage form development.

REFERENCES

Baumgartner S., Lahajnar G., Sepe A. and Kristl J. (2005). "Quantitative evaluation of polymer concentration profile during swelling of hydrophilic matrix tablets using ^{1}H NMR and MRI methods." European Journal of Pharmaceutics and Biopharmaceutics **59**: 299-306.

Bonferoni M. C., Caramella C., Sangalli M. E., Conte U., Hernandez R. M. and Pedraz J. L. (1992). "Rheological behaviour of hydrophilic polymers and drug release from erodible matrixes." Journal of Controlled Release **18**: 205-212.

Bonferoni M. C., Rossi S., Ferrari F., Bertoni M. and Caramella C. (1995). "Influence of medium on dissolution-erosion behaviour of Na carboxymethylcellulose and on viscoelastic properties of gels." International Journal of Pharmaceutics **117**: 41-48.

Colombo P. (1993). "Swelling-controlled release in hydrogel matrices for oral route." Advanced Drug Delivery Reviews **11**(1-2): 37-57.

Cunningham C. R. (1999). " Maize s tarch a nd super-disintegrants indirect c ompression formulation." Pharm. Manufac. Rev. **December**: 22-24.

Cutts L. S., Hibberd S., Adler J., Davis M. C. and Melia C. D. (1996). "Characterizing drug release processes within controlled release dosage form using the confocal laser scanning microscope." Journal of Controlled Release **42**(2): 115-124.

Durig T. and Fassihi R. (2002). "Guar-based monolithic matrix systems: effect of ionizable and non-ionizable substances and excipients on gel dynamics and release kinetics." Journal of Controlled Release **80**: 45-56.

Fujita H. (1961). "Diffusion in Polymer-Diluent Systems." Fortschr. Hochpolym.-Forsch. **3**(1): 1-47.

Fyfe C. A. and Blazek A. I. (1997). "Investigation of hydrogel formation from hydroxypropylmethylcellulose (HPMC) by NMR spectroscopy and NMR imaging techniques." Macromolecules **30**: 6230-6237.

Fyfe C. A. and Blazek-Welsh A. I. (2000). "Quantitative NMR imaging study of the mechanism of drug release from swelling hydroxypropylmethylcellulose tablets." Journal of Controlled Release **68**: 313-333.

Gao P. and Fagerness P. E. (1995a). "Diffusion in HPMC gels. I. Determination of drug and water diffusivity by pulsed-field-gradient spin-echo NMR." Pharmaceutical Research **12**: 955-964.

Gao P. and Meury R. H. (1996a). "Swelling of hydroxypropylmethylcellulose matrix tablets. 1. Characterization of swelling using a novel optical imaging method." Journal of Pharmaceutical Sciences **85**: 725-731.

Gao P., Nixon P. R. and Skoug J. W. (1995b). "Diffusion in HPMC gels. II. Prediction of drug release rates from hydrophilic matrix extended-release dosage forms." Pharmaceutical Research **12**(965-971).

Gao P., Skoug J. W., Nixon P. R., Ju R. C., Stemm N. L. and K.C. S. (1996b). "Swelling of Hydroxypropyl methylcellulose matrix tablets. 2. Mechanistic study of the influence of formulation variables on matrix performance and drug release." Journal of Pharmaceutical Sciences **85**(7): 732-740.

Hancock B. C. and Zografi G. (1994). "The relationship between the glass transition temperature and the water content of amorphous pharmaceutical solids." Pharmaceutical Research **11**: 471-477.

Harland R. S., Gazzaniga A., Sangalli M. E., Colombo P. and Peppas N. A. (1988). "Drug/polymer matrix swelling and dissolution." Pharmaceutical Research **5**: 488-494.

Hui C. Y., Wu K. C., Lasky R. C. and Kramer E. J. (1987). "Case II diffusion in polymers. I. Transient swelling." J. Appl. Phys. **22**: 1885-1900.

Ju R. T. C., Nixon P. R. and Patel M. V. (1995a). "Drug release from hydrophilic matrixes 1. New scaling laws for predicting polymer and drug release based on the polymer disentanglement concentration and the diffusion layer." Journal of Pharmaceutical Sciences **84**(12): 1455-1463.

Ju R. T. C., Nixon P. R., Patel M. V. and Tong D. M. (1995b). "Drug release from hydrophilic matrices. 2. A mathematical model based on polymer disentanglement concentration and the diffusion layer." Journal of Pharmaceutical Sciences **84**(12): 1464-1477.

Ju R. T. C., Nixon P. R., Patel M. V. and Tong D. M. (1995c). "A mechanistic model for drug release from hydrophilic matrices based on the structure of swollen matrices." Proceedings of the International Symposium on Controlled Release of Bioactive Materials. **22**: 59-60.

Katzhendler I., Hoffman A., Goldberger A. and Friedman M. (1997). "Modeling of drug release from erodible tablets." Journal of Pharmaceutical Sciences **86**(1): 110-115.

Katzhendler I., Mader K. and Friedman M. (2000). "Structure and hydration properties of hydroxypropyl methylcellulose matrices containing naproxen and naproxen sodium." International Journal of Pharmaceutics **200**(2): 161-179.

Kim H. and Fassihi R. (1997). "Application of a binary polymer system in drug release rate m odulation. 1. Characterization of r elease mechanism." J ournal of P harmaceutical Sciences **86**(3): 316-322.

Lee P. I. (1980). "Diffusional release of a solute from a polymeric matrix. Approximate analytical solutions." J. Membrane Sci. **7**: 255-275.

Lee P. I. and Peppas N. A. (1987). "Prediction of polymer dissolution in swellable controlled-release systems." Journal of Controlled Release **6**: 207-215.

Levina M. and Rajabi-Siahboomi A. R. (2004). "The influence of excipients on drug release from hydroxypropyl methycellulose matrices." Journal of Pharmaceutical Sciences **93**: 2746-2754.

Melia C. D. (1991). "Hydrophilic matrix sustained release systems based on polysaccharide carriers." Critical Reviews in Therapeutic Drug Carrier Systems **8**(4): 395-421.

Melia C. D., Hodsdon A. C., Davis M. C. and Mitchell J. R. (1994). "Polymer concentration profiles o f the s urface gel layer of x anthan, a lginate a nd H PMC m atrix systems." Proceedings of the International Symposium on Controlled Release of Bioactive Materials. **21th**: 724-725.

Melia C. D., Rajabi-Siahboomi A. R. and Davis M. C. (1992). "The development of structural features in the surface gel layer of hydrating HPMC hydrophilic matrices." Proceedings of the International Symposium on Controlled Release of Bioactive Materials. **19th**: 28-29.

Narasimhan B. and Peppas N. A. (1996). "Disentanglement and reptation during dissolution of rubbery polymers." Journal of Polymer Science: part B: Polymer Physics **34**: 947-961.

Narasimhan B. and Peppas N. A. (1997). "Molecular analysis of drug delivery systems controlled by dissolution of the polymer carrier." Journal of Pharmaceutical Sciences **86**: 297-304.

Papadimitriou E., Buckton G. and Efentakis M. (1993). "Probing the mechanism of swelling of hydroxypropylmethylcelloluse matrices." International Journal of Pharmaceutics **98**: 57-62.

Peppas N. A., Wu J. C. and Von Meerwall E. D. (1994). "Mathematical modeling and experimental characterization of polymer dissolution." Macromolecules **27**: 5626-5638.

Pham A. T. and Lee P. I. (1994). "Probing the mechanism of drug release from hydroxypropylmethyl cellulose matrices." Pharmaceutical Research **11**(10): 1379-1384.

Rajabi-Siahboomi A. R., Bowtell R. W., Mansfield P., Davis M. C. and Melia C. D. (1996). "Structure and behavior in hydrophilic matrix sustained release dosage forms: 4. Studies of water mobility and diffusion coefficients in the gel layer of HPMC tablets using NMR imagine." Pharmaceutical Research **13**: 376-380.

Rajabi-Siahboomi A. R., Bowtell R. W., Mansfield P., Henderson A., Davis M. C. and Melia C. D. (1994). "Structure and behavior in hydrophilic matrix sustained release dosage forms: 2. NMR imaging studies of dimensional changes in the gel layer and core of HPMC matrices undergoing hydration." Journal of Controlled Release **31**: 121-128.

Siepmann J., Kranz H., Bodmeier R. and Peppas N. A. (1999a). " HPMC-matrices for controlled drug deliver: a new model combining diffusion, swelling, and dissolution mechanisms and predicting the release kinetics." Pharmaceutical Research **16**(11): 1748-1756.

Siepmann J., Kranz H., Peppas N. A. and Bodmeier R. (2000). "Calculation of the required size and shape of hydroxypropyl methylcellulose matrices to achieve desired drug release profiles." International Journal of Pharmaceutics **201**: 151-164.

Siepmann J. and Peppas N. A. (2001). "Modeling of drug release from delivery systems based on hydroxypropyl methylcellulose (HPMC)." Advanced Drug Delivery Reviews **48**(2-3): 139-157.

Siepmann J., Podual K., Sriwongjanya M. and Peppas N. A. (1999b). "A new model describing the swelling and drug release kinetics from hydroxypropyl methylcellulose tablets." Journal of Pharmaceutical Sciences **88**: 65-72.

Siepmann J., Streubel A. and Peppas N. A. (2002). "Understanding and predicting drug delivery from hydrophilic matrix tablets using the "Sequential Layer" model." Pharmaceutical Research **19**(3): 306-314.

Tu Y.-O. and Ouano A. C. (1977). "Model for the kinematics of polymer dissolution." IBM J Res Develop **21**(2): 131-142.

Ueberreiter K. (1968). Diffusion in Polymers. New York, Academic Press.

Wan L. S. C., Heng P. W. S. and Wong L. F. (1993). "Relationship between swelling and drug release in a hydrophilic matrix." Drug Development and Industrial Pharmacy **19**(10): 1201-1210.

Yang L., Johnson B. and Fassihi R. (1998). "Determination of continuous changes in the gel layer thickness of poly(ethylene oxide) and HPMC tablets undergoing hydration: a texture analysis study." Pharmaceutical Research **15**(12): 1902-1906.

Table III-1 Estimate of the average water diffusion constant at HPMC gel layer and its dependence on the viscosity grade.

Grade	Slope	C_w* (%)	$C_{w,eq}$ (%)	$<D_w>$ (cm^2/s)	k_w	$D_{w,eq}$ (cm^2/s)	$D_{w,12\%}$ (cm^2/s)
K100LV	0.494	0.53	0.888	1.6E-05	2.86	3.23E-05	3.15E-05
K4M	0.546	0.53	0.950	1.7E-05	2.86	3.67E-05	2.97E-05
K15M	0.624	0.57	0.964	1.8E-05	2.86	3.83E-05	2.99E-05
K100M	0.733	0.62	0.975	2.1E-05	2.92	4.07E-05	3.07E-05

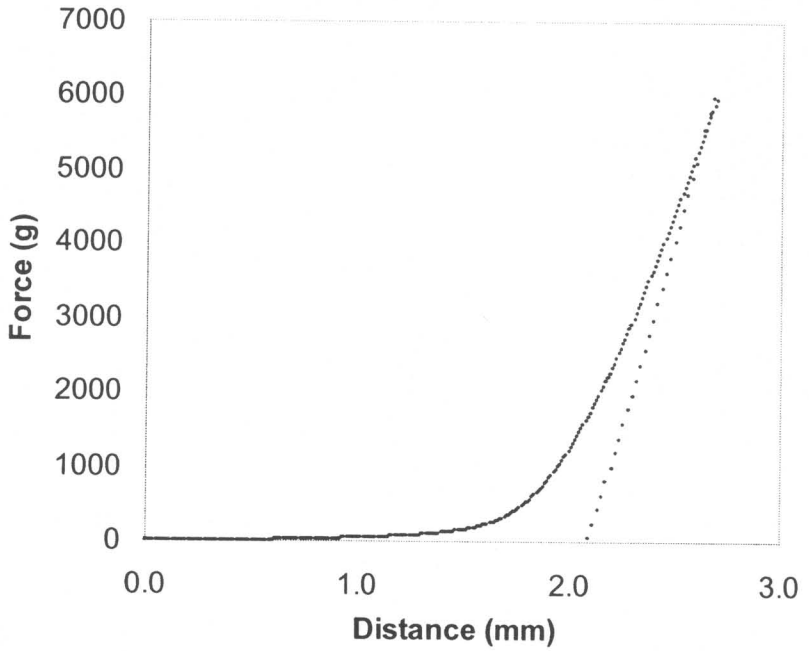

Figure III-1 The force-distance profile of HPMC K15M matrix tablets at two hours swelling

(a)

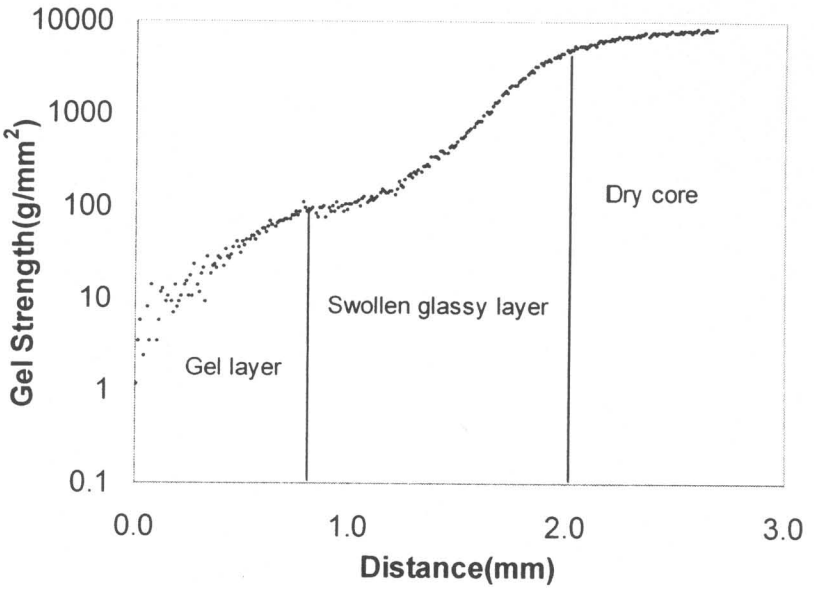

(b)

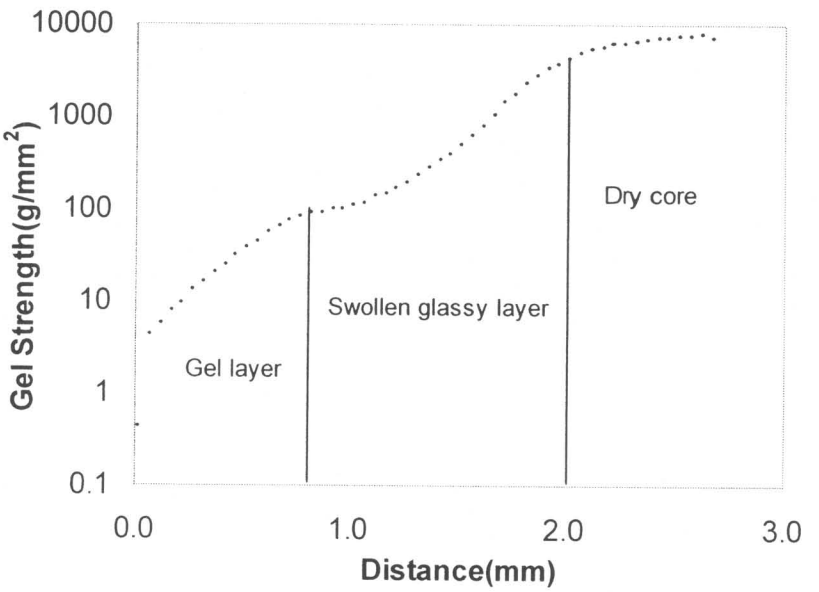

Figure III-2 The representative semi-log gel strength profile of HPMC K15M matrix at two hours swelling. (a) Average of three replicates (b) Average of five points from (a). The structure of a swelling tablet was characterized by three different layers: gel layer, swollen glassy layer and dry glassy core.

(a)

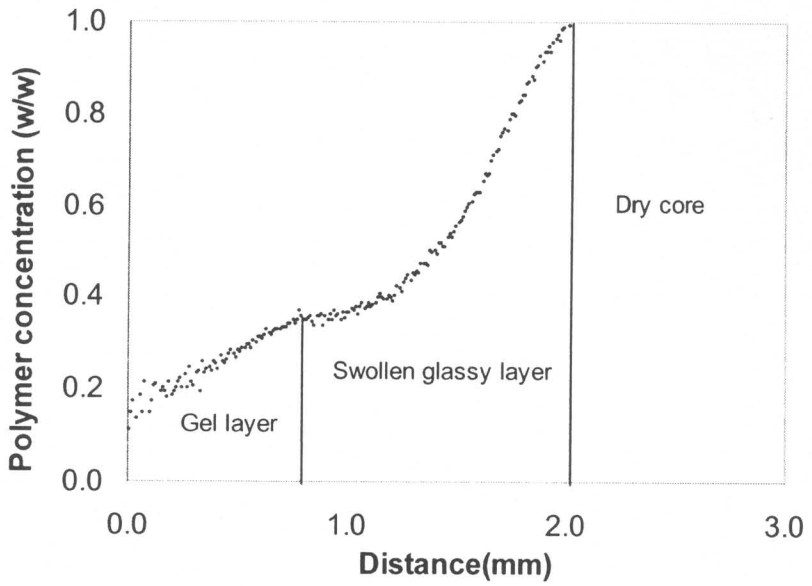

(b)

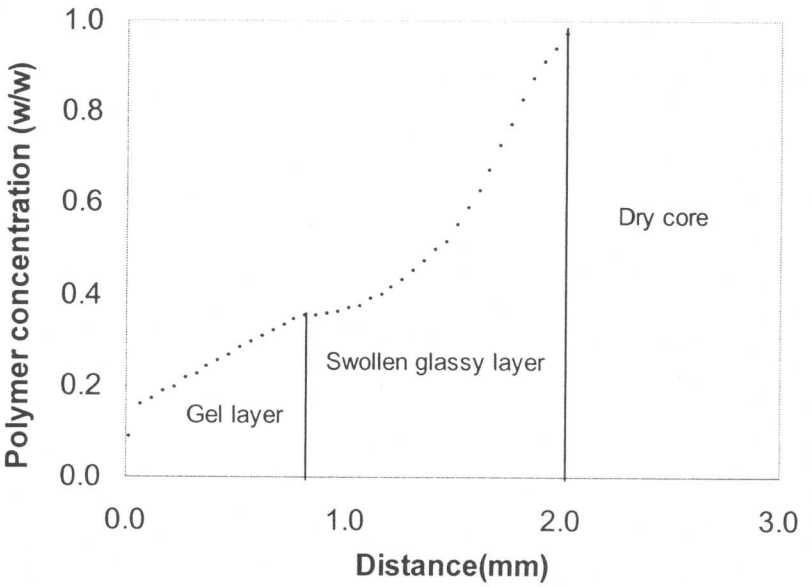

Figure III-3 The representative polymer concentration profile in swelling matrix of HPMC K15M at two hours. (a) Average of three replicates (b) Average of five points from (a).

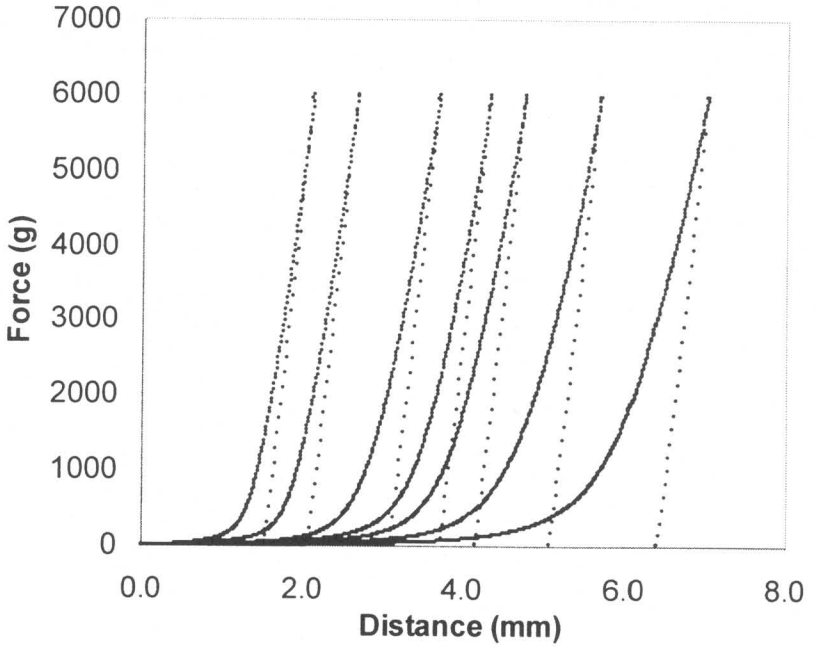

Figure III-4 The force-distance profiles of HPMC K15M matrices with varying time of swelling (from left to right: 1.0, 2.0, 4.0, 6.0, 8.0, 12.0, 18.0 hours)

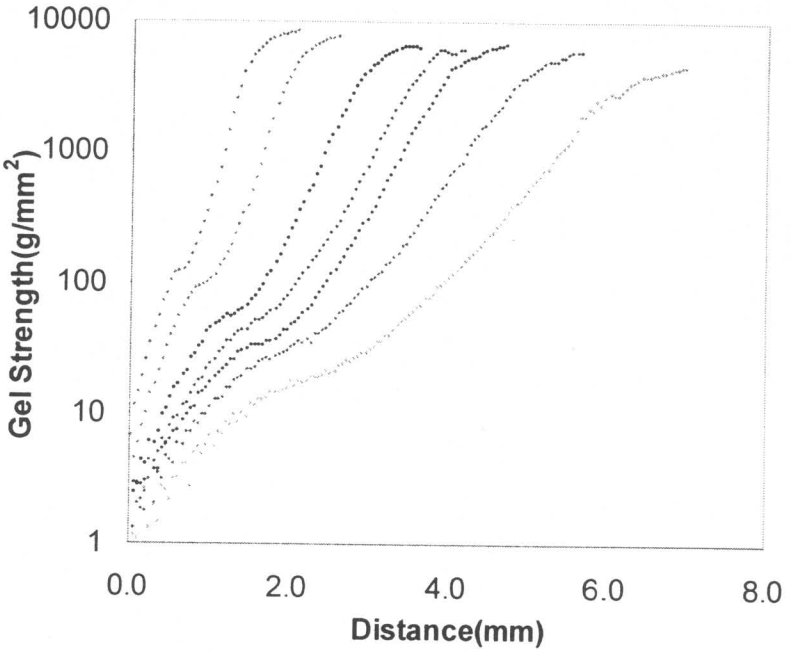

Figure III-5 The gel strength profiles of HPMC K15M matrices with varying time of swelling (from left to right: 1.0, 2.0, 4.0, 6.0, 8.0, 12.0, 18.0 hours)

(a)

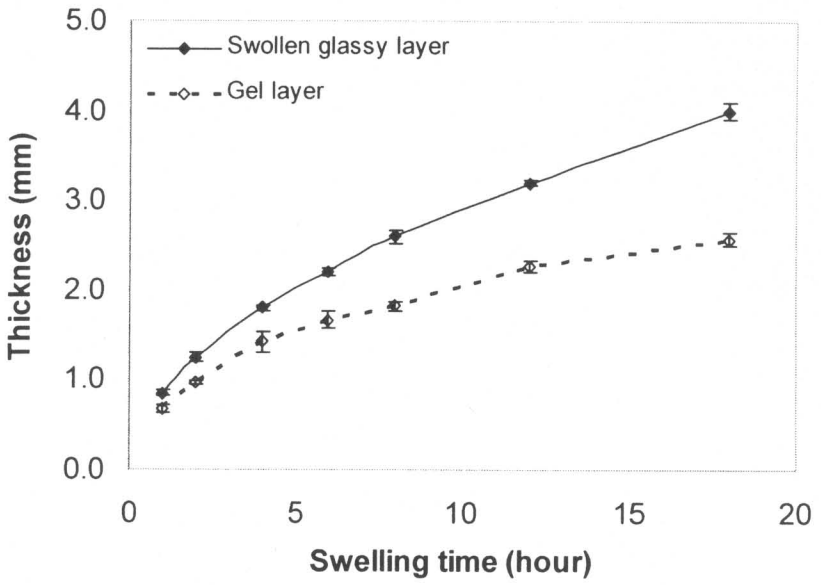

(b)

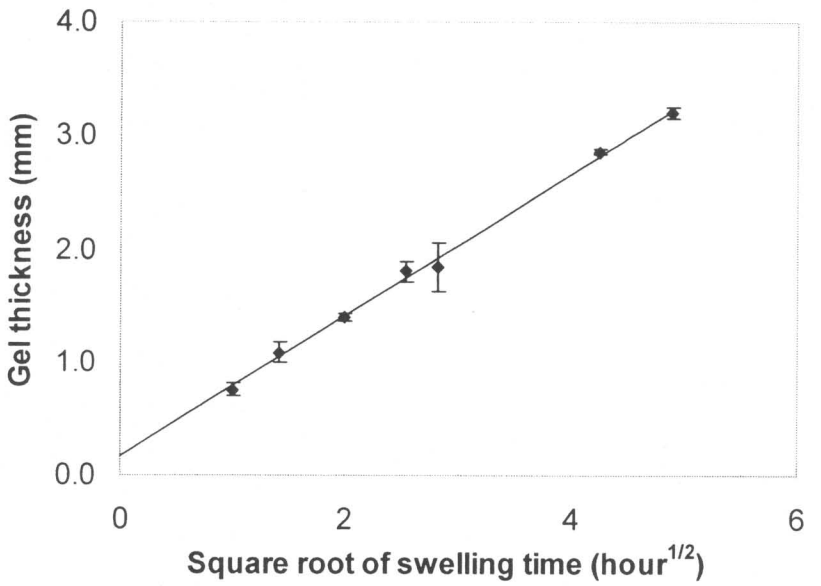

Figure III-6 (a) Dynamic changes in gel layer and swollen glassy layer thickness for HPMC K15M matrices as a function of time. (Standard deviations have been shown); (b) Dynamic changes of gel layer thickness as a function of square root of swelling time.

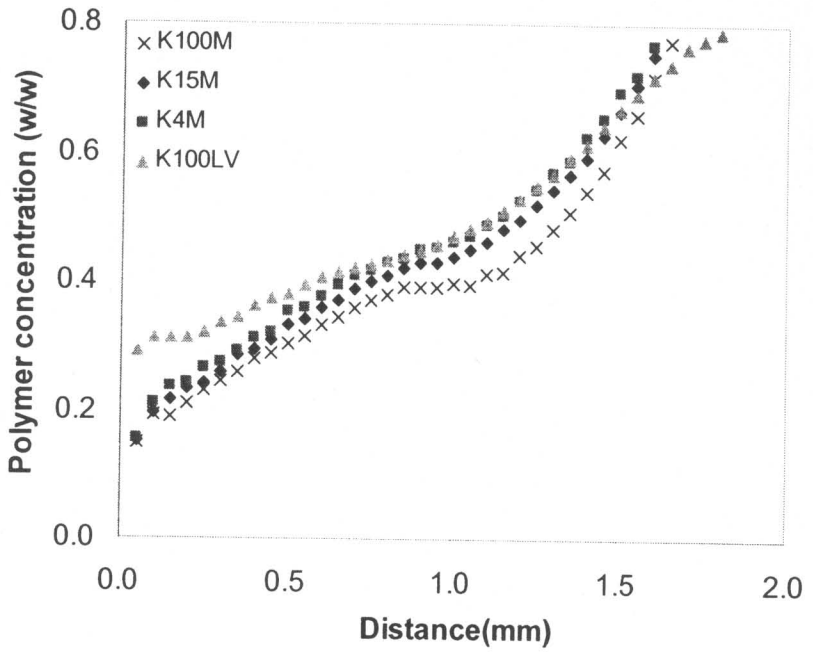

Figure III-7 The effect of viscosity grade on the polymer concentration profiles of swelling table at 2 hour hydration.

(a)

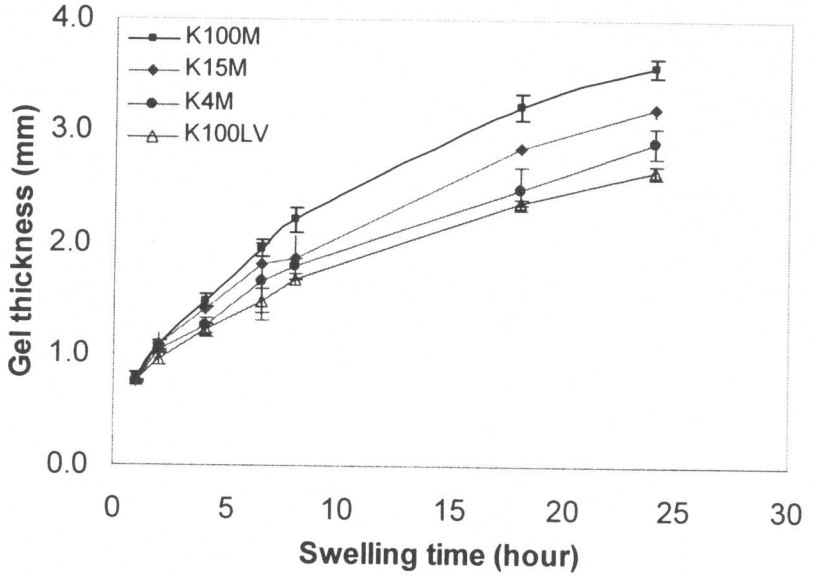

(b)

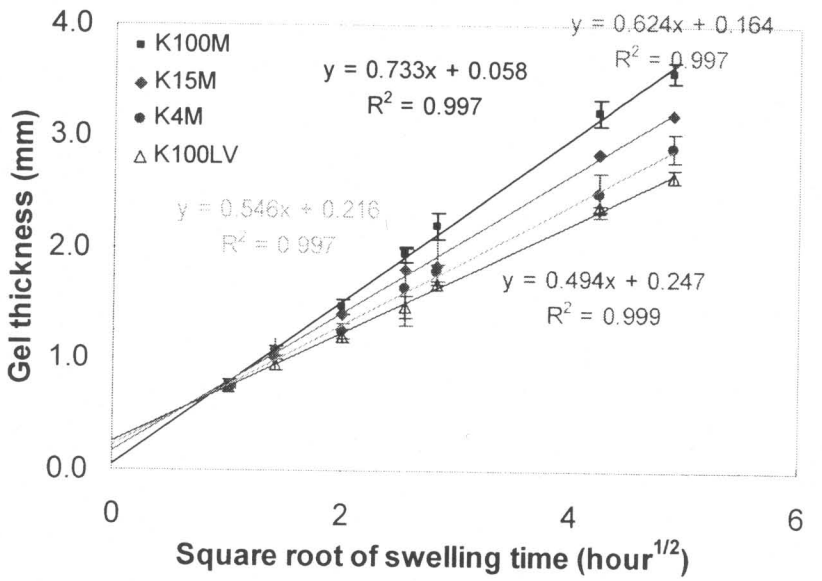

Figure III-8 The effect of HPMC viscosity grade on the gel layer thickness change as a function of time (a) and square root of time (b)

(a)

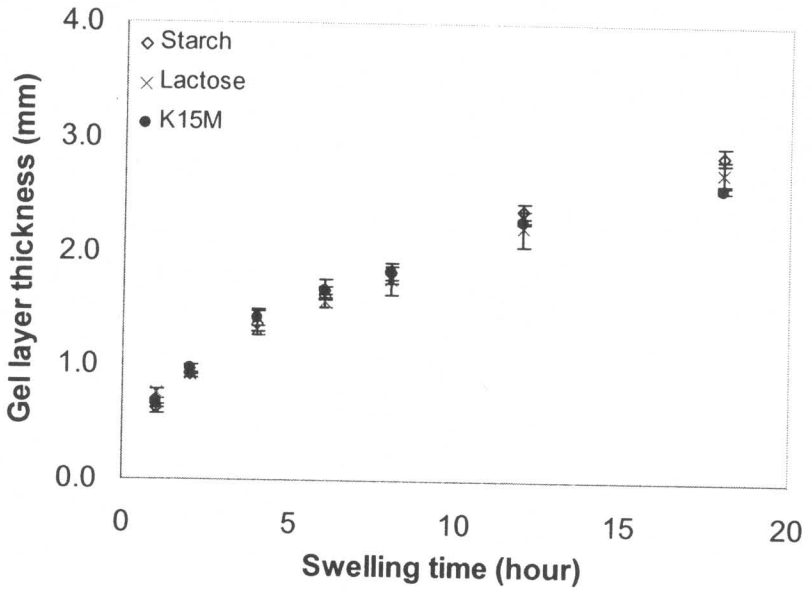

(b)

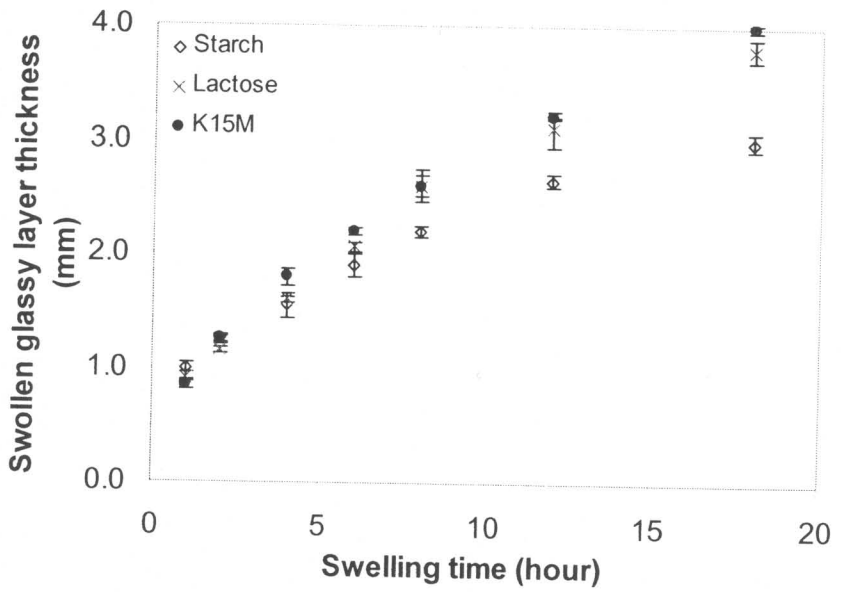

Figure III-9 Dynamic changes in (a) gel layer and (b) swollen glassy layer thickness of HPMC K15M matrices with and without different excipients versus time. (●, 100% K15M, ◊, 40% K15M with 60% Starch 1500, x, 40% K15M with 60% lactose).

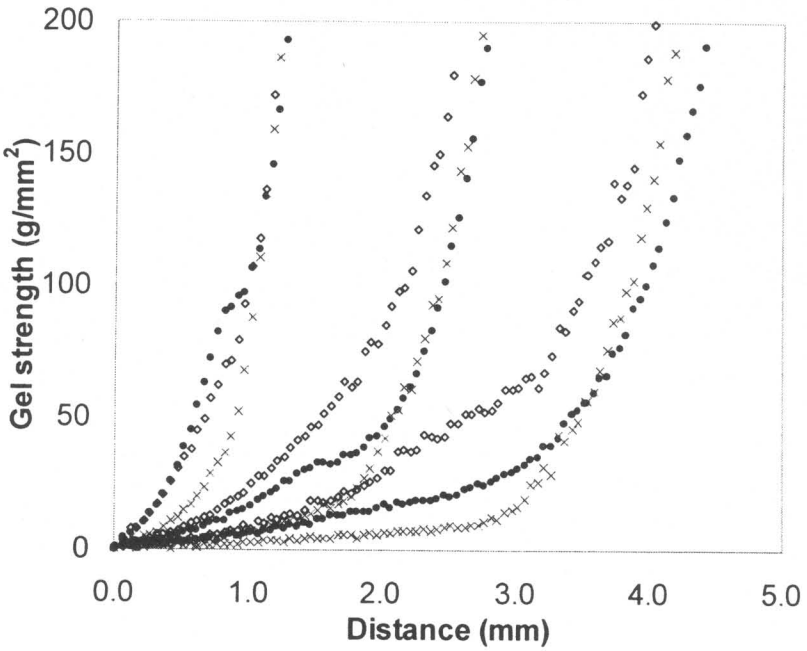

Figure III-10 The gel strength profile of HPMC K15M matrices containing different excipients at varying time of swelling (from left to right: 2.0, 8.0, 18.0 hours) (●, 100% K15M, ◊, 40% K15M with 60% starch 1500, x, 40% K15M with 60% lactose).

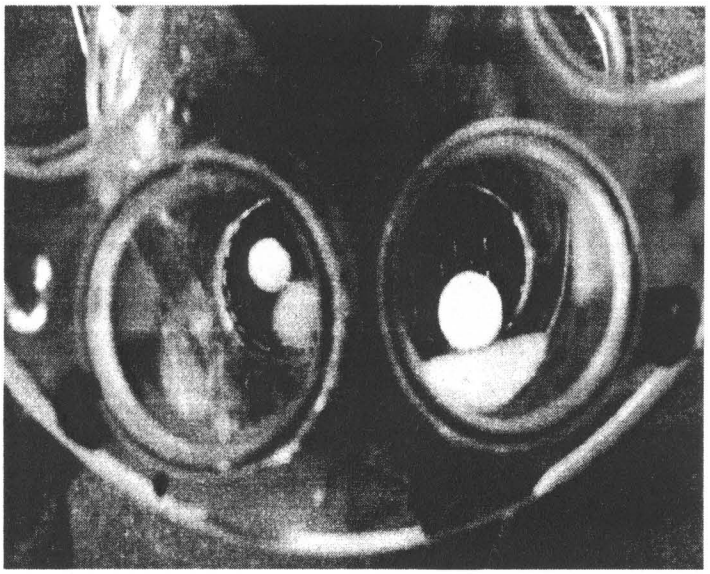

Figure III-11 Disintegration experiment of HPMC K15M tablet with different excipients in 0.25M phosphate buffer after 30 mins. The tablet in the left chamber is 40% K15M with 60% lactose and the one in the right chamber is 40% K15M with 60% Starch 1500.

CHAPTER IV Construction and Validation of Mathematical Model Correlating Gel Strength and Polymer Erosion

ABSTRACT

Purpose. The purpose of this study was to correlate HPMC dissolution with HPMC gel strength using mathematical modeling, and to study the effects of HPMC molecular weight, excipient type such as lactose and Starch 1500, and excipient content on HPMC dissolution. ***Methods.*** The gel strength was measured using Texture Analyzer. One dimensional HPMC dissolution tests were conducted in 0.05M phosphate buffer (pH 6.8) at 25 ^{0}C using USP dissolution apparatus II with a rotation speed of 100 rpm. HPMC release was determined using a size exclusion chromatography-HPLC-evaporative light scattering detector (SEC-HPLC-ELSD) method. ***Results.*** A mathematical model w as constructed to correlate HPMC dissolution rate to HPMC gel strength through the HPMC disentanglement concentration. Effects of HPMC molecular weight, excipient type and excipient content on HPMC dissolution were studied to validate the model. A power-law relationship was found between HPMC disentanglement concentration and HPMC molecular weight with an exponent of -0.68, consistent with a previous study report (Ju 1995a); Consequently, a power-law relationship between the HPMC dissolution rate and molecular weight was established experimentally, which was in good agreement with both model prediction and literature results. Release of a high molecular weight HPMC (HPMC K15M) was found independent of the content of lactose and a surfactant (SDS) but retarded by Starch 1500. ***Conclusions.*** Gel strength was successfully correlated to polymer erosion through polymer disentanglement concentration. Texture Analyzer was

demonstrated to be a reliable, convenient and new method of estimating polymer disentanglement concentration.

Key Words: Gel strength; polymer dissolution; polymer disentanglement concentration; ELSD; HPMC; Texture Analyzer

INTRODUCTION

Polymer dissolution is an important phenomenon in polymer science and engineering. It has found significant applications in a variety of areas. For example, in microlithography, the irradiated regions of a thin polymer film are dissolved by an appropriate solvent to form desired patterns (Iwayanagi 1988; O'Brien 1989). Polymer dissolution also finds application in membrane science, specifically for a technique called phase inversion to form asymmetric membranes. In this process, a polymer solution thin film is cast onto a suitable substrate followed by immersion in a coagulation bath for quenching (Tsay 1990; Kesting 1993; Narasimhan 1998). During the quenching period, solvent/non-solvent exchanges and eventual polymer precipitation occurs. The final structure of the membrane is determined by the extent of polymer dissolution. Polymer dissolution also plays an instrumental role in recycling plastics (Srivastava 1993; Nauman 1994), where a single solvent can be used to dissolve several unsorted polymers at different temperatures. Polymer dissolution is being currently investigated for tissue regeneration as well (Pappas 1994; Langer 1995), where the dissolution rate of the biodegradable polymer scaffolds is required to match the growth rate of tissue cells.

Within the field of controlled drug delivery, it is well recognized that the drug release process can be controlled either by drug diffusion or by polymer dissolution (Colombo 1987; Conte 1988). In the development of microcapsules for sustained release

dosage forms (Koida 1987), the mechanism of drug transport is governed by the dissolution of the polymer shell. Ozturk and co-workers (Ozturk 1988a, b) showed that the dissolution of polyacids, used in enteric-coated tablets, was the controlling step in drug release. It was also suggested that for drugs with low water solubility, drug release from the polymer matrix is mainly via polymer dissolution (Alderman 1984; Doelker 1987; Skoug 1993).

The dissolution of a polymer in a solvent involves two transport processes, namely solvent diffusion and chain disentanglement. When an uncross-linked, amorphous, glassy polymer is brought in contact with a thermodynamically compatible solvent, the latter diffuses into the polymer and polymer chains undergo a glass-to-gel transition. When the solvent concentration in the swollen polymer reaches a critical value, chain disentanglement begins to dominate and eventually the polymer is dissolved. Ueberreiter *et al.* (Ueberreiter 1968) summarized the various types of dissolution and the surface structure of glassy polymers during dissolution. Important parameters such as the polymer molecular weight, the solvent diffusion coefficient, the gel layer thickness, the rate of agitation and the temperature, were identified. Since then, various mathematical models have been proposed to understand polymer dissolution.

The approaches to model polymer dissolution can be broadly classified as 1) use of phenomenological models and Fickian equations (Tu 1977; Harland 1988; Devotta 1994; Devotta 1995; Vrentas 1998; Siepmann 1999a; Siepmann 1999b; Siepmann 2000a; Siepmann 2000b, 2001; Siepmann 2002; Vrentas 2004); 2) models based on stress relaxation (Brochard 1983; Herman 1990) and 3) analysis using anomalous transport models for solvent transport and scaling laws for chain disentanglement (Papanu 1989; Peppas 1994; Ju 1995a; Ju 1995b; Ju 1995c; Narasimhan 1996b, a; Ju 1997).

Tu *et al.* (Tu 1977) proposed a phenomenological model with Fickian equations for polymer dissolution. They studied the motions of both the liquid-gel boundary and the gel-glass boundary. These boundaries were observed due to the sharp changes in viscosity and refractive index at the interface. The important parameter in this model was the polymer disassociation rate, defined as the rate at which the polymer goes from a gel-like phase to a less viscous liquid solution. Harland *et al.* (Harland 1988) formulated a similar model for drug release in a dissolving polymer-solvent system. The important parameters identified in the phenomenon were the polymer concentrations at both interfaces of glass/gel transition and gel/solvent and the dissolution coefficient. Devotta *et al.* (Devotta 1994; Devotta 1995) considered the Fickian dissolution of a spherical polymeric particle. They modeled chain "disengagement" by defining a flux that was proportional to the concentration of the polymer at the polymer-solvent interface. The transport of the chains in the solvent was assumed to be controlled by an external mass transfer resistance. Numerical simulations yielded the effect of the particle size on the dissolution process. Siepmann *et al.* (Siepmann 1999a; Siepmann 1999b; Siepmann 2000a; Siepmann 2000b, 2001; Siepmann 2002) published a series of mathematical models describing drug release from dissolving hydroxypropyl methyl cellulose (HPMC) matrices. Diffusion coefficients for water and drug were taken to be concentration dependent following a generalized free volume theory. Dissolution was described using a reptation model. They proposed that the disentanglement processes begin to dominate when the polymer concentration was below a critical concentration at gel/solvent interface. A dissolution constant was defined to describe the velocity of the dissolution per unit area and could be controlled by either rate of disentanglement or by diffusion through a boundary layer, adjacent to the HPMC-water interface. These approaches using phenomenology, although valuable, do not discuss the molecular (or physical) origin of some of the important parameters used (such

as the polymer concentration at gel/solvent interface and the polymer dissolution coefficient).

On the basis of the idea that polymer swelling due to solvent influx results in an elastic-like stress opposing the solvent penetration, Brochard and de Gennes (Brochard 1983) proposed relaxation-controlled polymer dissolution kinetics. The dissolution flux was expressed as the difference between the polymer stress gradient and the solvent osmotic pressure gradient. After the formation of a swollen gel layer, the sequential dissolution of the polymer from the swollen state was assumed to be controlled by the local stress relaxation rate. This rate was shown to be of the order of the reptation time. Herman and Edwards (Herman 1990) extended the above approach by considering in detail the stress accompanying the swelling of the polymer within the reptation model. They proposed that the solvent swelling induces a nonrandom distribution of polymer chain orientation. This contribution to the free energy and the chemical potential of the polymer and the solvent were evaluated in closed form using reptation theory. This approach could account for both solvent penetration and polymer dissolution but required several parameters that were difficult to measure experimentally.

Recognizing the presence of entanglements in polymers, dissolution has been understood as the transformation undergone by the polymer from an entangled gel-like phase to a disentangled liquid solution. The dynamics of these chains have been described by means of the reptation idea. On the basis of the above arguments, Papanu *et al.* (Papanu 1989) proposed a reptation model for polymer dissolution. The dissolution rate was expressed as the ratio between the radius of gyration of the polymer and the reptation time. The dependence of the radius of gyration and the reptation time on the polymer molecular weight and the solvent concentration was derived using scaling laws (de Gennes

1979; de Gennes 1982). This model assumed that the dissolution rate is only related to the polymer concentration at the gel/solvent interface, but independent of the solvent concentration inside the polymer. The polymer concentration at gel/solvent interface was estimated by thermodynamics of the swollen network. Peppas *et al.* (Peppas 1994) proposed a polymer dissolution model using an anomalous transport model for solvent penetration coupled with a reptation model for dissolution. The disentanglement time was proposed to be of the order of the reptation time. This model introduced the concept of the "dissolution clock" that controls the dissolution process and proposed that the magnitude of a "dissolution number" determined the gel layer thickness. This approach assumes that the solvent concentration at the polymer-solvent interface is independent of the solvent concentration history. Ju *et al.* (Ju 1995a; Ju 1995b; Ju 1995c; Ju 1997) proposed a model to predict swelling/dissolution behavior of HPMC matrices. They introduced a polymer disentanglement concentration and a polymer diffusion layer into the model (Ju 1995a; Ju 1995b). The disentanglement concentration was defined as the concentration below which the chains detach off the matrix and diffuse through the diffusion layer into the bulk solution. By assuming that disentanglement concentration scales similarly with polymer molecular weight as the overlapping concentration of polymer solution, they derived a scaling law of polymer disentanglement concentration with polymer molecular weight.

Based on these models, measurements of both the structure of the gel layer and polymer dissolution kinetics are crucial to understand the polymer dissolution mechanism. The techniques to characterize the gel layer structure in a swelling tablet were briefly reviewed in Chapter III. And various techniques were utilized to measure the polymer dissolution kinetics. Some of these techniques include the gravimetric method, differential

refractometry, differential viscometry, optical microscopy, UV or fluorescence microscopy and NMR imaging.

The gravimetric method is the most common way to measure the polymer dissolution kinetics. Bonferoni *et al.* (Bonferoni 1992) determined the amount of polymer erosion using this method for matrices containing a blend of sodium carboxymethyl-cellulose and HPMC. In another study, Tahara *et al.* (Tahara 1995) examined the erosion of HPMC matrices containing lactose. Durig and Fassihi (Durig 2002) investigated the erosion kinetics of guar-based matrix tablets and the effect of ionic and non-ionic excipients. The gravimetric method is easy to operate but not applicable to systems where multiple components are released.

One of the earliest techniques used to study polymer dissolution was refractometry (Ueberreiter 1968). This technique is based on the refractive index change as the polymer concentration increases in the solvent. However, this technique is not sensitive enough to detect small amount of dissolved polymer in very large quantities of solvent.

Skoug *et al.* (Skoug 1993) qualitatively determined the relative contributions of polymer erosion and drug diffusion to overall drug release from commercial sustained release (SR) tablets by measuring polymer release into dissolution media using size exclusion chromatography and differential viscometric detection. The viscometric detector measures the pressure difference caused by a change in viscosity of the sample flow stream compared to the reference stream. This differential pressure signal is proportional to specific viscosity. Later, Ju *et al.* (Ju 1997) used this same technique to monitor the polymer concentration in aqueous solution for a serious of HPMC viscosity grades in sustained release dosage form containing an active ingredient and lactose.

Optical microscopy allows direct visual observation of the dissolution process and the formation of a gel layer. Therefore, it provides information about the structure of the different layers (solution, gel, and dry core) formed. In cases where both the solvent and the polymer are transparent, it is necessary to use either a dye in the solvent or carbon black in the polymer to track both the penetration of the solvent into the polymer matrix and the dissolution of polymer in the solvent. Ouano and Carothers (Ouano 1980) improved this method by using critical angle illumination microscopy and eliminated the need for dye or carbon black tracer. Good contrast between the different layers of the dissolving polymer could be achieved by changing the angle of illumination of the sample. The use of optical microscopy has provided valuable insight into the behavior of polymers in contact with solvent, but there is limited chemical specificity with an optical microscopic system.

NMR imaging offers a convenient way to obtain both qualitative and quantitative data about the polymer dissolution. Devotta *et al.* (Devotta 1994) measured the integrated proton signal area as a function of time to examine the time variation of the population of the dissolved polymeric molecules in the swelling-dissolving polymer. This method is based on the direct linear relationship between the integrated signal area and the population of the dissolved polymer in the NMR intensity measurement. As we reviewed in Chapter III, NMR imaging method is also able to detect the structure of swelling tablet non-invasively, so it is possible to conduct experiments *in situ*. However, limitations do exist. For example, the spin-spin and spin-lattice relaxation processes that characterize the return of the spin system to equilibrium following perturbation by radio frequency pulse, can cause attenuation of the NMR signal (Weisenberger 1989).

If the polymer is UV active or exhibits fluorescence, UV and fluorescence microscopy provides sensitive ways to measure the polymer concentration in the dissolution medium. However, in most of the cellulose-based formulation, macromolecules are stealth (transparent) to UV-VIS detection and they do not exhibit fluorescence either. The evaporative light scattering detector (ELSD) is gaining popularity in pharmaceutical analysis due to its high sensitivity and universal detection. ELSD measures the amount of light scattered by particles of mobile phase that have been dried through evaporation. In general, evaporative light-scattering detectors deliver a signal for all compounds that do not evaporate or decompose during the mobile-phase evaporation stage. ELSD is considered to be universal, as is the more traditional refractive index detector. However, ELSD offers advantages over refractive index detection in that it is compatible with a much wider range of solvents and modifiers, and it produces stable baselines during gradient elution chromatography because its response is independent of the spectral properties of the analyte and solvent (Johnson 1990; Herbreteau 1992; Churms 1996).

With the efforts from both theoreticians and experimentalists, the molecular understanding of polymer dissolution mechanisms becomes possible. It is well recognized that the solvent/polymer interaction and molecular diffusion are the key parameters to affect the polymer dissolution. Specifically, polymer dissolution could be affected by polymer molecular weight and polydispersity, polymer structure, composition and conformation, the solvent properties, the environmental parameters and processing conditions. Recently, it was suggested that the rheology of polymer gel such as gel strength could be correlated to the polymer dissolution (Bonferoni 1992), however, systematic investigation between the gel strength and polymer dissolution was lack of.

In this chapter, we will try to use mathematical modeling to correlate HPMC dissolution with the gel strength of HPMC through the concept of polymer disentanglement concentration proposed by Ju *et al.* (Ju 1995a; Ju 1995b) and study the effects of polymer viscosity grade, excipient type and content on HPMC dissolution to validate our model.

MATERIALS AND METHODS

Materials

METHOCEL®, commercially available hydroxypropylmethyl cellulose (HPMC) with four viscosity grades, K100M, K15M, K4M and K100LV, were same as those used in Chapter II. Lactose monohydrate and Starch® 1500 were obtained from Fast-Flo and Colorcon, respectively. Sodium dodecyl sulfate (SDS) was from BDH laboratory supplies. 0.05 M phosphate buffer (pH 6.8) was used as dissolution medium.

Sample Preparation

The tablets containing 100% hydroxypropylmethylcellulose (Methocel™, K100M, K15M, K4M and K100LV) were prepared using a reciprocating tabletting machine (model EKO, Korsch, Berlin, Germany), equipped with a flat-faced punch of 1.0 cm diameter, in order to manufacture tablets weighing 0.4 g with a thickness of 4.0 mm. The tablets containing HPMC K15M and excipients (lactose, SDS and Starch 1500) were prepared by first mixing them in a blender and then compressing them using the same machine under the same conditions. The mass of HPMC and excipents were predetermined to give desired HPMC/excipient ratios. The HPMC/Starch 1500 ratios included 2:1, 1:1 and 1:2; HPMC/lactose ratios included 3:2 and 2:3; HPMC/SDS ratios included 15:1, 15:2 and 15:3. The total weight of tablets was also 0.4 g.

One-dimensional *In Vitro* Dissolution Study

The tablet was put into a sample holder with exact the same diameter of the tablet. The depth of the sample holder was designed to be same as the thickness of the dry tablet. The dissolution testing was performed using a USP II rotating paddle apparatus (Vankel 7000) at a rotation speed of 100±1 rpm and a temperature of 25±0.5 ^{0}C. The dissolution medium (900ml) was measured into each of the six vessels of the bath and allowed to equilibrate before starting the experiments. Before each experiment, sampling times (up to 24h) were programmed into the Dissoette system. Samples were filtered through a 45-μm polyethylene filter and collected for further HPLC analysis. In case of the HPMC concentration in the sample was beyond 100 ppm, the sample was first diluted using the dissolution medium to appropriate concentration. All dissolution studies were performed at least in triplicate for each batch of tablet.

Matrix erosion studies were also performed using the gravimetric method. The dissolution conditions were the same as above. At regular intervals, sample holders with tablets were withdrawn from the dissolution vessels, and lightly blotted with a tissue paper to remove excess test liquid and re-weighted. Then the sample holders with tablets were put into a vacuum oven (50^{0}C) and dried to a constant weight. The amount of polymer erosion was calculated as the difference between the original and dry weight of the tablets after dissolution test. Weighing method was only used for pure HPMC tablets and tablets of K15M/Starch 1500, and the dissolution of HPMC with excipients (SDS, lactose and Starch 1500) was studied using HPLC analysis.

HPLC Assays

A size exclusion chromatography method with evaporative light scattering detector was used to measure the release of HPMC. The HPLC column used in this work was a silica-based size exclusion column (Bio-Rad Laboratories) with the following specifications: Bio-Sil SEC 250-5 column, 7.8 mm x 30 cm, 5 μm particle size. The HPMC response was measured using an evaporative light scattering detector (Shimadzu ELSD-LT). In addition to the detector and the column, the chromatographic system also contained two LC-10ADvp pumps, a SIL-10Avp auto-sampler, a DGU-14A Online degasser, a SCL-10Avp system controller, a 100μL Semi-Micro gradient mixer) (all from Shimadzu, Colombia, MD). For data acquisition, an in-house computer system installed with the Atlas software system was used.

The mobile phase used was 0.1M ammonium acetate with pH 6.8. The flow rate was 1.0 ml/min and the injection volume was 50 μl. The ELSD was operated with nitrogen gas maintained at 350 kPa, the nebulizer temperature kept at 70±1 ^{0}C and the gain set at 9. Because the average molecular weight of HPMC used exceeded the molecular weight cut-off of the column, the HPMC retention volume was close to the exclusion limit (5.5 min). The HPMC standards are prepared with the concentration range from 2ppm to 100ppm. The HPMC concentrations were determined by measuring the peak area and comparing with the standard curve of HPMC.

Evaporative Light Scattering Detection (ELSD)

The principle of ELSD operation is shown in Figure IV-1: A nebulizer using an inert gas such as helium or nitrogen creates a plume of droplets. The eluent is evaporated, creating a plume of non-volatile particles, which enters the temperature controlled

evaporation tube. The plume passes through a focused high intensity visible light beam. The light striking the dried particles is scattered and the photons are detected by a photomultiplier tube at a fixed angle from the incident light. Because the evaporative light scattering detector is not a spectroscopic detector, its response does not obey Beer's law (Lafosse 1987). Instead, the light scattering phenomenon is described by three mathematical terms, all of which are influenced by particle size. The observed peak area (A) is related to the quantity of analyte on-column (m) through the relationship

$$A = am^x \qquad \text{Equation IV-1}$$

where x is the slope of the response line and a is the response factor. This data treatment is well established in the literature (Lafosse 1987; Mengerink 1991).

RESULTS AND DISCUSSION

1. Mathematical Model Construction

By envisioning polymer matrix dissolution as consisting of polymer detachment off the matrix followed by diffusion of the dissolved polymer chains through the diffusion layer towards the bulk solution, Ju *et al.* built and tested the following model of polymer erosion (Ju 1995a; Ju 1995b):

$$J_p = f_p \left\langle D_p \right\rangle^{2/3} \nu^{-1/6} \varpi^{1/2} C_{p,dis} \qquad \text{Equation IV-2}$$

where J_p is matrix dissolution flux, f_p is the prefactor, $<D_p>$ is an averaged polymer diffusion coefficient within the diffusion layer, ν is the solvent kinematic viscosity, ϖ is the stirring rate, and $C_{p,\,dis}$ is the polymer disentanglement concentration, defined as the polymer concentration at the gel layer/diffusion layer interface. Among these parameters, only $<D_p>$ and $C_{p,\,dis}$ are properties related to the matrix system.

It is known that the diffusion coefficient of polymers, D_p, is strongly concentration dependent due to the entanglement of polymer chains (Doi 1989). The correlation between D_p and polymer concentration, combined with the significant polymer concentration variation, justifies the need to employ an average polymer diffusion coefficient, $<D_p>$, within the diffusion layer to model the polymer dissolution flux. Assuming the concentration profile of the polymer within the diffusion layer is close to that of small molecules dissolved from a rotating disk, it was described by Levich (Levich 1962) as:

$$C_p(r) = C_{p,dis} \frac{\int_0^r e^{-u^3} du}{\int_0^\infty e^{-u^3} du} \qquad \text{Equation IV-3}$$

As demonstrated by Ju *et al.*(Ju 1997), the $C_p(r)$ profile in the diffusion layer exhibits a linear decline with distance away from the gel layer/diffusion layer interface, except when the diffusion layer/bulk solution interface is approached and the profile becomes less linear. To simplify the mathematics, we further assumed the concentration profile is linear, so

$$C_p(r) = C_{p,dis} \frac{r}{L} \qquad \text{Equation IV-4}$$

where L is the diffusion layer thickness, and r is the distance away from the gel layer/diffusion layer interface. Furthermore, Ju *et al.* (Ju 1997) found that the polymer diffusion coefficient has the following relationship with polymer concentration:

$$D_p = D_{p,0}(1+[\eta]_p C_p/8)^{-2} \qquad \text{Equation IV-5}$$

where $D_{p,0}$ is the diffusion coefficient of the polymer in a dilute solution and $[\eta]_p$ is the polymer intrinsic viscosity. Based on Equation IV-4 and IV-5, we are able to calculate $<D_p>$ as

$$\langle D_p \rangle = \frac{\int_0^L D_p(r) r dr}{\int_0^L r dr} = \frac{2D_{p,0}}{L^2}\int_0^L \frac{r}{(1+\alpha r)^2} dr \qquad \text{Equation IV-6}$$

and $$\alpha = \frac{[\eta]_p C_{p,dis}}{8L} \qquad \text{Equation IV-7}$$

Integrating the right side of Equation IV-6 leads to

$$\langle D_p \rangle = \frac{2D_{p,0}}{(\alpha L)^2}\left[\ln(1+\alpha L) + \frac{1}{1+\alpha L} - 1\right] \qquad \text{Equation IV-8}$$

or

$$\langle D_p \rangle = \frac{2D_{p,0}}{([\eta]_p C_{p,dis}/8)^2}\left[\ln(1+[\eta]_p C_{p,dis}/8) + \frac{1}{1+[\eta]_p C_{p,dis}/8} - 1\right] \qquad \text{Equation IV-9}$$

Based on Equation IV-2 and IV-9, we can see that the polymer dissolution flux is a function of the polymer disentanglement concentration, i.e. $C_{p,dis}$. Therefore, our objective now is to correlate the gel strength with polymer disentanglement concentration.

The viscosity of a polymer solution is, in general, related to C_p as follows (Dow Chemical):

$$\eta \approx \eta_s (1+[\eta]_p C_p / 8)^8 \qquad \text{Equation IV-10}$$

As our preliminary study has shown, the gel strength derived from TA is proportional to the viscosity of the gel, so

$$G_{p,dis} = K(1+[\eta]_p C_{p,dis} / 8)^8 \qquad \text{Equation IV-11}$$

or

$$\frac{[\eta]_p C_{p,dis}}{8} = \left(\frac{G_{p,dis}}{K}\right)^{1/8} - 1 \qquad \text{Equation IV-12}$$

here K is the proportion constant between gel strength and viscosity of the gel. Now Equation IV-9 can be rearranged into:

$$\langle D_p \rangle = \frac{2D_{p,0}}{\left(\left(\frac{G_{p,dis}}{K}\right)^{1/8} - 1\right)^2}\left[\frac{1}{8}\ln\left(\frac{G_{p,dis}}{K}\right) + \left(\frac{G_{p,dis}}{K}\right)^{-1/8} - 1\right] \qquad \text{Equation IV-13}$$

In reality it is not possible to get $G_{p,dis}$ before knowing $C_{p,dis}$. A method to obtain $C_{p,dis}$ using TA will be described below. Both theory and our previous experimental results showed that there is a power-law relationship between the viscosity/gel strength and concentration of polymer solution in good solvent above $C_{p,dis}$ as we demonstrated in Chapter II:

$$G = kC_p^{\beta} \qquad \text{Equation IV-14}$$

Hence, if we measure the gel strength (G_{exp}) at a polymer concentration higher than $C_{p,dis}$, the following relationship should be existed:

$$\frac{G_{p,\exp}}{G_{p,dis}} = \left(\frac{C_{p,\exp}}{C_{p,dis}}\right)^{\beta} \qquad \text{Equation IV-15}$$

Therefore, for system 1 and 2 (1 is a reference system with known $C_{p,dis}$), at the same polymer concentration (C_{exp}), the following equations can be obtained similarly:

$$\frac{G_{1,\exp}}{G_{1,dis}} = \left(\frac{C_{\exp}}{C_{1,dis}}\right)^{\beta_1} \qquad \text{Equation IV-16}$$

and

$$\frac{G_{2,\exp}}{G_{2,dis}} = \left(\frac{C_{\exp}}{C_{2,dis}}\right)^{\beta_2} \qquad \text{Equation IV-17}$$

Dividing Equation IV-16 by IV-17 leads to

$$\frac{G_{1,\exp}}{G_{2,\exp}} = \frac{C_{2,dis}^{\ \beta_2}}{C_{1,dis}^{\ \beta_1}} \left(C_{\exp}\right)^{\beta_1-\beta_2} \left(\frac{G_{1,dis}}{G_{2,dis}}\right) \qquad \text{Equation IV-18}$$

By substituting Equation IV-11 into IV-18, we obtained

$$\frac{G_{1,\exp}}{G_{2,\exp}} = \frac{C_{2,dis}^{\ \beta_2}}{C_{1,dis}^{\ \beta_1}} \left(C_{\exp}\right)^{\beta_1-\beta_2} \left(\frac{1+[\eta]_{p,1} C_{1,dis}/8}{1+[\eta]_{p,2} C_{2,dis}/8}\right)^{8} \qquad \text{Equation IV-19}$$

Equation IV-19 provides a convenient and theoretical basis for estimating the polymer disentanglement concentration. After a reference (denoted as 1) is selected, its polymer disentanglement concentration can be obtained from literature. $G_{1,exp}$ (reference) and $G_{2,exp}$ (test system) can be obtained from TA experiments, and thus $C_{2,dis}$ can be calculated according to Equation IV-19. The calculated polymer disentanglement concentration is then substituted into Equation IV-2 to calculate the polymer dissolution

flux. Equation IV-19 also implies that the polymer disentanglement concentration is directly correlated to the gel strength.

2. Model Validation

2.1. Effect of HPMC Viscosity Grade on HPMC Dissolution

A typical SEC-HPLC-ELSD chromatogram of HPMC K15M was shown in Figure IV-2. Since the average molecular weight of HPMC K15M exceeded the molecular weight cut-off of the column, the HPMC retention volume was close to the exclusion limit (5.5 min). This is in agreement with a previous study (Sung 1996). The concentrations of the HPMC K15M standards were between 2 ppm and 100 ppm. The peak area of each concentration was measured to establish the standard curve, as shown in Figure IV-3. In agreement with Equation IV-1, logarithm of peak area linearly increased with logarithm of HPMC concentration. HPMC concentrations of each sample were then determined by measuring the peak area and comparing with the standard curve.

We also measured the HPMC K15M dissolution using gravimetric method, and found that the data was identical to the result obtained by SEC-HPLC-ELSD method. For the data reported below, gravimetric method was used for the dissolution of HPMC K100M, K15M, K4M, K100LV and K15M/Starch 1500. SEC-HPLC-ELSD analysis was used for the dissolution of HPMC K15M, K15M/Starch 1500, K15M/lactose and K15M/SDS.

The dissolution of HPMC with four viscosity grades K100M, K15M, K4M and K100LV was shown in Figure IV-4. Since it is one dimensional dissolution, the dissolution amount was linear with the dissolution time for all the samples; therefore, the

dissolution rate could be extracted from the slope of the line. The data was listed in Table IV-1.

As we discussed in Chapter II, the gel strength of HPMC follows a power-law relationship with polymer concentration. Using the parameters obtained from the power-low relationship, disentanglement concentrations for HPMCs of various viscosity grades could be determined based on Equation IV-19. The disentanglement concentration of HPMC K4M, 5%, was used as a reference (Ju 1995a). As such, disentanglement concentrations for all other viscosity grades were calculated accordingly and the corresponding values were listed in Table IV-1. The experimental concentration was chosen as 20% for all the viscosity grades and it was verified that the calculated disentanglement concentration was not affected by the selection of experimental concentration as it is supposed to be.

Based on Table IV-1, HPMC disentanglement concentration as a function of the molecular weight was plotted in Figure IV-5. A power-law relationship was derived using linear regression, and the value of the power exponent was –0.68. Ju *et al.* (Ju 1995a) also proposed a power-law relationship between disentanglement concentration and the molecular weight of HPMC by assuming that the disentanglement concentration obeyed the same scaling law as overlapping concentration in polymer solution. The power they derived was –0.8. The agreement between these two exponents suggested that the gel strength derived from Texture Analyzer measurement is reliable and TA is a proven and convenient tool for measuring the disentanglement concentration, a key parameter for polymer dissolution. The slight difference of the two exponents might be attributed to several reasons. First, as the authors pointed out in their paper (Ju 1995a), the overlapping concentration is far below the disentanglement concentration; therefore, powers for

overlapping and disentanglement concentrations could be different. Secondly, we assumed that polymer viscosity at disentanglement concentration can be described either by Equation IV-10 as in concentrated polymer solution or from gel strength data as in gel state. Such extrapolations might bring some deviations.

Once the disentanglement concentration was determined, the ratio of (average diffusion coefficient in the diffusion layer) over (the diffusion coefficient in bulk solution) could be determined using Equation IV-9 and the intrinsic viscosity data was obtainable from the Dow Chemical's technical handbook. The data were also listed in Table IV-1. The ratios decrease with increase of molecular weight, but they are all very close to unity. This indicates that the effect of polymer concentration on the self-diffusion was not significant. The diffusion coefficient of HPMC in water was estimated using the following equation (Ju 1997).

$$D_{p.0} = 7.4 \times 10^{-5} \times M_n^{-0.6} \qquad \text{Equation IV-20}$$

The dissolution rates of HPMC for all the viscosity grades were calculated based on Equation IV-2. To eliminate the prefactor and other constants in Equation IV-2, the dissolution rate of HPMC K4M was used as a reference. The results were listed in Table IV-1. Both theoretical calculation and experimental measurements of HPMC dissolution rates were compared and plotted as function of molecular weight in Figure IV-6. As we can see, model predictions were in good agreement with experimental data. A power-law relationship exists between dissolution rate and the molecular weight, as reported elsewhere (Ju 1995a). The power obtained from theoretical calculation was –1.09, similar to the experimental value of -1.0. This difference could be attributed to several reasons: 1) The dissolution was not strictly on the interface of gel/diffusion layer, a prerequisite for the validity of Equation IV-2; 2) The diffusion coefficients of HPMC estimated using

Equation IV-20 might cause some variations. 3) The polydispersity effect was not taken into the consideration in the model. Polydispersity is expected to affect both the diffusion coefficient and the disentanglement concentration. Nevertheless, the overall agreement between the experimental data and model prediction was satisfactory.

2.2. Effect of Excipient Type and Content on HPMC Dissolution

As we discussed in Chapter II, the addition of lactose did not have effect on HPMC K15M gel strength. Based on our model, HPMC dissolution rate would not be affected by the presence of lactose, this was verified experimentally, as shown in Figure IV-7. Several groups have investigated the effect of lactose on HPMC dissolution (Ju 1995a; Sung 1996). Ju *et al.* (Ju 1995a) proposed to use "apparent molecular weight" to explain the effects of non-polymer ingredients (excipients and drug molecules) on the dissolution of HPMC from a formulation. The apparent molecular weight was defined as the weight average molecular weight of HPMC and lactose. The authors found that the dissolution rate of HPMC K4M was inversely linearly to the apparent molecular weight. The dissolution rate in their study was expressed as the ratio of release amount of HPMC to the amount of dry tablet. After converting the release fraction to the absolute amount of HPMC release, we found their data also suggested that HPMC release amount in given time interval was independent on the content of lactose for all the formulations they investigated. Sung *et al.*(Sung 1996) also investigated the effect of lactose content on the release of HPMC K4M. Their result was shown in Figure IV-8 (a), where HPMC release was expressed as the percent of initial dry weight. After converting such release fraction to the absolute amount of HPMC released at 3 and 6 hours, we found that the release amount did not change with the lactose content as shown in Figure IV-8 (b).

The effect of lactose on HPMC dissolution is a good example to demonstrate that HPMC dissolution rate was only affected by the polymer disentanglement concentration and thus potentially gel strength. It suggested that lactose exerted insignificant impact on the gel properties of HPMC-based tablets. Upon the tablet contacts with the dissolution medium, water molecules start to diffuse into the HPMC/lactose matrix and dissolve lactose molecules, which further diffuse out of the matrix and leave HPMC behind. Therefore, at the interface of gel/dissolution medium, lactose concentration is very low, and HPMC disentanglement concentration should be the same as that of pure HPMC tablets. As a result, HPMC dissolution rate would be same, as long as there is enough polymer in the matrix to maintain the shape of the tablet.

On the other hand, addition of SDS into HPMC gels increased the gel strength, as we discussed in Chapter II. Based on our model, SDS would be expected to retard the dissolution rate of HPMC K15M. However, this did not agree with experimental data, as shown in Figure IV-9. For all three ratios of HPMC/SDS (15:1, 15:2 and 15:3) investigated, the dissolution rates of HPMC K15M were identical to that of a pure HPMC tablet. This is not surprising if we use the same argument as in the case of HPMC/lactose. Since SDS is small molecule and will diffuse out of the matrix prior to the dissolution of HPMC, SDS concentration at the interface of gel/dissolution medium was very low. Previous study (Nilsson 1995) showed that SDS adsorption to the HPMC chain only occurred when SDS concentration was above a critical adsorption concentration. Therefore, SDS molecules at the interface of gel/diffusion layer are very likely in solution state, having minimum effect on HPMC disentanglement concentration, same as lactose. As a result, SDS content had no effect on HPMC dissolution rate at all.

Based on the above argument, in order for the excipient to affect HPMC disentanglement concentration, the excipient should not diffuse out of the matrix prior to HPMC dissolution. In this regard, Starch 1500 is an ideal excipient, since it is only partially soluble and has much larger size than SDS and lactose. We used both gravimetric method and SEC-HPLC-ELSD analysis to measure the dissolution of HPMC from tablets having the binary mixtures of HPMC K15M and Starch 1500. It was found that Starch 1500 did not significantly contribute to the ELSD signal probably because it was filtered out before entering the column. Therefore, ELSD signal was only contributed by HPMC in the sample. On the other hand, the gravimetric method measured the total amount of HPMC and starch released from the tablet. The ratio of HPMC detected by the ELSD to the total release amount measured by gravimetric method was identical to the ratio in the original tablet, indicating that HPMC and starch dissolve simultaneously at the interface of gel/dissolution medium.

HPMC K 15M release from tablets containing HPMC and starch was shown in Figure IV-10. The HPMC/starch ratios studied were 1:2, 1:1 and 2:1, the same as those studied in homogeneous gel systems in Chapter II. For the purpose of comparison, the release rate of pure HPMC K15M tablet was also shown in the figure. Once again, since it is one dimensional dissolution and the surface area of tablet was maintained constant during the experiment, the HPMC release linearly increased with time. Therefore, the release rate was extracted from the slope of the lines shown in Figure IV-10. Apparently, presence of Starch 1500 in the tablets has significantly modulated the release profiles of HPMC, which is in line with the model prediction since Starch 1500 increases the gel strength of HPMC.

The effect of starch content on HPMC gel strengths was discussed in Chapter II in details. The constant and the exponent obtained from the curve fitting were listed in Table IV-2. Based on Equation IV-19, disentanglement concentrations of HPMC K15M at different Starch 1500 levels were calculated. The calculated $C_{p,dis}$ values of HPMC K15M were plotted as a function of the ratio of HPMC to Starch 1500 in Figure IV-11, where the presence of starch was shown to decrease the disentanglement concentration of HPMC.

After the disentanglement of HPMC K15M and starch, the effect of starch on HPMC diffusion would be very minimal considering the nature of partially soluble Starch 1500, therefore, the intrinsic viscosity of the mixture of HPMC and starch would be the same as that of pure K15M. Therefore, the average diffusion constants of HPMC at different Starch 1500 concentrations could be determined using Equation IV-13 and the results were summarized in Table IV-2. As we can see, the ratio of average diffusion constant in diffusion layer to the diffusion constant in solvent was close to unity due to low disentanglement concentration of HPMC. Based on Equation IV-2, the release rate of HPMC would be proportional to the disentanglement concentration of HPMC, and it was verified in Figure IV-12.

After knowing the disentanglement concentration and average diffusion constant, we are able to calculate the release rate based on Equation IV-2. To get ride of the effects of prefactor and the parameters that were kept constant during the experiments, all release rates were calculated using pure HPMC K15M as a reference. The results were listed in Table IV-2 and plotted in Figure IV-13. The experimental release rates of pure HPMC K15M and the mixture of HPMC and Starch 1500 were also shown in Figure IV-13 and the model predictions were in good agreement with experimental data.

CONCLUSIONS

A mathematical model was constructed to correlate HPMC dissolution rate and HPMC gel strength through HPMC disentanglement concentration, $C_{p,dis}$. Effects of HPMC viscosity grade, excipient type, and excipient content on HPMC dissolution were studied to validate the model, while $C_{p,dis}$ was calculated using the model and TA gel strength data. A power-law relationship was found between HPMC disentanglement concentration and HPMC molecular weight and the exponent value was in agreement with previous literature results. Further, a power-law relationship between HPMC dissolution rate and molecular weight was found experimentally, consistent with both model predictions and literature results. HPMC K15M dissolution was also found to be independent of the content of lactose and SDS, but was retarded by Starch 1500. Therefore, gel strength was successfully correlated to polymer erosion through the polymer disentanglement concentration. Texture Analyzer demonstrated to be a new, reliable, and convenient method to estimate the polymer disentanglement concentration.

REFERENCES

Alderman D. A. (1984). "A review of cellulose ethers in hydrophilic matrices for oral controlled-release dosage forms." Int. J. Pharm. Tech. Prod. Mfr. **5**: 1-9.

Bonferoni M. C., Caramella C., Sangalli M. E., Conte U., Hernandez R. M. and Pedraz J. L. (1992). "Rheological behaviour of hydrophilic polymers and drug release from erodible matrixes." Journal of Controlled Release **18**: 205-212.

Brochard F. and de Gennes P. G. (1983). "Kinetics of polymer dissolution." Phys Chem Hydrodynam **4**(4): 313-322.

Churms S. C. (1996). "Recent progress in carbohydrate separation by high-performance liquid chromatography based on size exclusion." Journal of Chromatography **720**(1+2): 151-166.

Colombo P., Gazzaniga A., Caramella C., Conte U. and La Manna A. (1987). "In vitro programmable zero-order release drug delivery system." Acta Pharmaceutica Technologica **33**(1): 15-20.

Conte U., Colombo P., Gazzaniga A., Sangalli M. E. and La Manna A. (1988). "Swelling-activated drug delivery systems." Biomaterials **9**(6): 489-493.

de Gennes P. G. (1979). Scaling Concepts in Polymer Physics. Ithaca, NY, Cornell University Press.

de Gennes P. G. and Leger L. (1982). "Dynamics of entangled polymer chains." Annu. Rev. Phys. Chem. **33**: 49-61.

Devotta I., Ambeskar V. D., Mandhare A. B. and Mashelkar R. A. (1994). "The life time of a dissolving polymeric particle." Chem Eng Sci **49**(5): 645-654.

Devotta I., Badiger M. V., Rajamohanan P. R., Ganapathy S. and Mashelkar R. A. (1995). "Unusual retardation and enhancement in polymer dissolution: role of disengagement dynamics." Chem Eng Sci **50**(16): 2557-2569.

Doelker E. L. (1987). Water-swollen cellulose derivatives in pharmacy. Hydrogels in Medicine and Pharmacy. N. A. Peppas. Boca Raton, FL, CRC Press. **2:** 115-160.

Doi M. and Edwards S. F., Eds. (1989). The Theory of Polymer Dynamics. Chapter 5. Oxford, Clarendon.

Durig T. and Fassihi R. (2002). "Guar-based monolithic matrix systems: effect of ionizable and non-ionizable substances and excipients on gel dynamics and release kinetics." Journal of Controlled Release **80**: 45-56.

Harland R. S., Gazzaniga A., Sangalli M. E., Colombo P. and Peppas N. A. (1988). "Drug/polymer matrix swelling and dissolution." Pharmaceutical Research **5**: 488-494.

Herbreteau B., Lafosse M., Morin-Allory L. and Dreux M. (1992). "High performance liquid chromatography of raw sugars and polyols using bonded silica gels." Chromatographia **33**(7-8): 325-330.

Herman M. F. and Edwards S. F. (1990). "A repetition model for polymer dissolution." Macromolecules **23**(15): 3662-3671.

Iwayanagi T., Ueno T., Nonogaki S., Ito H. and Willson C. G. (1988). Materials and processes for deep-UV lithography. Electronic and Photonic Applications of Polymers. **218:** 109-224.

Johnson D. C. and LaCourse W. R. (1990). "Liquid chromatography with pulsed electrochemical detection at gold and platinum electrodes." Analytical Chemistry **62**(10): 589A-597A.

Ju R. T. C., Nixon P. R. and Patel M. V. (1995a). "Drug release from hydrophilic matrixes 1. New scaling laws for predicting polymer and drug release based on the polymer disentanglement concentration and the diffusion layer." Journal of Pharmaceutical Sciences **84**(12): 1455-1463.

Ju R. T. C., Nixon P. R. and Patel M. V. (1997). "Diffusion coefficients of polymer chains in the diffusion layer adjacent to a swollen hydrophilic matrix." Journal of Pharmaceutical Sciences **86**(11): 1293-1298.

Ju R. T. C., Nixon P. R., Patel M. V. and Tong D. M. (1995b). "Drug release from hydrophilic matrices. 2. A mathematical model based on polymer disentanglement concentration and the diffusion layer." Journal of Pharmaceutical Sciences **84**(12): 1464-1477.

Ju R. T. C., Nixon P. R., Patel M. V. and Tong D. M. (1995c). "A mechanistic model for drug release from hydrophilic matrices based on the structure of swollen matrices." Proceedings of the International Symposium on Controlled Release of Bioactive Materials. **22**: 59-60.

Kesting R. E. and Fritzsche A. K. (1993). Polymeric Gas Separation Membranes., NY: Wiley.

Koida Y., Takahata H., Kobayashi M. and Samejime M. (1987). "Studies on dissolution mechanism of drugs from ethylcellulose microcapsules." Chem. Pharm. Bull. **35**: 1538-1545.

Lafosse M., Dreux M. and Morin-Allory L. (1987). "Application fields of a new evaporative light scattering detector for high-performance liquid chromatography and supercritical fluid chromatography." Journal of Chromatography **404**(1): 95-105.

Langer R. and Vacanti J. P. (1995). "Artificial organs." Scientific American **273**(3): 130-133.

Levich V. G., Ed. (1962). Physicochemical Hydrodynamics. Englewood Cliffs, NJ,, Prentice-Hall.

Mengerink Y., De Man H. C. J. and Van der Wal S. (1991). "Use of an evaporative light scattering detector in reversed-phase high-performance liquid chromatography of oligomeric surfactants." Journal of Chromatography **552**(1-2): 593-604.

Narasimhan B. and Mallapragada S. K. (1998). "Dissolution of amorphous and semicrystalline polymers: mechanisms and novel applications." Recent Research Developments in Macromolecules Research **3**(Part 2): 311-324.

Narasimhan B. and Peppas N. A. (1996a). "Disentanglement and reptation during dissolution of rubbery polymers." journal of polymer science:part B: polymer physics **34**: 947-961.

Narasimhan B. and Peppas N. A. (1996b). "On the importance of chain reptation in models of dissolution of glassy polymers." Macromolecules **29**: 3283-3291.

Nauman E. B. and C. L. J. (1994). US.

Nilsson S. (1995). "Interactions between water-soluble cellulose derivatives and surfactants. 1. The HPMC/SDS/Water system." Macromolecules **28**: 7837-7844.

O'Brien M. J. and Soane D. S. (1989). Microelectronics Processing: Chemical Engineering Aspects, American Chemical Society: Washington, DC.

Ouano A. C. and Carothers F. A. (1980). "Dissolution dynamics of some polymers: solvent-polymer boundaries." Polym. Eng. Sci. **20**(2): 160-166.

Ozturk S. S., Palsson B. O. and Dressman J. B. (1988a). "Dissolution of ionizable drugs in buffered and unbuffered solutions." Pharmaceutical Research **5**: 272-282.

Ozturk S. S., Palsson B. O. and Dressman J. B. (1988b). "Kinetics of release from enteric-coated tablets." Pharmaceutical Research **5**: 550-565.

Papanu J. S., Hess D. W., Bell A. T. and Soane D. S. (1989). "In situ ellipsometry to monitor swelling and dissolution of thin polymer films." J. Electrochem. Soc **136**(4): 1195-1200.

Pappas N. A. and Langer R. (1994). "New challenges in biomaterials." Science **263**(5154): 1715-1720.

Peppas N. A., Wu J. C. and Von Meerwall E. D. (1994). "Mathematical modeling and experimental characterization of polymer dissolution." Macromolecules **27**: 5626-5638.

Siepmann J., K ranz H ., Bodmeier R. a nd P eppas N. A. (1999a). " HPMC-matrices for controlled drug deliver: a new model combining diffusion, swelling, and dissolution mechanisms and predicting the release kinetics." Pharmaceutical Research **16**(11): 1748-1756.

Siepmann J., Kranz H., Peppas N. A. and Bodmeier R. (2000a). "Calculation of the required size and shape of hydroxypropyl methylcellulose matrices to achieve desired drug release profiles." International Journal of Pharmaceutics **201**: 151-164.

Siepmann J. and Peppas N. A. (2000b). "Hydrophilic matrices for controlled drug delivery: an improved mathematical model to predict the resulting drug release kinetics (the "Sequential Layer" model)." Pharmaceutical Research **17**(10): 1290-1298.

Siepmann J. and Peppas N. A. (2001). "Modeling of drug release from delivery systems based on hydroxypropyl methylcellulose (HPMC)." Advanced Drug Delivery Reviews **48**(2-3): 139-157.

Siepmann J ., P odual K., Sriwongjanya M. and Peppas N. A. (1999b). "A new m odel describing the swelling and drug release kinetics from hydroxypropyl methylcellulose tablets." Journal of Pharmaceutical Sciences **88**: 65-72.

Siepmann J., Streubel A. and Peppas N. A. (2002). "Understanding and predicting drug delivery from hydrophilic matrix tablets using the "Sequential Layer" model." Pharmaceutical Research **19**(3): 306-314.

Skoug J. W., Mikelsons M. V., Vigneron C. N. and Stemm N. L. (1993). "Qualitative evaluation of the mechanism of release of matrix sustained release dosage forms by measurement of polymer release." Journal of Controlled Release **27**: 227-245.

Srivastava A. P. and Nauman B. E. (1993). "Kinetics of solvent induced melting of semicrystalline polymers." Polymeric Materials Science and Engineering **69**: 307-308.

Sung K. C., Nixon P. R., Skoug J. W., Ju T. R., Gao P., Topp E. M. and Patel M. V. (1996). "Effect of formulation variables on drug and polymer release from HPMC-based matrix tablets." International Journal of Pharmaceutics **142**(1): 53-60.

Tahara K., Yamamoto K. and Nishihata T. (1995). "Overall mechanism behind matrix sustained release (SR) tablets prepared with hydroxypropylmethylcellulose 2910." J. Controlled Release **35**: 59-66.

Tsay C. S. and McHugh A. J. (1990). "Mass transfer modeling of asymmetric membrane formation by phase inversion." J. Polym. Sci. **28**(8): 1327-1365.

Tu Y.-O. and Ouano A. C. (1977). "Model for the kinematics of polymer dissolution." IBM J Res Develop **21**(2): 131-142.

Ueberreiter K. (1968). Diffusion in Polymers. New York, Academic Press.

Vrentas J. S. and Vrentas C. M. (1998). "Dissolution of rubbery and glassy polymers." J. Polym. Sci., B, Polym Phys **36**(14): 2607-2614.

Vrentas J. S. and Vrentas C. M. (2004). "Diffusion-controlled polymer dissolution and drug release." Journal of Applied Polymer Science **93**: 92-99.

Weisenberger L. A. and Koenig J. L. (1989). "NMR imaging of solvent diffusion in polymers." Appl Spectrosc **43**: 1117-1126.

Table IV-1 The parameters used for the calculation of disentanglement concentration of HPMC of four viscosity grades and the corresponding results.

Parameters	K100M	K15M	K4M	K100LV
Intrinsic Viscosity, η_p(dL/g)	19.2	11.0	7.5	2.6
Molecular Weight, M_n (kDa)	267	134	96	29
Gel strength at 20% (w/w), G (g/mm^2)	7.643	4.497	2.591	0.867
Disentanglement Conc., $C_{p.dis}$ (%w/w)	2.52	3.65	5.00	11.24
$<D_p>/D_{p.0}$	0.925	0.937	0.941	0.953
Dissolution rate, J_p (mg/hr)	0.880	1.695	2.660	9.738

Table IV-2 The parameters used for the calculation of disentanglement concentration of HPMC K15M with the presence of Starch 1500 and the corresponding results.

Parameters	K15M	K15M:Starch = 2:1	K15M:Starch =1:1	K15M:Starch =1:2
Intrinsic Viscosity, η_p(dL/g)	11.0	11.0	11.0	11.0
Gel strength at 5% (w/w), G (g/mm^2)	0.027	0.105	0.398	2.735
Disentanglement Conc., $C_{p,dis}$ (%)	3.65	3.01	2.28	1.54
$<D_p>/D_{p,0}$	0.937	0.947	0.960	0.972
Dissolution rate, J_p (mg/hr)	1.88	1.56	1.19	0.81

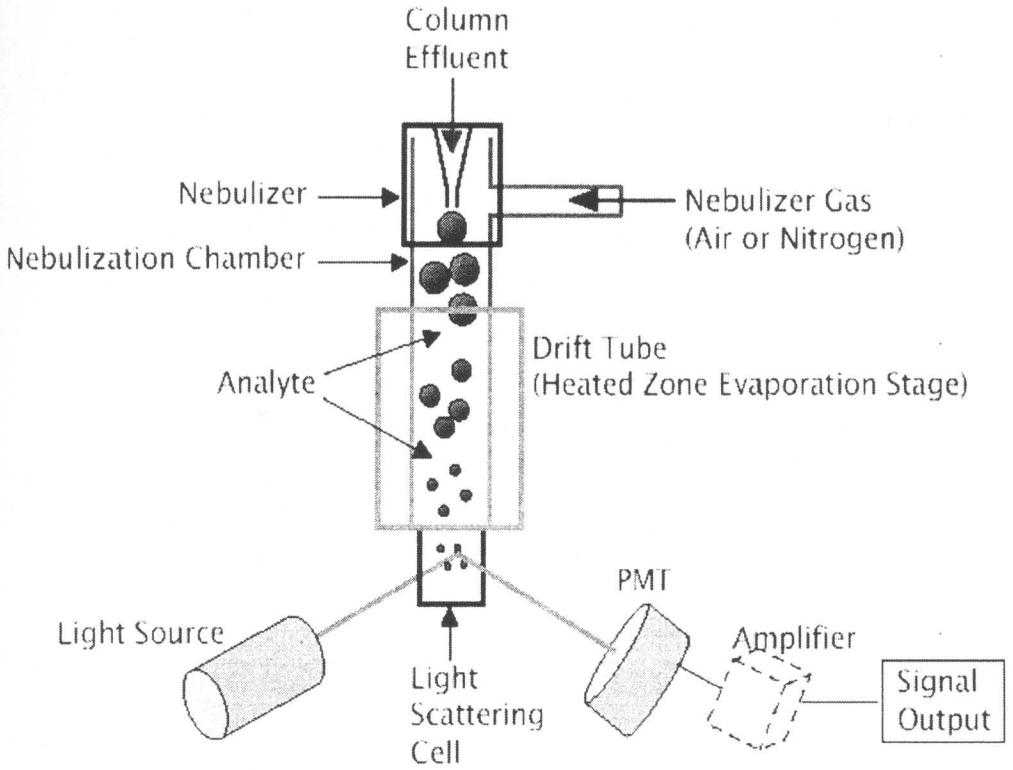

Figure IV-1 The schematic illustration of evaporative light scattering detector (ELSD).

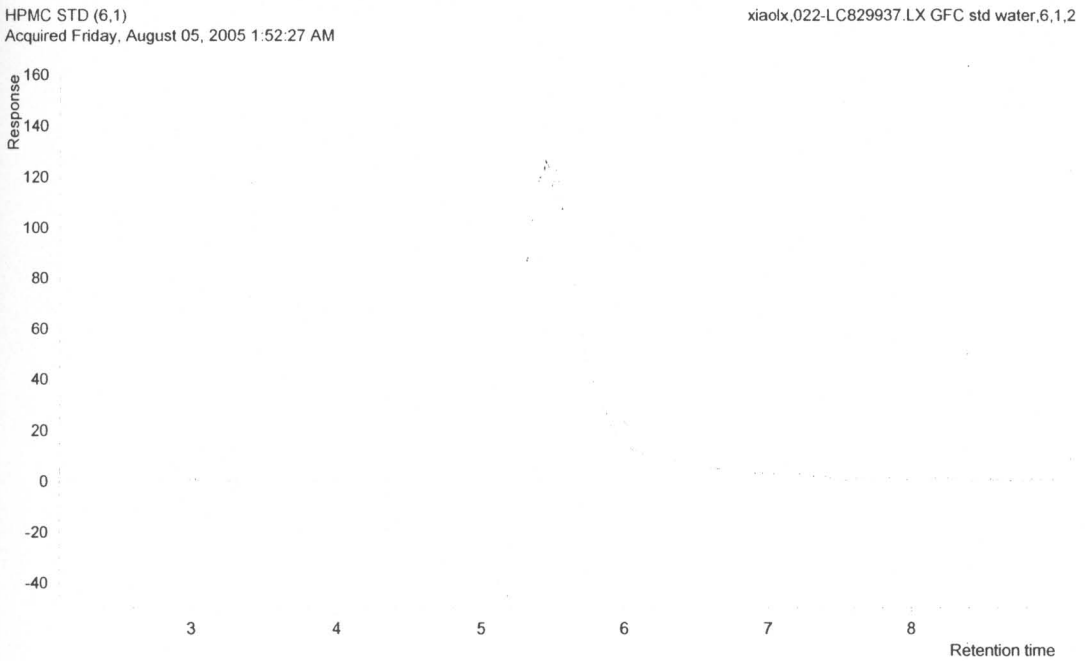

Figure IV-2 A typical chromatogram of HPMC K15M detected by SEC-HPLC-ELSD.

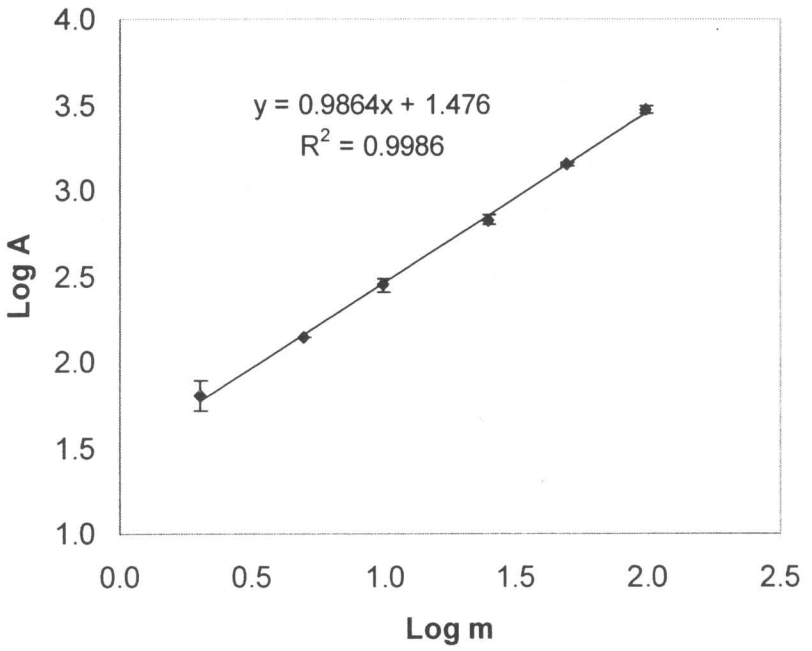

Figure IV-3 The standard curve of peak area of ELSD and the concentration of HPMC K15M.

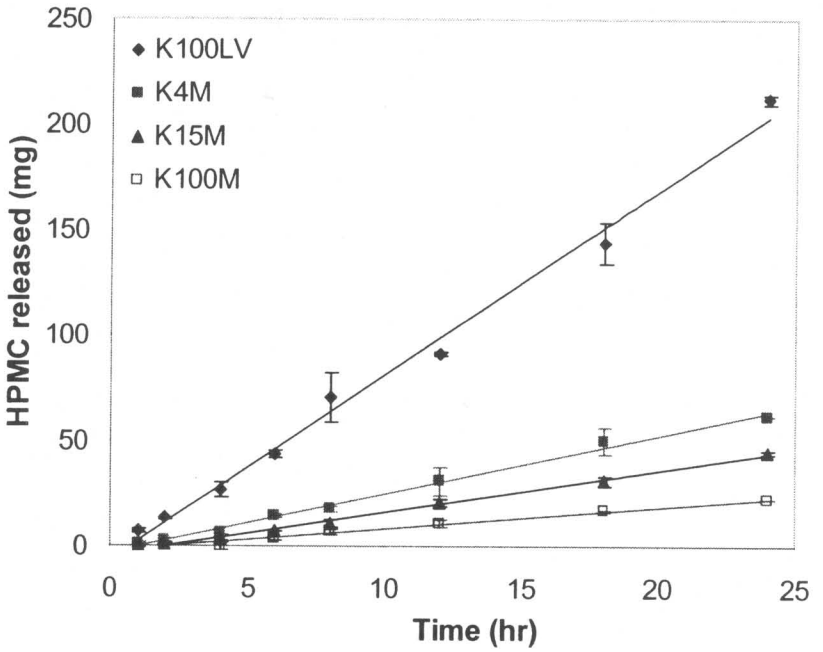

Figure IV-4 One dimensional dissolution kinetics of HPMC with four viscosity grades.

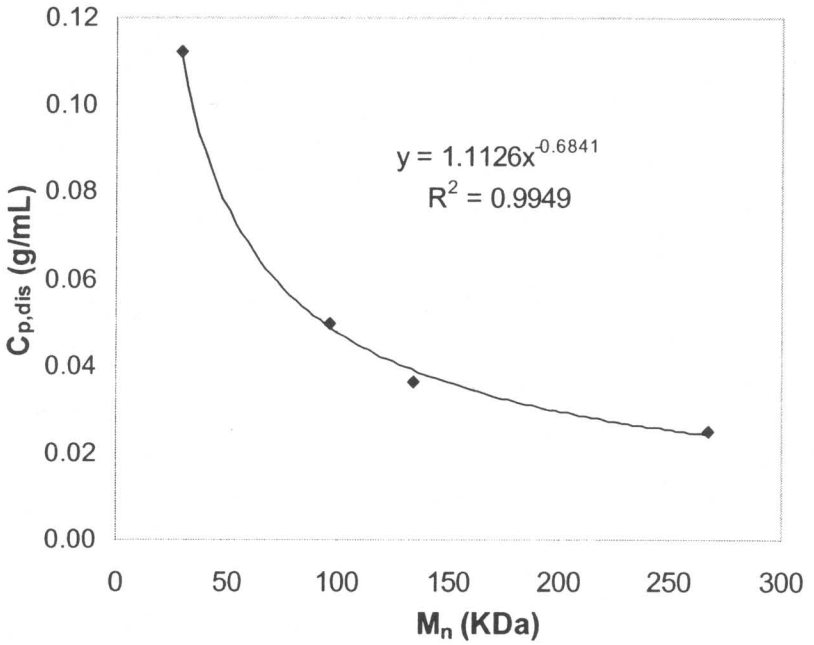

Figure IV-5 The effect of HPMC molecular weight on the disentanglement concentration. The disentanglement concentration was calculated based on Equation IV-19.

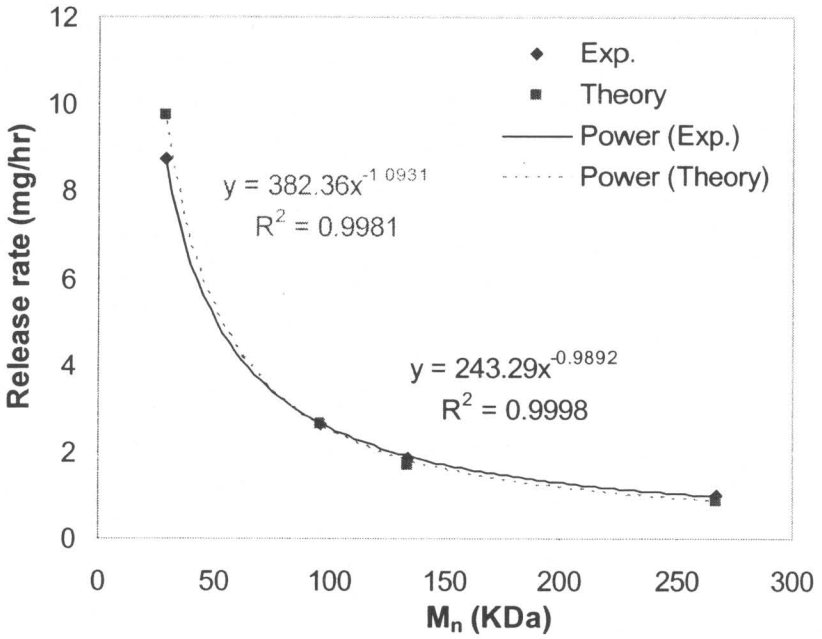

Figure IV-6 The effect of molecular weight on HPMC dissolution rate. The experimental data and the theoretical predictions were compared.

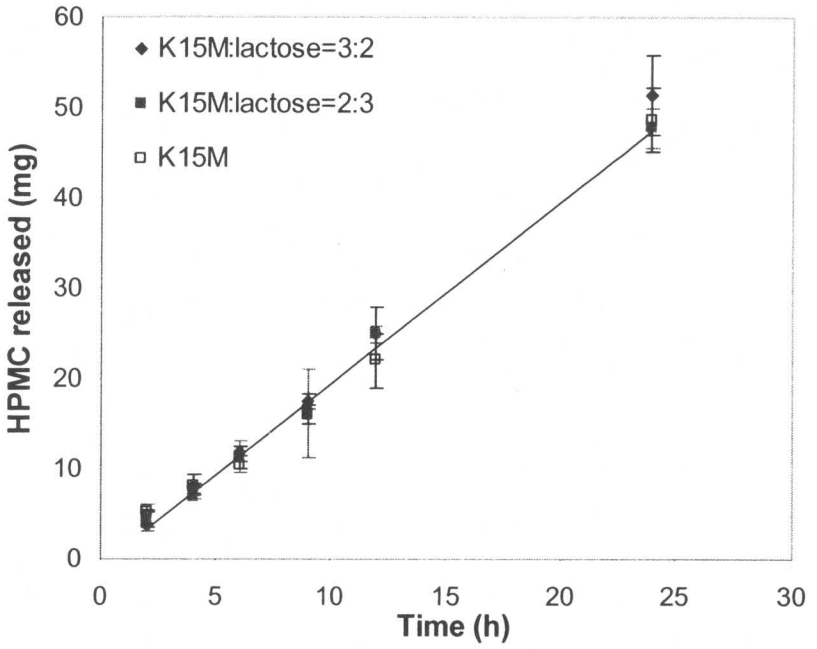

Figure IV-7 Effect of lactose on HPMC K15M release.

(a)

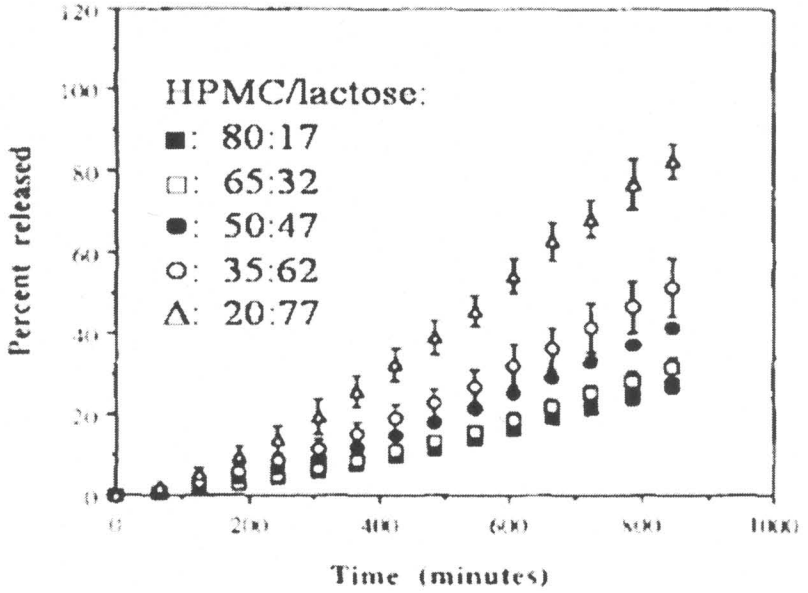

(b)

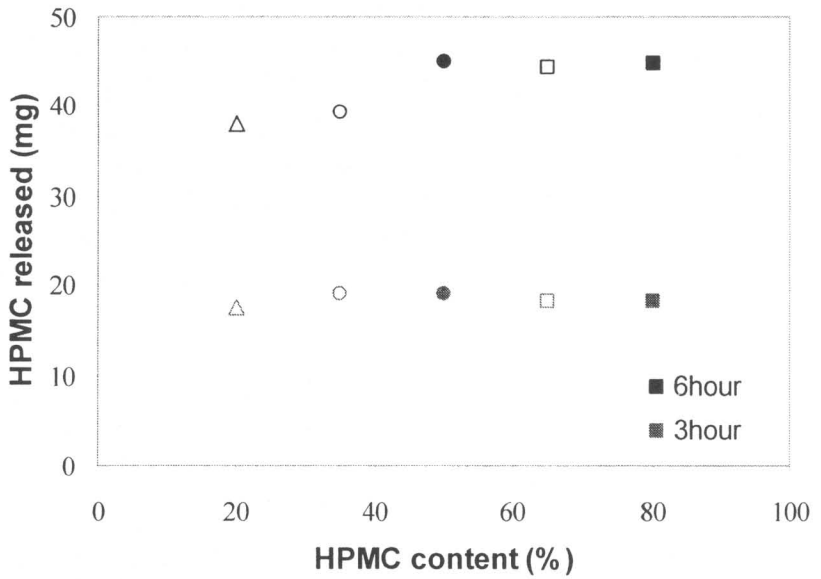

Figure IV-8 Lactose effect on HPMC K4M erosion. (a) % HPMC release at different HPMC/lactose ratios. (data adapted from (Sung 1996)) (b) Absolute HPMC released as a function of HPMC content at 3 hour and 6 hour.

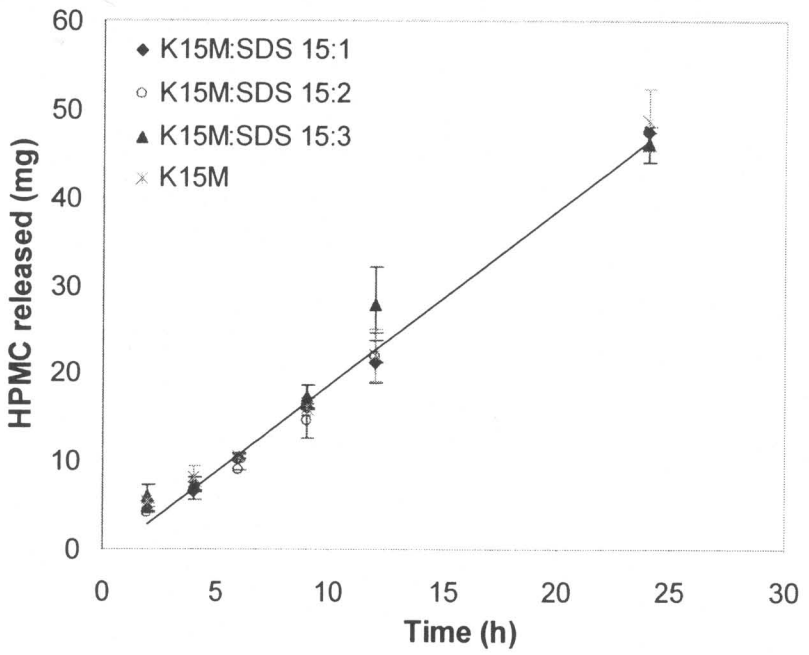

Figure IV-9 Effect of SDS on the release of HPMC K15M at different K15M:SDS ratios.

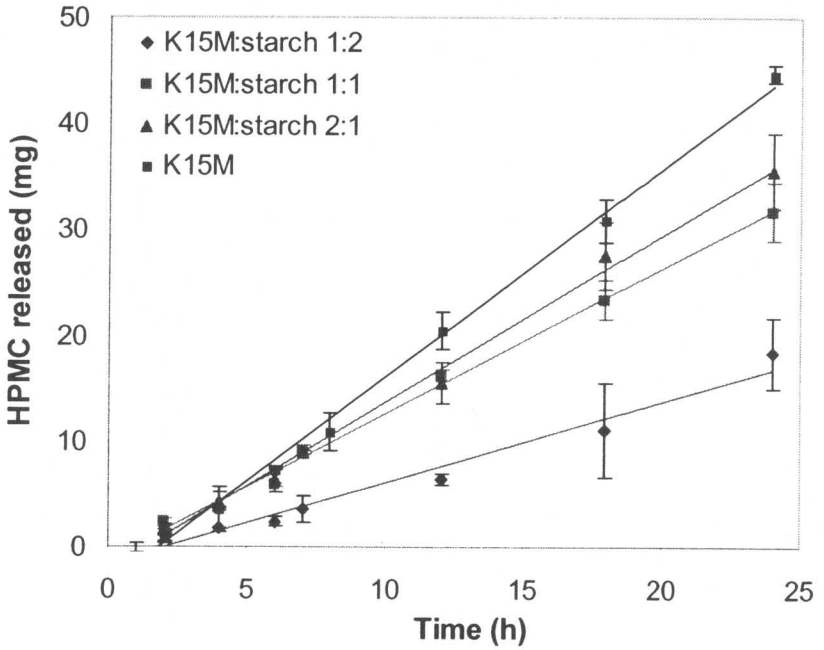

Figure IV-10 The effect of Starch 1500 on the dissolution of HPMC K15M.

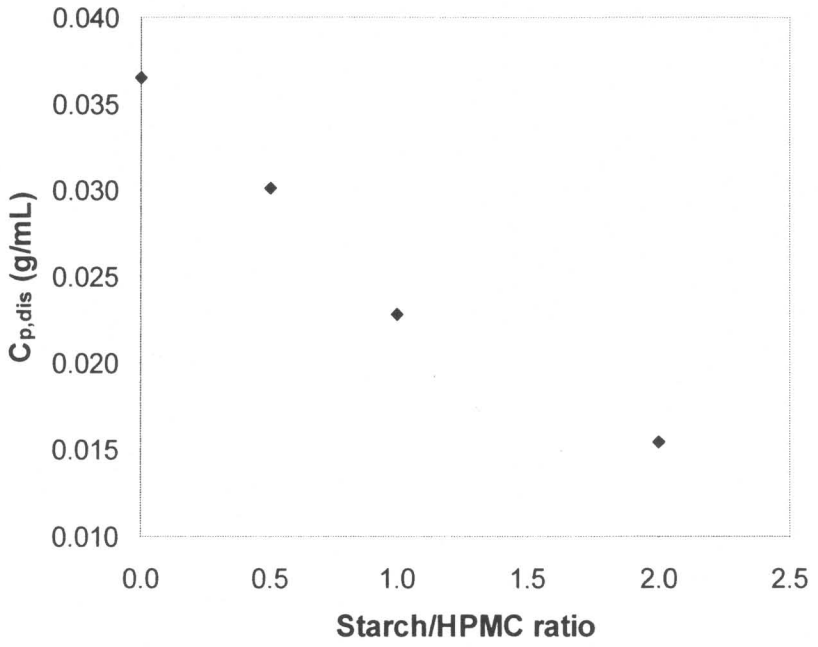

Figure IV-11 Effect of Starch 1500 on the disentanglement concentration of HPMC K15M.

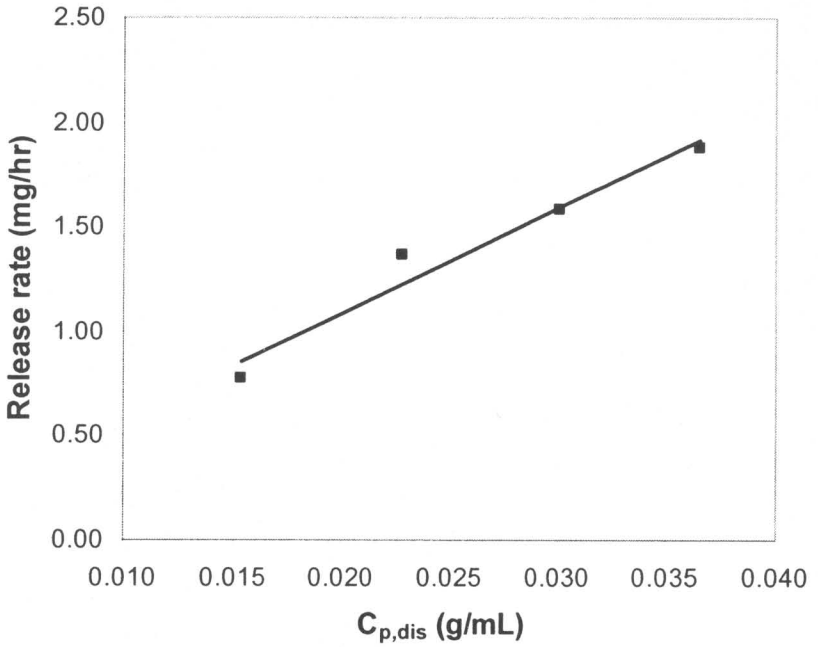

Figure IV-12 The correlation of HPMC K15M release rate with the calculated polymer disentanglement concentration of K15M at different ratios of HPMC/Starch 1500.

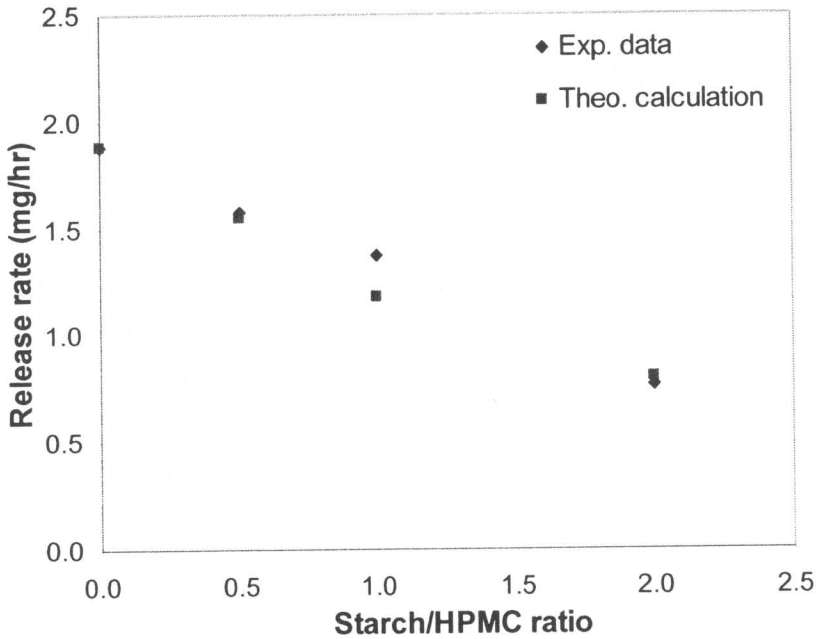

Figure IV-13 The effect of HPMC/Starch 1500 ratio on the dissolution rate of HPMC K15M. The experimental data and the theoretical prediction were compared.

CHAPTER V Understanding the Effect of SDS-HPMC Interaction on Drug Release from Depakote® ER Tablets

ABSTRACT

Purpose. The purpose of this study was to investigate the interaction between HPMC and a surfactant, SDS, in the dissolution medium and to c orrelate HPMC gel strength to the release of divalproex sodium from Depakote® ER tablet. ***Methods.*** HPMC gel strengths were measured using Texture Analyzer. Dissolution tests of Depakote® ER tablets were conducted in 0.05M phosphate buffer with and without 75mM SDS (pH 5.5) using USP dissolution apparatus II with a rotation speed of 100rpm. HPMC release was analyzed using a size exclusion chromatography-HPLC-evaporative light scattering detector (SEC-HPLC-ELSD) method. Divalproex sodium release was analyzed using TD_x® fluorescence polarization immunoassays following dilution with dissolution medium using an automated TD_x® system (Abbott TD_x® Analyzer). ***Results.*** Divalproex sodium release from Depakote® ER tablets in PBS buffer was diffusion-controlled; while the addition of 75mM SDS into the PBS dissolution medium increased drug release rate significantly a nd the r elease mechanism became e rosion-controlled. It was found that neither the interaction of active ingredient, divalproex sodium, with HPMC nor with SDS was the major cause for such dramatic drug release rate and mechanism changes in different dissolution media. Interactions between SDS and HPMC chains were found to be responsible for the changes in drug release rate and release mechanism. Our studies demonstrated that SDS enhanced HPMC gel strength at low concentrations and collapsed HPMC gel network at high concentrations. A unique structure of the swelling tablets was observed in the SDS-containing medium and helped explain the above changes of drug

release characteristic. That is, unlike normal HPMC-based tablets, gel strengths of swollen Depakote ER tablets exhibited a flat profile in the outer portion of the gel layer. This was attributed to SDS concentration gradients and its interaction with HPMC in the gel layer. Further, addition of 0.2M NaCl decreased both HPMC erosion and drug release rates in 75mM SDS dissolution medium, but increased drug release rate in PBS buffer although HPMC release rate decreased. ***Conclusions.*** A qualitative relationship between HPMC release and the gel strength was demonstrated, i.e., HPMC erosion decreased with gel strength increase by adding salt into PBS dissolution medium with and without 75mM SDS; HPMC erosion increased with gel strength decrease by adding 75mM SDS into PBS dissolution medium to collapse the gel at the dissolution interface, and the corresponding drug release was completely controlled by HPMC erosion.

Key Words: divalproex sodium; *in vitro/in vivo* correlation; gel strength, polymer dissolution, SEC-HPLC-ELSD, HPMC, Texture Analyzer, SDS

INTRODUCTION

Divalproex sodium, or sodium hydrogen divalproate, is a stable coordination compound containing equimolar proportions of sodium valproate and valproic acid. Chemically it is de signated a s s odium hy drogen bis(2-propylpentanoate) (Figure V-1). The anhydrous divalproex sodium exists as crystalline aggregates that appear as waxy white flakes with melting point of approximately 100^0C. It has high aqueous solubility at neutral pH (e.g., 36 mg/mL at pH 6.2) and solubility decreases at pH values below its pKa value of 4.8 (e.g., 2 mg/mL at pH4.7)(Qiu 2003a). The molecular weight of divalproex sodium is 310.41 g/mol.

Divalproex sodium is widely used antiepileptic agent. It has also been found to be effective in the treatment of bipolar disorder and in the prophylaxis of migraine headaches. Because divalproex sodium is a narrow therapeutic index drug commonly used for long-term therapy, a once-daily controlled release (CR) dosage form was designed to improve clinical therapy via increased patient compliance and reduced adverse events. Depakote ER® tablet (Abbott Laboratories, IL, USA) is a commercially available ER tablet of divalproex sodium based on a hydrophilic matrix platform. In this formulation, 53.8% is active ingredient, divalproex sodium, 30% is hydroxypropyl methylcellulose (HPMC) K15M acting as a rate-controlling polymer and 16.2% is filler/lubricant. It provides nearly 24 h of apparent zero-order *in vivo* absorption of divalproex sodium that allows once daily administration (Qiu 2003a).

During the formulation design of Depakote® ER tablet, an initial *in vitro* dissolution test (USP II, 100rpm, pH 6.8 phosphate buffer) was found to result in release rates that were slower than *in vivo* absorption and the release mechanism was diffusion-controlled. The test method was also unable to sufficiently differentiate formulations containing HPMC K15M with various concentrations (Table V-1), although these formulations have different *in vivo* absorption rates as shown in Figure V-2 (Qiu 2003b). To develop an *in vitro* method that is directly correlated with *in vivo* absorption, statistically designed studies were carried out to investigate the effects of various *in vitro* testing variables on drug release using USP dissolution apparatuses. The variables studied included agitation intensity, apparatus, pH, surfactant and ionic strength of the dissolution medium. A series of factorial studies indicated that higher pH, addition of sodium dodecyl sulfate (SDS) to the dissolution medium, and higher agitation intensity increased the release rate from the matrix tablet. Use of SDS not only lead to increased release rates

that are more comparable to *in vivo* absorption rates, but also improved differentiation among formulations with varying release rates. Based on the above findings, a predictive *in vitro* dissolution method was identified by adding 75mM SDS into 0.05M phosphate buffer and lowering the pH to 5.5. As a result, the drug release rate using this new method was increased and a good correlation between *in vitro* and *in vivo* data was obtained. The drug release mechanism was changed to apparent erosion-controlled and different formulations can also be adequately differentiated (Figure V-3). Comparing these two sets of test conditions, we found the significant difference is with and without addition of 75mM SDS into the dissolution medium. Among possible causes, the interaction between SDS and non-ionic polymer HPMC could be pivotal for understanding this system.

Interactions between surfactants and non-ionic, water-soluble polymers in aqueous solution has been the focus of intense research, originating from the study of protein-surfactant interaction (Klotz 1953; Breuer 1972). The general conclusion emerging from these studies is that surfactant molecules interact with polymer chains at a critical aggregation concentration (CAC), forming micelle-like clusters along the polymer backbones. Although polymer-surfactant micelle complexes find applications in many industries, such as enhanced oil recovery, food preparations, cosmetic formulations, laundry detergents and pharmaceutical compositions, many problems are still unsolved. Particularly, the question of how the precise chemical structure of the surfactant and the morphology of the unperturbed micelle are related to the tendency for association with polymers poses a challenge for chemists.

In 1957, Saito published the first extensive study on polymer-surfactant complexation. Two major observations were 1) an increase in viscosity of an aqueous poly(vinylpyrrolidone) (PVP) solution upon addition of SDS and 2) an increase in

solubilizing power of an SDS solution upon addition of PVP. Though it was suggested that the aggregation of surfactant molecules in the presence of polymer resembled normal micellization, Saito proposed that, at a low surfactant-to-polymer ratio, the surfactant molecules bind individually to the polymer. This binding was thought to occur by dipolar interaction of the surfactant head groups with polar sites on the polymer, while the surfactant chain was thought to lie parallel to the polymer chain. However, Saito wisely stated that the structure of the polymer-micelle or polymer-surfactant complex had not yet been clearly established.

The major concept emerged in the following decade, summarized in Breuer and Robb's review (Breuer 1972), was the picture of individual molecules along the polymer, together with some kind of micellization occurring above the critical micelle concentration (CMC) of the surfactant in pure water (Jones 1967; Saito 1969b, a). Many details of polymer-micelle interaction were revealed in that period; including the finding that complexation takes place even below the normal CMC (Jones 1967). This has long been used as support for individual binding. It was found that above a minimum molecular weight of the polymer, the interaction is independent of MW (Jones 1967; Schwuger 1973; Tokiwa 1973) and that certain saturation takes place at increasing surfactant concentration (Jones 1967). The importance of hydrophobic interaction in polymer-surfactant complex formation was deduced from the stronger interactions obtained as polymer hydrophobicity and surfactant alkyl chain length were increased (Saito 1957; Jones 1967). Much later, in 1987, measurements of heat capacities and apparent molar volumes also revealed a shift of these thermodynamic properties, upon addition of polymer, in the direction of enhanced hydrophobic association (Perron 1987).

The presently accepted model was proposed by Cabane (Cabane 1977) in 1977 on the basis of his comprehensive studies of the poly(ethylene oxide) (PEO)-sodium dodecylsulfate (SDS) system. According to this model, segments of the polymer bind to the surface region of the surfactant micelles and the polymer is converted into a "necklace" decorated with surfactant micelles. Stabilization of the interface between the hydrophobic core of the micelles and water is considered to be a major driving force for polymer-micelle interaction.

Although thorough understanding of polymer-surfactant interaction in the solution has been obtained, very few studies were found in the literature about the interactions between surfactant and polymer gel. In this work, we studied the effect of SDS in dissolution medium on the gel strength of HPMC swelling tablets, and its effect on corresponding drug and polymer release profiles from Depokate ER® tablet.

MATERIALS AND METHODS

Materials

METHOCEL®, commercially available hydroxypropylmethyl cellulose (HPMC) K15M, was same as that used in Chapter II. Sodium dodecyl sulfate (SDS) was from BDH laboratory supplies. Depokate ER® tablet was manufactured at Abbott Laboratories (Pharmaceutical Products Division, North Chicago, IL). Valproic acid was from Abbott Laboratories.

Sample Preparation

5.4% w/w HPMC K15M hydrogel with divalproex sodium at ratio of 30:53.8 was prepared by first mixing HPMC and divalproex sodium in a mortar and then adding

precisely weighed powder mixture into appropriate amount of 80-90^{0}C 0.05M phosphate buffer with or without 75mM SDS to form gel. 6.4% w/w HPMC K15M hydrogels at different SDS concentrations were prepared by dispersing K15M powders with predetermined mass into 80-90^{0}C 0.05M phosphate buffer (pH 5.5) with varying SDS concentrations (0, 2, 4, 6, 7.5, 10, 25, 50, 75, 115, 150 and 347mM) to form gel. Different concentrations of NaCl (0.1, 0.2 and 0.3M) were added into 0.05M phosphate buffer containing 50, 75, 115 and 150mM SDS and used to prepare HPMC gels with different ionic strength. The detailed procedures of gel preparation were as same as being described in Chapter II. The preparation of tablets containing 100% hydroxypropylmethyl cellulose (Methocel^{TM}, K15M) was as same as that described in Chapter III.

Cloud Point Measurement

0.5% w/v HPMC K15M solution was prepared by dispersing the pre-weighed polymer (500mg) or mixture of polymer (500mg) and sodium valproate (896.7mg) into 50mL of 0.05M phosphate buffer (pH 5.5) with or without 75mM SDS at 80^{0}C, cooling the dispersion down under stirring until the solution became clear, transferring the solution into 100mL volumetric flask and adding cold phosphate buffer with or without 75mM SDS to bring the total solution volume to 100mL. The HPMC solutions were stored overnight in a 4^{0}C refrigerator to hydrate fully. Samples were transferred to 1cm^2 cuvettes and placed in a water bath with a temperature regulator. During gradual increasing the temperature of water bath by 0.1^{0}C as increments, the transmitted light density through the samples was measured at 400nm. The cloud point was taken to be the temperature corresponding to 50% light transmission.

Solubility Test

A super-saturated valproic acid solution was prepared by adding 0.57570g valproic acid into a scintillation vial containing 4 mL of 0.05M phosphate buffer with 75mM SDS, pH 5.5. The vial was further covered using alumina foil and mounted onto a rotating shaker. After shaking for 15 hours, the vial was taken out from the shaker and stood still for phase separation. The oil (upper) phase was trashed and sample was withdrawn from aqueous (lower) phase and assayed using TD_x analysis after the phase separation reached the equilibrium.

One-dimensional Swelling Experiments

One planar side of the tablet was covered with organic coating (14.0 g Eudragit® RS in the mixture of 50 mL acetone and 50 mL isopropanol) impermeable to water in order to prevent deformation during the determination of the glass/gel interface, and the tablet was subsequently glued to the tablet mold with the same diameter as that of the tablet to provide one-dimensional swelling. The samples prepared in this manner were then placed in 0.05 M phosphate buffer with or without 75mM SDS (pH 5.5) under a static condition at room temperature or subjected to a dissolution test. The swelling tablets were carefully taken out at predetermined time intervals for texture analysis.

Texture Analyzer Measurements

Both homogeneous gel samples and swelling tablets were tested using TA.XT Plus Texture Analyzer (Texture Technologies Co., Algonquin, IL). The test probe used was a flat-tipped, round steel probe of 2mm in diameter and 30mm in length. The test conditions and procedures were as same as those in Chapter II and III.

***In Vitro* Dissolution Tests and Assays**

In vitro dissolution rates from the Depakote ER® tablet were determined using the USP Apparatus II (Vankel 7000). The paddle rotation speed was kept at 100rpm, and a temperature of 37.0±0.5 ^{0}C was maintained. Release testing was carried out in 900mL of pH 6.8 phosphate buffer or pH 5.5 phosphate buffers with or without 75mM SDS. 0.2M NaCl was added into pH 5.5 phosphate buffers with or without containing 75mM SDS to study the ionic strength effect on drug and HPMC release. Samples of 10mL were withdrawn at predetermined time intervals up to 24 h. Samples were filtered through a 35-μm polyethylene filter.

The valproic acid was assayed by TD_x® fluorescence polarization immunoassays following dilution with dissolution medium using an automated TD_x® system (Abbott TD_x® Analyzer). Valproate calibrators consisting of six standard concentrations (0, 12.5, 25, 50, 100, and 150 μg/mL) were used to perform an assay specific calibration prior to sample analysis. Dissolution samples were then pipetted into a sample cartridge and loaded into the analyzer along with valproate controls and monoclonal II reagent pack for automated sample analysis. The sensitivity of the assay was 0.70μg/mL. High accuracy and precision were also confirmed. The HPMC K15M was assayed using SEC-HPLC-ELSD method described in Chapter IV, except that the mobile phased used in this study was 0.1M ammonium acetate with pH 5.5. All dissolution studies were performed in triplicate.

One-dimensional *in vitro* dissolution tests were conducted under the same conditions as those in three-dimensional tests, except that only upper face of tablet

exposed to the dissolution medium by putting the tablet in a sample holder of the same size of tablet.

RESULTS AND DISCUSSION

1. Interaction between Active Ingredient and HPMC

Cloud Point Measurement

It is well known that the hydration of HPMC in aqueous solution is affected by temperature. At lower temperatures, polymer chains are fully hydrated and there is little polymer-to-polymer interaction other than simple entanglement when the polymer concentration is above overlapping concentration. As the temperature of the solution increases, the cellulose polymers gradually lose the water of hydration and solution viscosity decreases. As the polymer loses more water of hydration, a polymer-polymer interaction takes place, primarily induced through hydrophobic interactions among methoxy-substituents. As such, polymer chains start to aggregate and eventually precipitate out of solution, leading to a cloudy solution. As a beam of light passes through the solution, the light transmission is reduced due to cloudiness of the solution. The temperature at which light transmission reaches 50 % of initial value is defined as the cloud point. Therefore, cloud point is a measure of the interaction between polymer and solvent, and thus, hydrophobicity of the polymer. In addition, any change in cloud point of a polymer/water system due to the addition of a third component can be referred to alterations of interaction and changes of the hydrophobic/hydrophilic balance in the system.

The percent transmittance profiles of 0.5% w/w HPMC K15M in the solution of 0.05M phosphate buffer with and without sodium valproate (SV) were presented in Figure

V-4. The ratio of HPMC/SV is 30:53.8, as same as that in Depakote® ER formulation. The cloud points obtained from the corresponding transmittance profiles were 63.2 and 64.9 ^{0}C for K15M with and without presence of SV, respectively. The decrease in cloud point with the addition of surfactant (SV is a surfactant like molecule) has been reported in the literature (Löefroth 1991; Drummond 1992), and it might be due to the conformational changes of the polymer that promotes the hydrophobic-hydrophobic polymer interaction (Carlsson 1986). Nevertheless, this minor difference in cloud point suggested that there is no significant interaction between HPMC and SV in the solution.

The same measurement was also done in PBS buffer containing 75mM SDS, and no cloud point was detected up to 100^{0}C, as shown in Figure V-4. This is in agreement with the result obtained by Nilsson (Nilsson 1995), who measured cloud point of 0.3% HPMC salt free solution with various SDS concentrations and found that cloud point was beyond 100^{0}C when SDS concentration was above 16 mM.

Cloud point data indicates that the interaction between HPMC and SDS is much stronger than the interaction between HPMC and the active ingradient, sodium valproate, in aqueous solution.

Gel Strength Measurement

To study the interaction between divalproex sodium and HPMC at gel state, the strength of 5.5% HPMC K15M homogeneous gel with and without divalproex sodium (DS) was measured using Texture Analyzer. The ratio of HPMC to divalproex sodium was 30:53.8 w/w, as same as that in Depakote® ER formulation. As shown in Figure V-5, divalproex sodium increased the strength of K15M gel slightly. On the other hand, the effect of SDS is much more significant than divalproex sodium, indicating greater

HPMC/SDS interactions than HPMC/divalproex sodium. In addition, the gel strength of HPMC/DS/SDS was slightly lower than HPMC/SDS, as shown in Figure V-5.

The gel strength data demonstrated that HPMC/SDS interactions were much stronger than those of HPMC/divalproex sodium, in agreement with cloud point data obtained in solution state.

2. Interaction between Active Ingredient and SDS

It is known that divalproex sodium dissociates into equal molar of sodium valproate and valproic acid in aqueous medium. And valproic acid is a hydrophobic compound with low water solubility (Qiu 2003a), we expected that high concentration of SDS in dissolution medium could increase the solubility of valproic acid by forming mixed micelles. This was proven experimentally. The solubility tests of valproic acid in 0.05M phosphate buffers at different pH with or without 75mM SDS were conducted and the results were listed in Table V-2. The solubility of valproic acid in 0.05M phosphate buffer at pH 5.5 was 7.3mg/mL, and increased to 22.5mg/mL with addition of 75mM SDS into the buffer solution. When the pH of buffer solution increased to 6.8, the solubility of valproic acid increased to 126.9mg/mL

The drug release studies in different media were performed and the results were shown in Figure V-6. Both higher pH and inclusion of 75mM SDS in the dissolution medium increased drug release, but the enhancement by 75mM SDS was much more significant than by pH increase, which was not consistent with solubility data. Therefore, we concluded that the solubility increase by SDS couldn't fully explain the fast drug release in SDS medium.

3. Interaction between SDS and HPMC

Effect of SDS Concentration on HPMC Gel Strength in Homogeneous Gel Systems

The strength of HPMC K15M homogeneous gels at different SDS concentrations (from 0 to 347mM) was measured, and the gel strength enhancement was plotted as a function of SDS concentration in Figure V-7. It is shown that the gel strength profile can be classified as two regions: SDS increases HPMC gel strength at low total SDS concentration, up to ~120mM, and collapses the HPMC gel at higher total SDS concentration, i.e. ~150mM.

A similar trend was also reported when Nilsson *et al.* studied the effect of SDS on the viscosity of HPMC solutions (Nilsson 1995). They found the reduced specific HPMC viscosity started to increase sharply when the SDS concentration was above 4mM, and reached a maximum at SDS concentration between 5 to 8mM depending on the concentration of HPMC. As the total SDS concentration exceeded 12mM, the reduced specific HPMC viscosity approached the same value lower than that of HPMC solutions without SDS irrespective of polymer concentration. This suggests that interactions of SDS and HPMC chains are sensitive to SDS concentration. The mechanism of SDS/HPMC interaction was suggested by Nilsson (Nilsson 1995) and shown in Figure V-8. The author discussed the difference between high and low HPMC concentration, and here we only focus on high HPMC concentration, which is more related to the gel system. When SDS concentration is above 4mM, SDS starts to adsorb to the HPMC chain in a cooperative manner in the form of small micelles. The adsorbed micelles increase in both size and number with surfactant concentration up to a certain limiting plateau value, while SDS concentration in the solution, $[SDS]_{eq}$, kept constant as shown in Figure V-9. If the

polymer concentration is above the overlapping concentration, the micelles adsorption tends to become intermolecular in nature; i.e., one micelle is shared by two or more polymer molecules creating a three dimensional network. This explains the high viscosity observed by Nilsson (Nilsson 1995), and gel strength enhancement in Figure V-7. When more SDS is added, normal micelles begin to form in the solution and SDS concentration in the solution starts to increase as shown in Figure V-9. A particular polymer molecule may then solubilize its hydrophobic sites also in normal free micelles. This competition will favor the normal micelles as their relative number increases with increasing the total SDS concentration and the networking tendency of the polymer solution will eventually be lost. This effect shows itself in Figure V-7 as the gel was very weak or gel network was completely collapsed.

Effect of SDS on HPMC Homogeneous Gel Strength at Different Ionic Strength

The effect of SDS on HPMC gel strength under different ionic strength was also studied and presented in Figure V-10(a). And such effect was not only the function of the ionic strength as shown in Figure V-10(b). As more salts added in, the relative gel strength profile shifted toward the right and the maximum gel strength increased as salt concentration increased. Two different gel strength dependencies on salt concentration were observed: the relative gel strength decreases as salt concentration increases when SDS concentration is equal and lower than 75mM, while gel strength increases as salt concentration increases when SDS concentration is higher than 90mM. The effect of salt concentration (ionic strength) on SDS micelle formation in aqueous solution was studied by Nagarajan *et al.* (Nagarajan 1991). They found that the aggregation number of SDS micelle increases with salt concentration, while critical micelle concentration (CMC) decreases as shown in Table V-3. Based on this data, the concentration of SDS micelle at

different salt concentration was calculated and also shown in Table V-3. We expect the effect of salt on SDS micelle formation in the presence of HPMC to follow the same trend, i.e. the number of SDS micelles formed in polymer network decreased with salt concentration resulted in less gel strength enhancement at low SDS concentration. On the other hand, at high SDS concentration, HPMC chains were saturated with SDS micelles, so the number of SDS micelles interacting with HPMC network would be same at all salt concentration. But higher salt concentration could shield negative charges from SDS and prevent gel collapsing; as a result, gel strength increases.

Effect of SDS on Gel Strength of HPMC and Depakote® ER Swelling Tablets

The effect of SDS on gel strengths of HPMC-based swelling tablets was investigated. As shown in Figure V-11(a), gel strength profiles of the swollen HPMC tablets in phosphate buffer were significantly modulated by 75mM SDS. SDS increased the gel strength at given penetration depth and slightly decreased the gel layer thickness, as shown in Figure V-11. SDS's effect became more apparent as swelling progressed. As clearly demonstrated in Figure V-11(b), a typical gel strength profile was observed in phosphate buffer, i.e. the gel strength increases gradually with the penetration depth as described in Chapter III. However, a new and unique structure was rendered by 75mM SDS. A sudden plateau of gel strength was observed at the outer gel layer, followed by further gradual increase in gel strength. This indicates a sharp phase transition at the interface of gel/dissolution medium.

The effect of SDS on gel strength of Depakote® ER swelling tablets followed the same trend described above as shown in Figure V-12 (a), and a characteristic gel strength plateau was also seen in SDS medium as shown in Figure IV-12 (b). The lower gel

strength of Depakote® ER tablets compared with pure HPMC tablet was probably due to the lower level of HPMC used in the former.

While the cause of the sharp interface is unknown and beyond the scope of this study, we hypothesize as follow. Once HPMC tablet started to swell, SDS molecules and or micelles in the solution diffused into the swelling tablet, interacting with HPMC chains and thus enhancing the gel strength. Furthermore, a SDS concentration gradient across the gel layer is expected to form. High SDS concentrations at the "outer" region should increase the gel strength to a greater extent than lower SDS concentrations do at the "inner" region. Thus, it is likely the typical increase of gel strengths toward the inside of gel layers is balanced by the extent of gel strength enhancement due to the SDS concentration gradient, forming a plateau region when these two factors cancel each other out.

Since there are abundant SDS molecules and or micelles in the solution, SDS micelles continued to accumulate at the gel surface until the saturation point and HPMC gel started to collapse. However, this could not be detected by gel strength measurement since the collapsed gel is so weak as shown in Figure V-7 at high SDS concentration end. This explains the sharp phase transition at the interface of gel/dissolution medium and why the gel layer thickness in SDS solution was shorter than in phosphate buffer.

4. Drug and HPMC Dissolution

Release of divalproex sodium and HPMC from Depakote® ER tablets was shown in Figure V-13. Without SDS, the release of divalproex sodium was much faster than the release of HPMC, suggesting that diffusion played a major role in to the overall drug release. We also found that the drug release was proportional to the square root of time,

while HPMC was proportional to time. Therefore, we concluded that divalproex sodium release from Depakote® ER tablet in PBS buffer was diffusion-controlled.

The divalproex sodium and HPMC release from Depakote® ER tablet in PBS buffer containing 75mM SDS was shown in Figure V-14. Contrary to the above data, the release of divalproex sodium was identical to that of HPMC, and both were proportional to time. The results definitely proved that polymer erosion was the predominant mechanism for divalproex sodium release. Further, SDS increased HPMC release by more than 3 times than that from SDS-free solution. As we discussed above, the accumulation of SDS at the surface of HPMC gels significantly weakened or collapsed the gel structure, leading to accelerated HPMC release. The gel structure at the dissolution interface was significant different as shown in Figure V-16. The gel interface was very smooth at PBS buffer but relative rough and irregular in SDS solution due to the gel at the interface was too weak to maintain its shape.

One-dimensional release of divalproex sodium from Depakote® ER tablet in PBS buffer without and with 75mM SDS was also studied and the results were shown in Figure V-15. In agreement with three-dimensional release, divalproex sodium release was mainly controlled by diffusion and had minimal contribution from HPMC release in PBS buffer, while the drug release was identical to HPMC release in SDS solution. We further found that HPMC release from both PBS and SDS was proportional to the dissolution area, in agreement with the model we proposed in Chapter IV.

The effect of ionic strength on divalproex sodium and HPMC release in PBS buffer containing 75mM SDS was also studied and the results were shown in Figure V-17. The ionic strength was changed by the addition of 0.2M NaCl. In agreement with previous data (Qiu 2003b), addition of 0.2M NaCl decreased drug release. On the contrary, addition

of 0.2M NaCl into SDS-free buffer increased divalproex sodium release as shown in Figure V-18 (a), while HPMC release decreased in both situations (Figure V-17 (b) and Figure V-18 (b)). As we discussed above, accumulation of SDS at HPMC gel interface collapsed the gel structure, promoting the polymer erosion. And the increase of ionic strength shielded negative charge from SDS and prevented gel collapsing, as a result, the gel strength increases at given SDS concentration as shown in Figure V-10 at high end of SDS concentration. As the result of increased gel strength, both HPMC and drug releases decreased. However, in PBS buffer, the addition of 0.2M NaCl increased the gel strength of HPMC as shown in Figure V-10 (b), which resulted in lower HPMC release. It is not clear why divalproex sodium release increased with the addition of 0.2M NaCl into PBS buffer. Nevertheless, the fact that the addition of 0.2M NaCl into PBS buffer had opposite effect on divalproex sodium and HPMC releases further proved that the latter had little contribution on the former.

CONCLUSIONS

Divalproex sodium release from Depakote® ER tablet was diffusion-controlled in the PBS buffer without SDS; while the drug release became erosion-controlled when 75mM SDS was added to the same buffer. The most likely cause of SDS's effect was interactions between SDS and HPMC chains in the gel layer. SDS increased HPMC gel strength at low concentration and collapsed HPMC gel network at high concentration. A unique structure of swollen HPMC tablets was observed in SDS-containing PBS buffer, reflected as a plateau of high gel strengths at the outer portion of gel layer. This was further attributed to the SDS concentration gradient inside the HPMC gel layer. Accumulation of SDS at the HPMC gel surface would eventually collapse HPMC gel structure, promoting HPMC erosion. Addition of NaCl into the dissolution medium of

PBS buffer with 75mM SDS decreased both HPMC erosion and drug release. On the contrary, addition of NaCl into the dissolution medium of SDS-free PBS buffer increased drug release, while HPMC release was retarded. In summary, a qualitative relationship between HPMC release and HPMC gel strength was demonstrated.

REFERENCES

Depakote® Tablet. 2002. Physicians' desk reference.

Depakote® Tablet. 2003. Physicians' desk reference.

Breuer M. M. and Robb I. D. (1972). "Interaction between macromolecules and detergent products." Chemistry & Industry **530**(13): 5.

Cabane B. (1977). "Structure of some polymer-detergent aggregates in water." J. Phys. Chem. **81**(17): 1939-1945.

Carlsson A., Karlström G. and Lindman B. (1986). "Synergistic surfactant-electrolyte effect in polymer solutions." Langmuir **2**(5): 536.

Drummond C. J., Albers S. and Furlong D. N. (1992). "Polymer-surfactant interactions: (Hydroxypropyl) cellulose with ionic and non-ionic surfactants." Colloids and Surfaces **62**(1-2): 75-85.

Jones M. N. (1967). "The interaction of sodium dodecyl sulfate with polyethylene oxide." J. Colloid Inter. Sci. **23**(1): 36-42.

Klotz L. M. (1953). The Proteins. New York, Academic Press.

Löefroth J. E., Johansson D., Norman A. C. and Wettström K. (1991). "Interactions between surfactants and polymers. I: HPMC." Prog. Colloid Polym. Sci. **84**(73): 7.

Nagarajan R. (1991). Langmuir **7**: 2934-2969.

Nilsson S. (1995). "Interactions between water-soluble cellulose derivatives and surfactants. 1. The HPMC/SDS/Water system." Macromolecules **28**: 7837-7844.

Perron G., Francoeur J., Desnoyers J. E. and Kwak J. C. T. (1987). "Heat capacities and volumes in aqueous polymer and polymer-surfactant solutions." Can. Journal Chem. **65**(5): 990-995.

Qiu Y., Cheskin H. S., Engh K. R. and Poska R. P. (2003a). "Once-a-Day Controlled-Release Dosage Form of Divalproex Sodium I: Formulation Design and *In Vitro/In Vivo* Investigations." Journal of Pharmaceutical Sciences **92**(6): 1166-1173.

Qiu Y., Garren J., Samara E., Gao G., Abraham C., Cheskin H. S. and Engh K. R. (2003b). "Once-a-Day Controlled-Release Dosage Form of Divalproex Sodium II: Development of a Predictive *In Vitro* Drug Release Method." Journal of Pharmaceutical Sciences **92**(11): 2317-2325.

Saito S. (1957). "Adsorption complexes of polymers with ions of wetting agents." Kolloid-Zeitschrift **154**: 19-29.

Saito S. and Yukawa M. (1969a). "Interaction of polymers and cationic surfactants with thiocyanate as counterions." J. Colloid Inter. Sci. **30**(2): 211-218.

Saito S. and Yukawa M. (1969b). "Solubilization of poly(vinyl acetate) by dodecylammonium thiocyanate." Kolloid Z.-Z. Polym. **234**(1): 1015-1017.

Schwuger M. J. (1973). "Mechanism of interaction between ionic surfactants and polyglycol ethers in water." J. Colloid Inter. Sci. **43**(2): 491-498.

Tokiwa F. and Tsujii K. (1973). "Solubilization behavior of mixed micelles of anionic and nonionic surfactants in relation to their micellar structures." Bull. Chem. Soc. Jpn **46**(5): 1338-1342.

Table V-1 Formulations of controlled-release hydrophilic matrix tablets of divalproex sodium (Qiu 2003b)

Formulation	B	F	G
Divalproex sodium	53.8%	53.8%	53.8%
HPMC K15M	30%	20%	40%
Filler/lubricant	16.2%	26.2%	6.2%

Table V-2 Solubility data of valproic acid at different conditions

pH	5.5	5.5 with 75mM SDS	6.8
Solubility (mg/mL)	7.3	22.5	126.9

Table V-3 SDS micelle concentration at different salt concentration.(* data adapted from (Nagarajan 1991))

Added salt concentration (M)	Aggregation number*	CMC (mM)*	Concentration of micelle (mM)
0.1	93	1.5	0.79
0.2	106	0.8	0.70
0.3	120	0.6	0.62

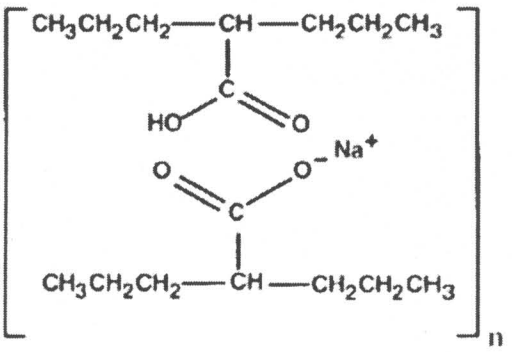

Figure V-1 Chemical structure of divalproex sodium.

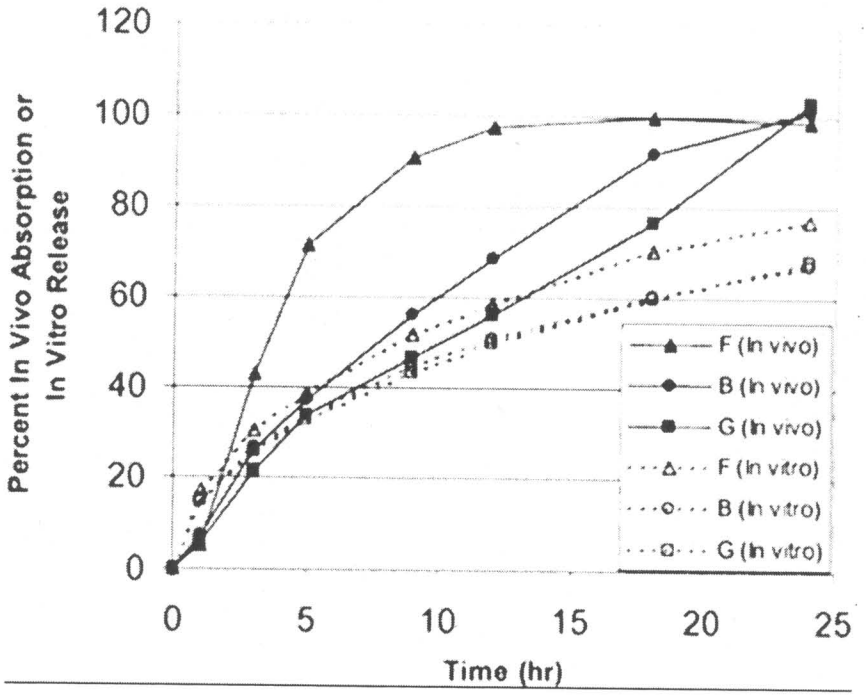

Figure V-2 Mean *in vivo* absorption versus *in vitro* release profiles of divalproex sodium extended release formulations B, F and G based on initial *in vitro* test method (USP II, 100rpm, pH 7.5 phosphate buffer) (Qiu 2003b).

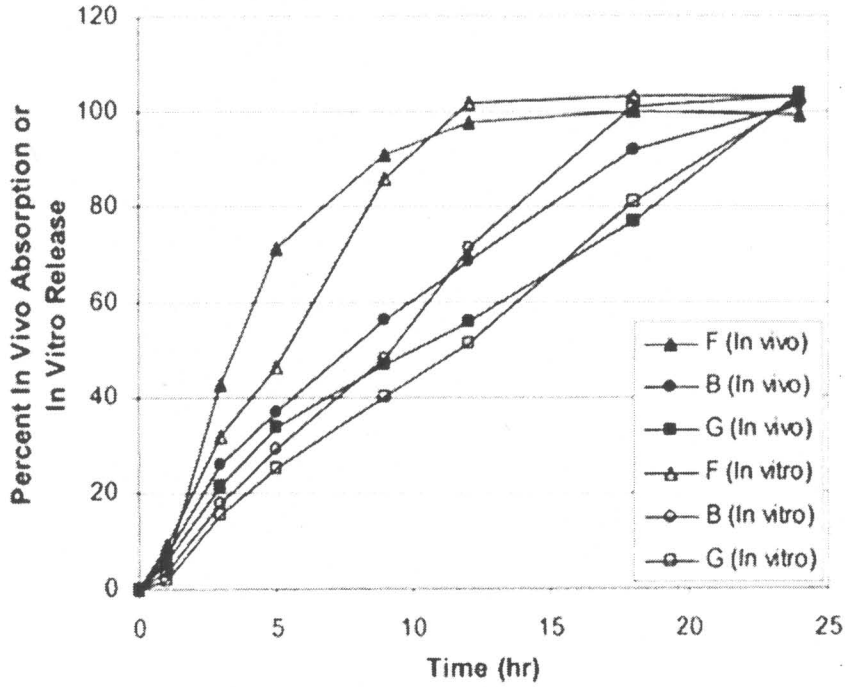

Figure V-3 Mean *in vivo* absorption versus *in vitro* release profiles of Formulations B, F and G based on predictive *in vitro* test method (USP II, 100rpm, 0.75 h 0.1N HCl followed by 0.05M phosphate buffer containing 75mM SDS at pH 5.5) (Qiu 2003b)

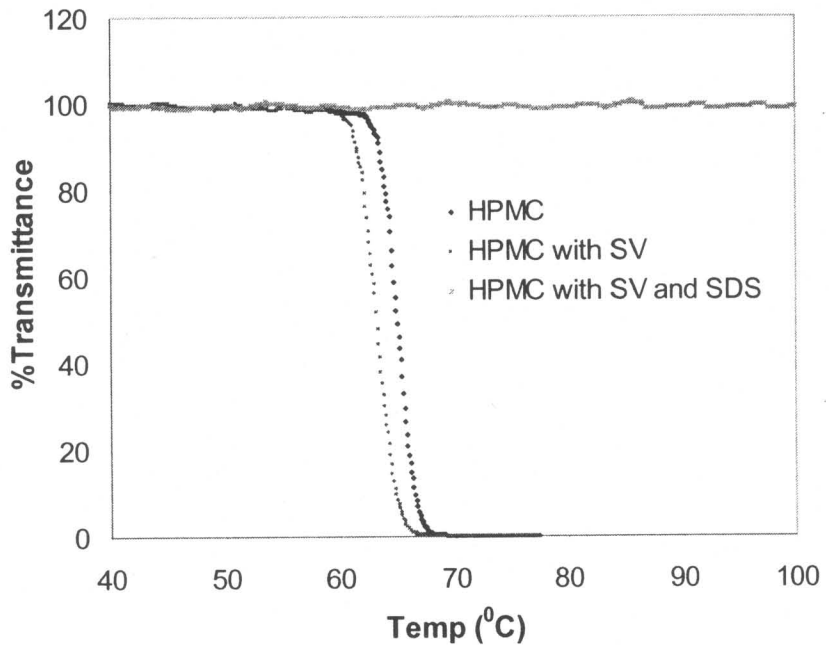

Figure V-4 The transmittance profiles of 0.5% w/w HPMC K15M in the solution of 0.05M phosphate buffer with or without sodium valproate (at ratio of 30:53.8 w/w) and mixture of 0.5% w/w HPMC K15M and sodium valproate (at ratio of 30:53.8 w/w) in the solution of 0.05M phosphate buffer with 75mM SDS.

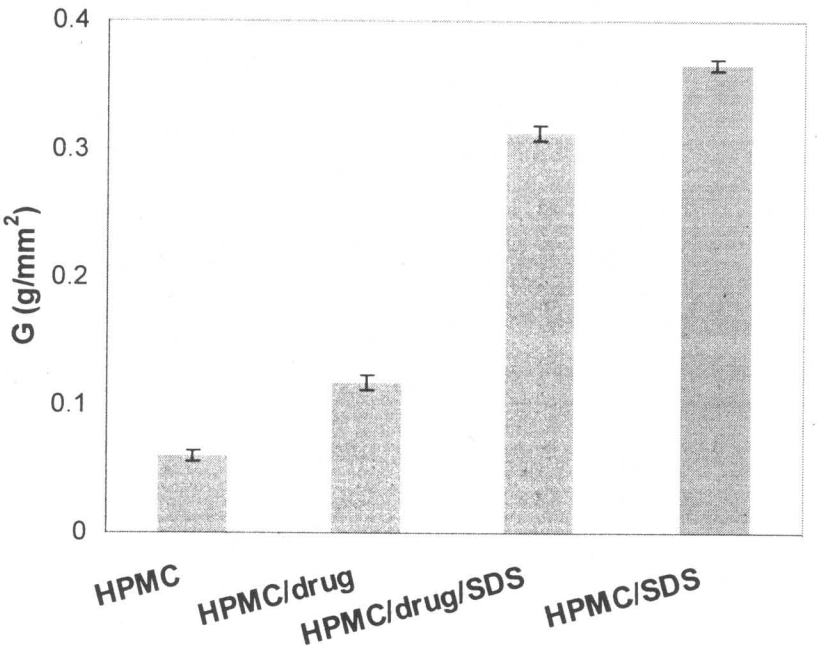

Figure V-5 Effect of divalproex sodium on the strength of HPMC K15M homogeneous gels with and without 75M SDS. 5.5% w/w HPMC was used and the ratio of K15M:divalproex sodium was 30:53.8 w/w.

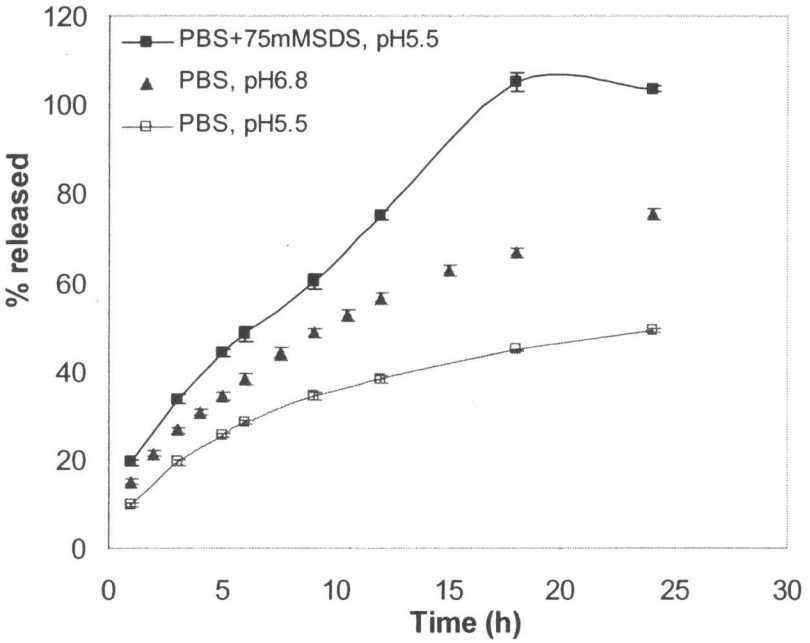

Figure V-6 Effect of pH or SDS on drug release from Depakote® ER tablets.

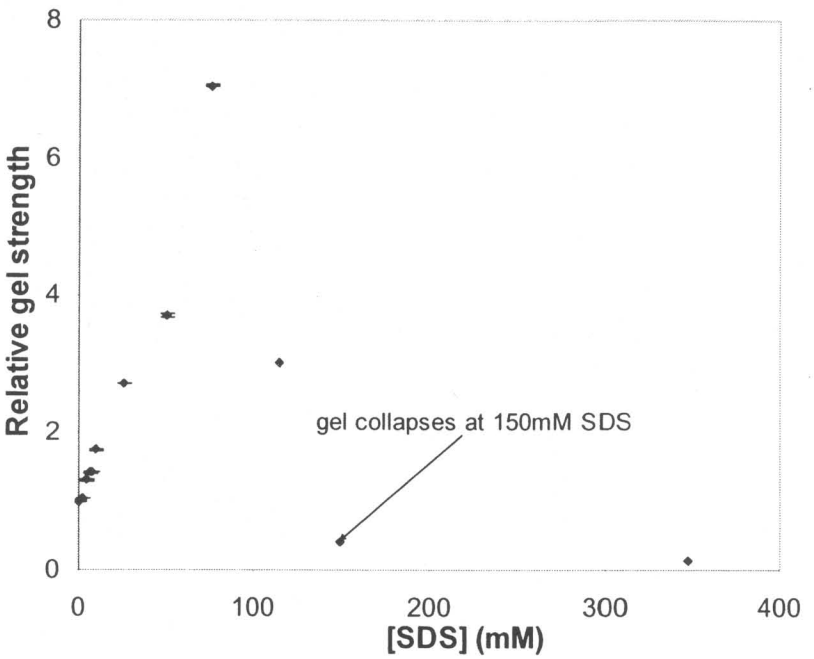

Figure V-7 Effect of SDS concentration on HPMC K15M gel strength.

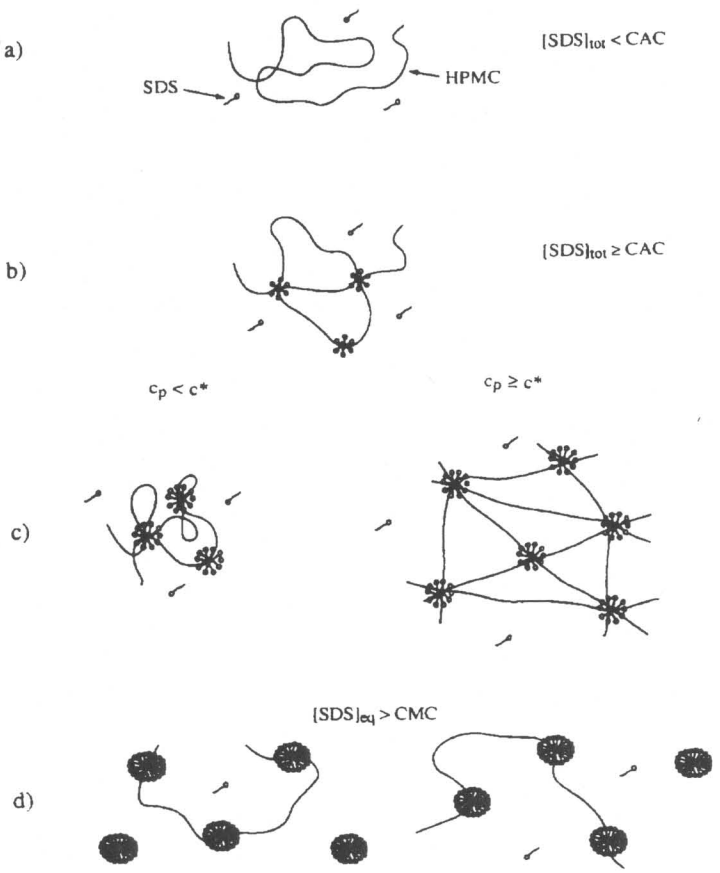

Figure V-8 Schematic representation of the model proposed for the interaction between HPMC and SDS: (a) At low SDS concentrations, $[SDS]_{tot} < CAC$, there is no adsorption of SDS to the HPMC chain. (b) SDS starts to adsorb as clusters to the HPMC chain at $[SDS]_{tot} \geq CAC$. (c) At high polymer concentration ($c > c^*$, c^* is polymer overlapping concentration), there is an intermolecular clustering creating a three-dimensional network. (d) At high SDS concentrations, normal micelles form in solution, competing HPMC chains from polymer network (Nilsson 1995).

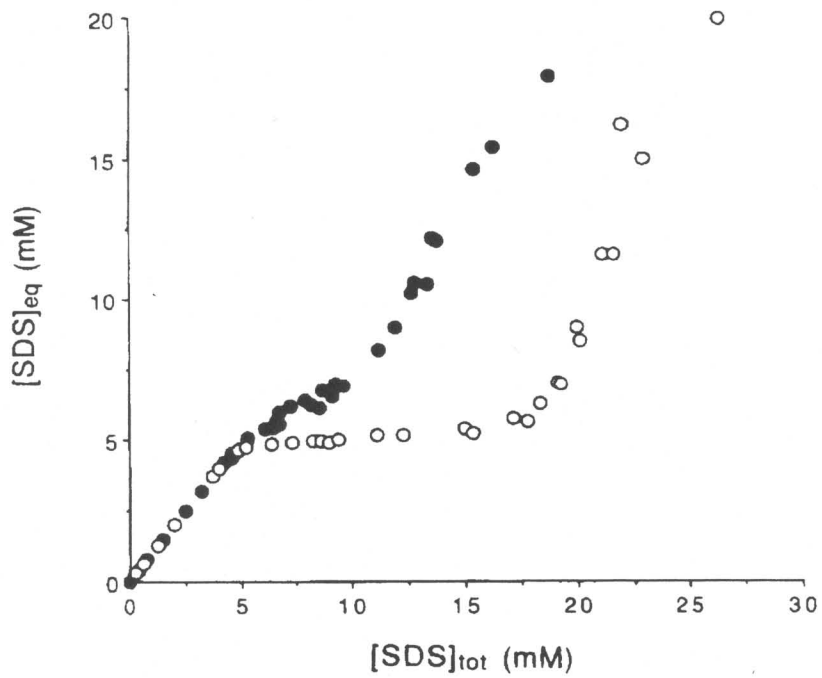

Figure V-9 Equilibrium SDS concentration vs. the total SDS concentration: (o) 0.20 and (•) 0.05% HPMC (Nilsson 1995)

(a)

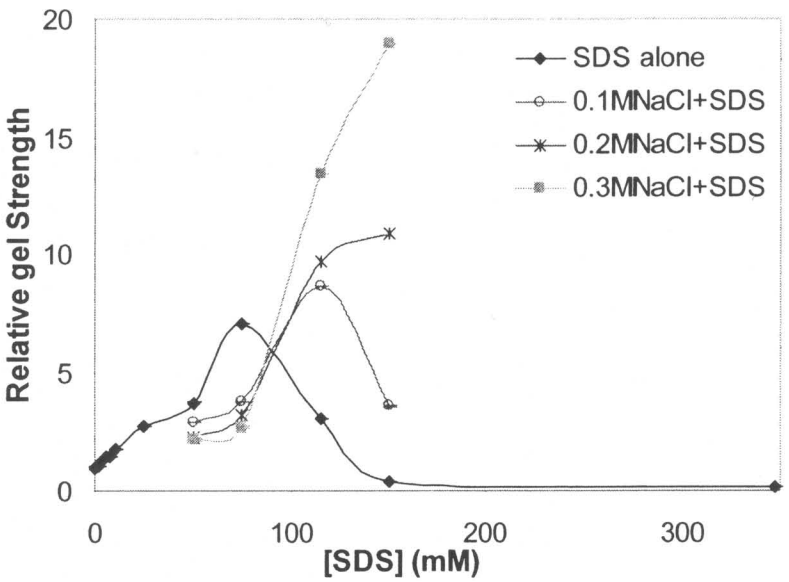

(b)

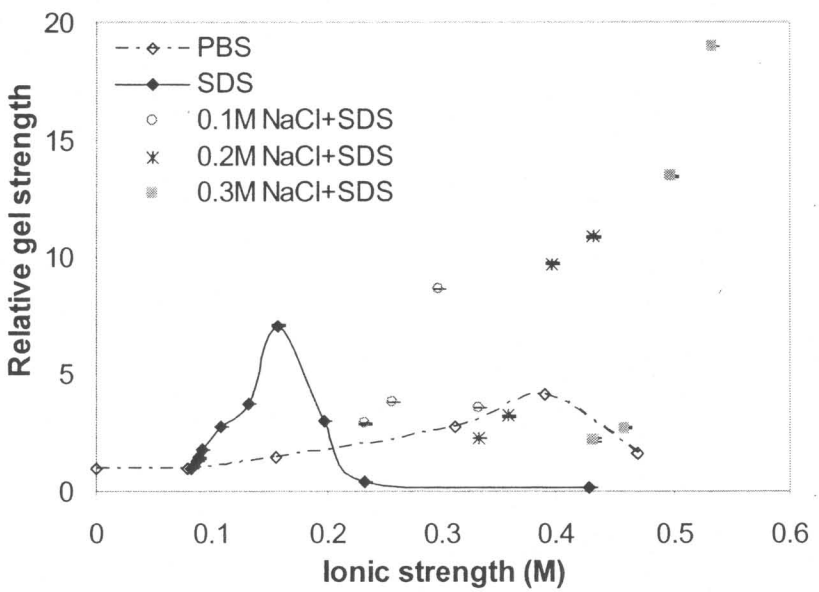

Figure V-10 Effect of SDS on HPMC gel strength at different ionic strength. (a) Relative gel strength as a function of SDS concentration. (b). Relative gel strength as a function of ionic strength.

(a)

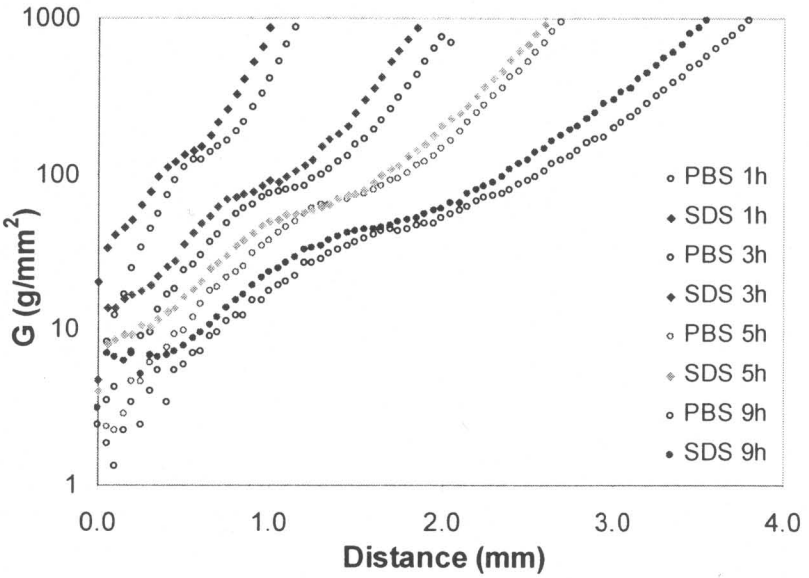

(b)

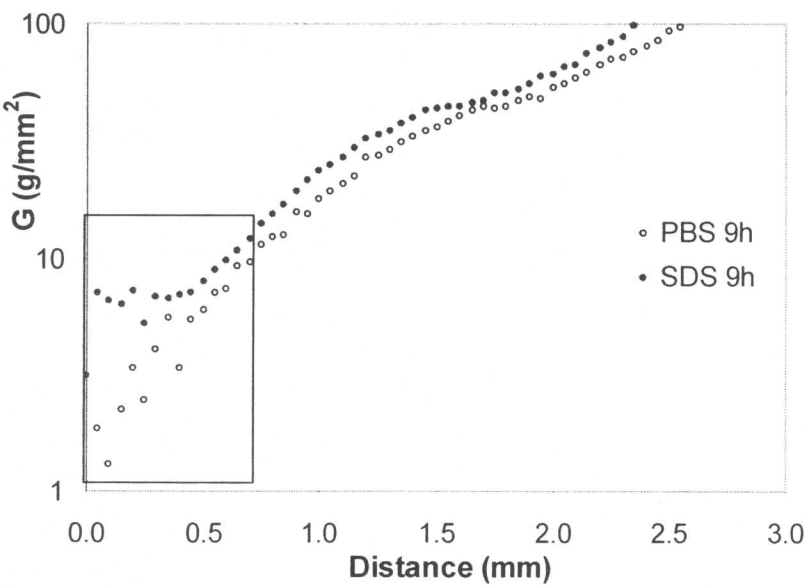

Figure V-11 Effect of 75mM SDS on the strength of HPMC swelling compacts. (a) Different swelling time (from left to right 1, 3, 5, 9 hour). (b) Enlarged gel strength profile at 9 hour swelling.

(a)

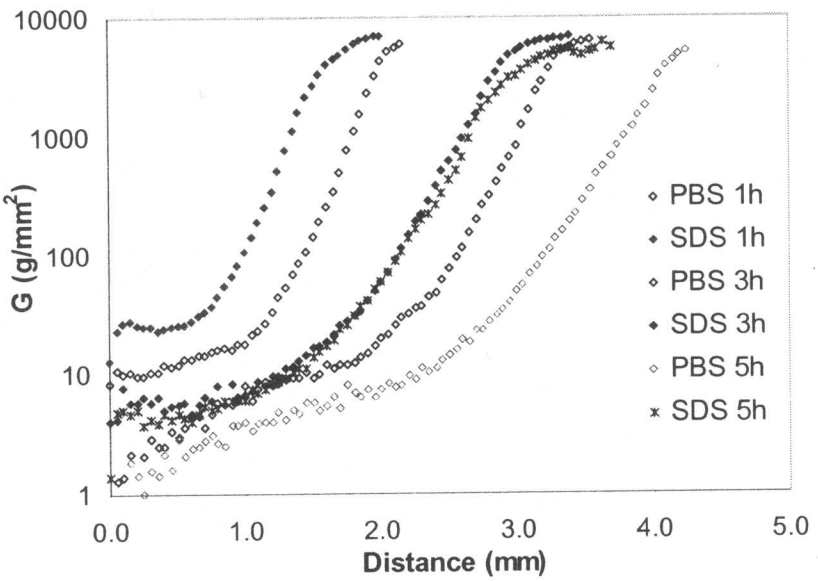

(b)

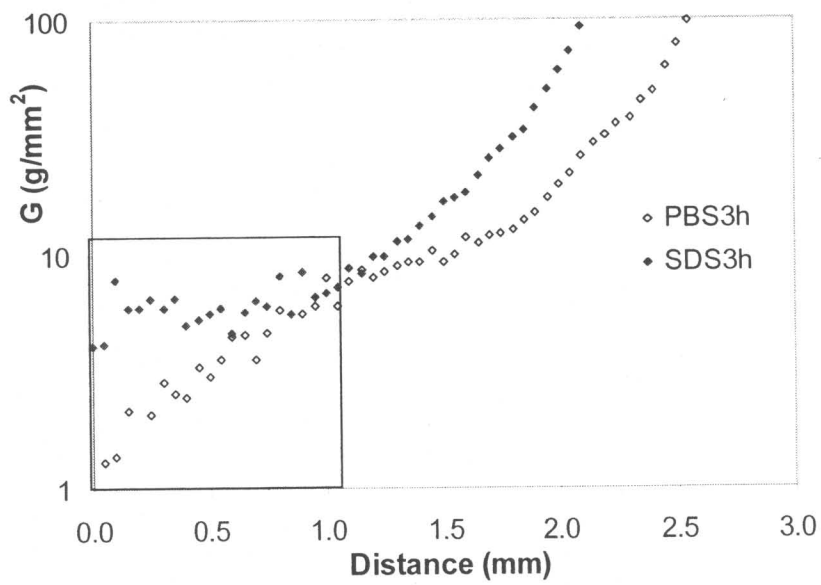

Figure V-12 Effect of 75mM SDS on the strength of Depakote ER swelling tablets. (a) Different swelling time (from left to right 1, 3, 5 hour). (b) Enlarged gel strength profile at 3 hour swelling.

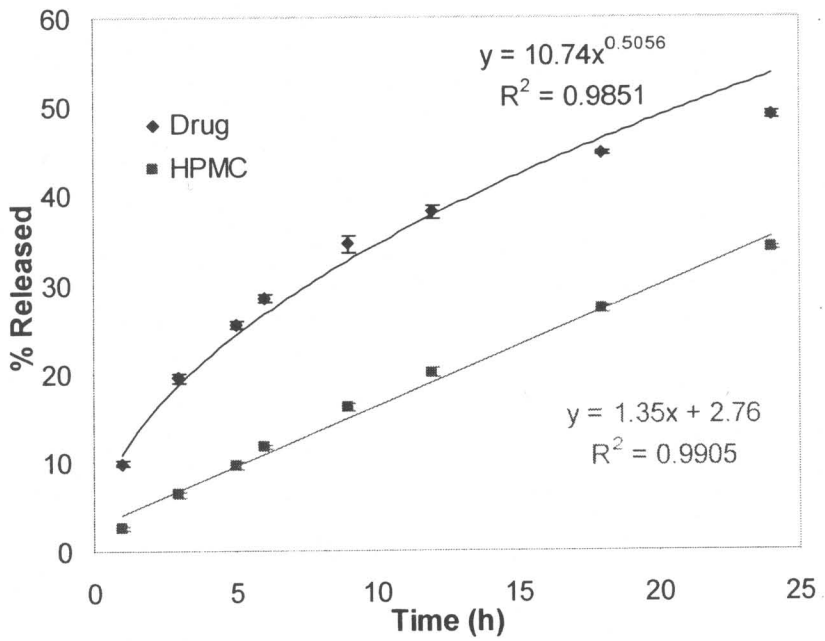

Figure V-13 HPMC and drug release comparison in 0.05M PBS, pH 5.5 medium.

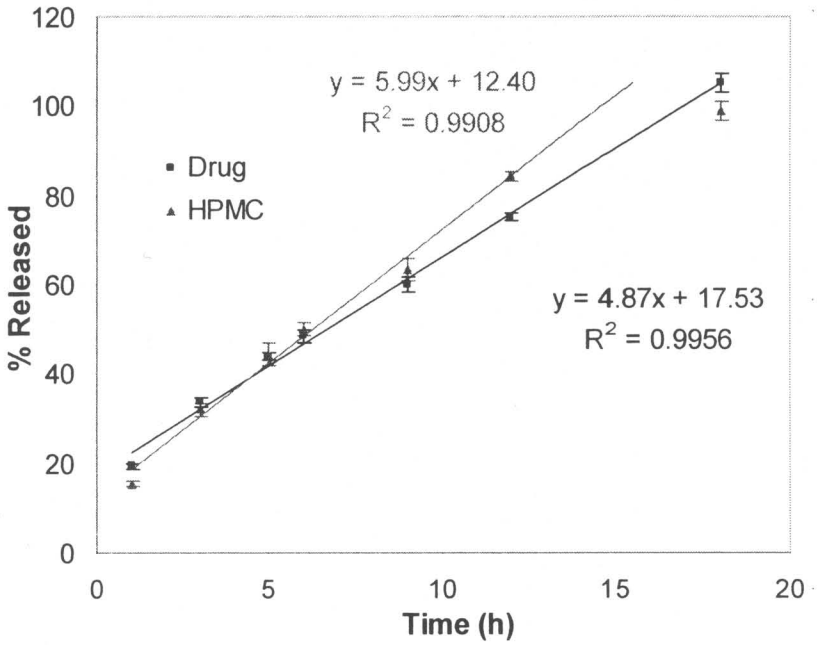

Figure V-14 HPMC and drug release comparison in 0.05M PBS + 75mM SDS, pH 5.5 medium.

(a)

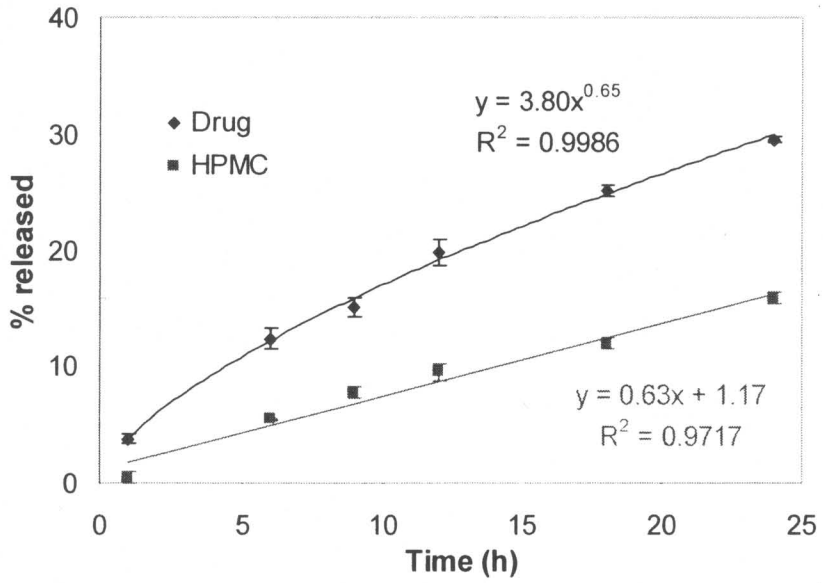

(b)

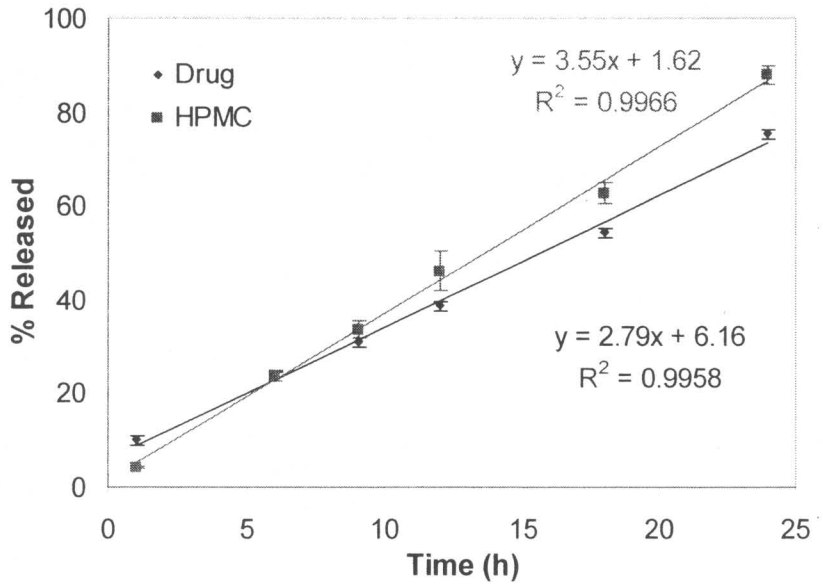

Figure V-15 One-dimensional HPMC and drug release comparison in (a) 0.05M PBS without and (b) with 75mM SDS, pH 5.5

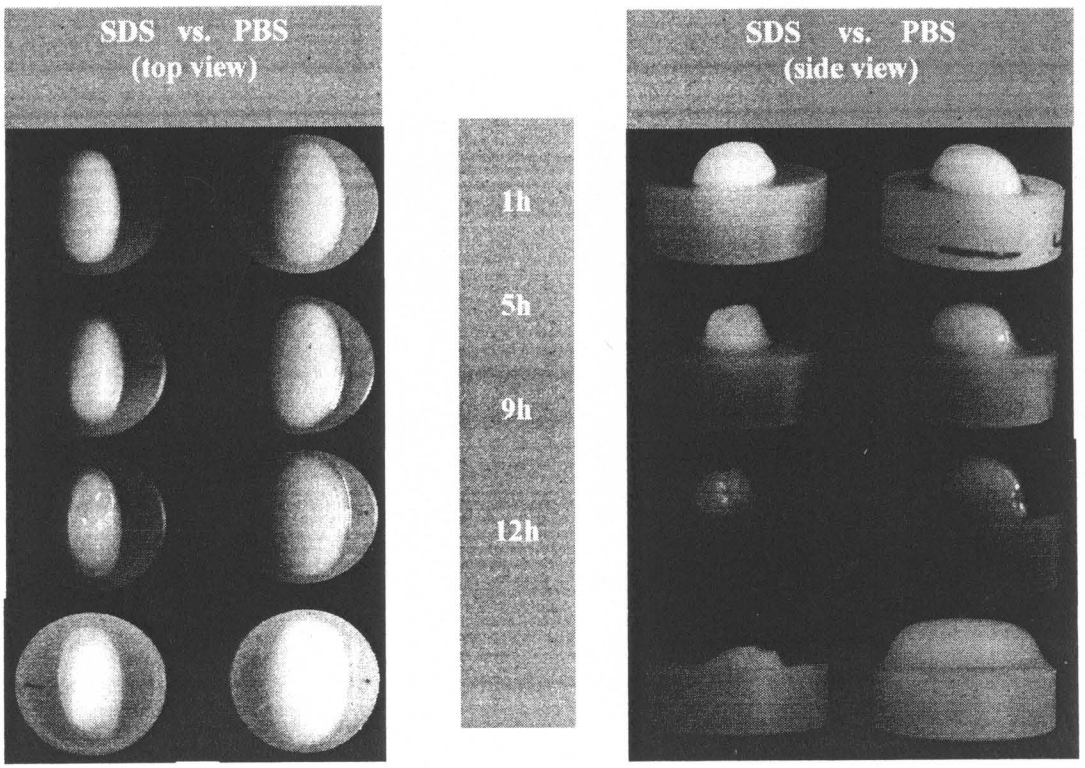

Figure V-16 Visual observation of Depakote® ER tablet dissolution in PBS buffer with and without 75mM SDS at different dissolution times.

(a)

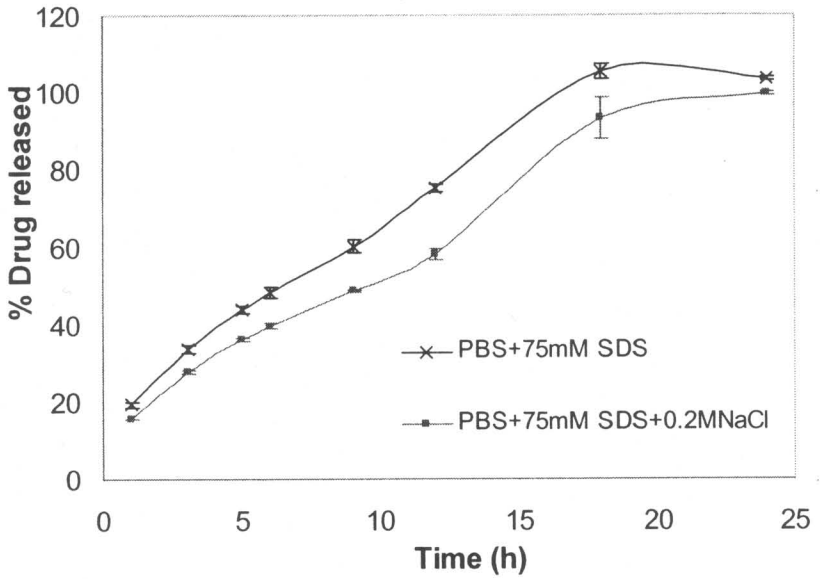

(b)

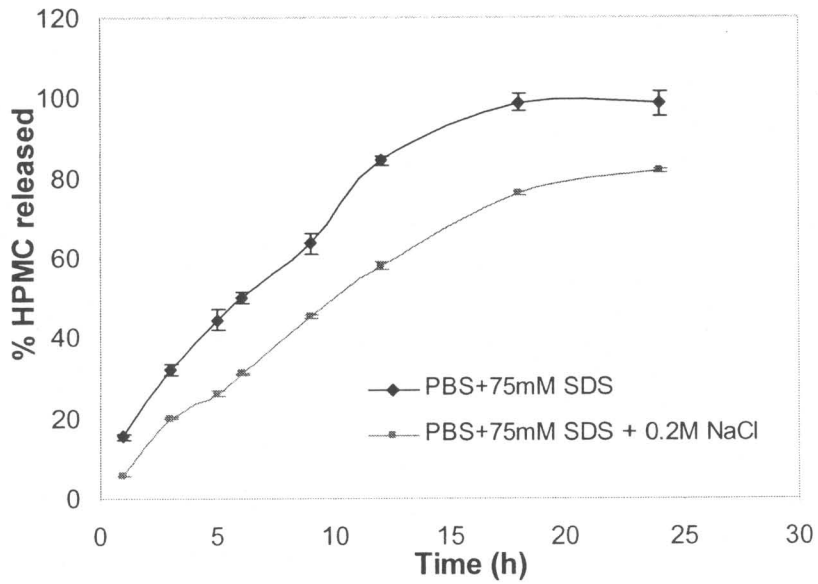

Figure V-17 Effect of ionic strength on (a) drug and (b) HPMC release in 0.05M PBS + 75mM SDS, pH 5.5 medium.

(a)

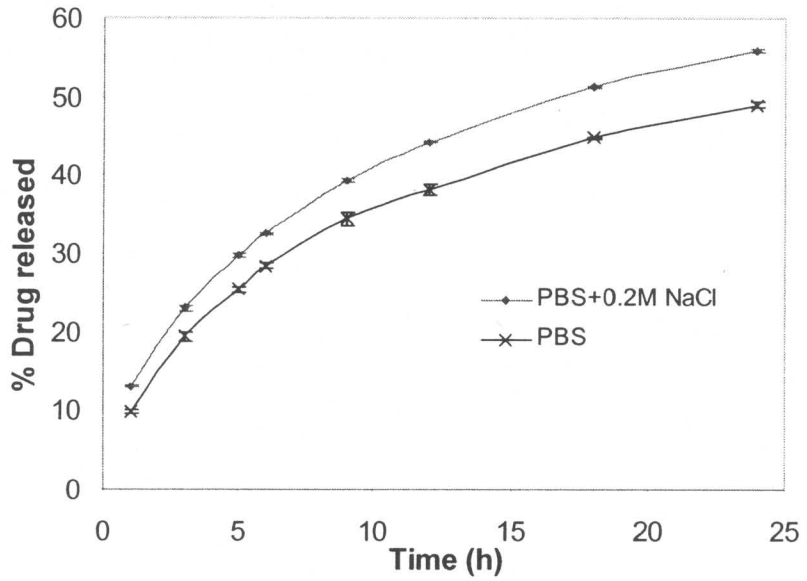

(b)

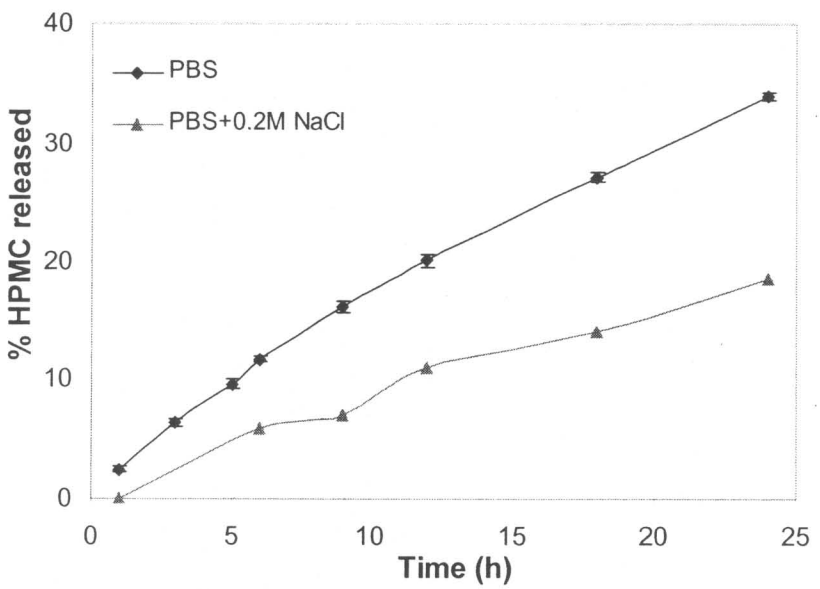

Figure V-18 Effect of ionic strength on (a) drug and (b) HPMC release in 0.05M PBS, pH 5.5 medium.

CHAPTER VI Suggested Future Studies

1. Application of Texture Analyzer to other polymer systems

Texture Analyzer has been utilized for the first time to delineate the structure of swollen HPMC tablet in this thesis. HPMC hydrogels were demonstrated to show true solution behavior in the literature (Ferrari 1994; Talukdar 1996), however, many other hydrogels, such as *k*-carrageenan and carboxyvinyl polymer gels, do not show the same behavior. It will be of interest to investigate if TA is able to characterize the structure of such tablets.

We also demonstrated that TA is a new, reliable, and convenient method to estimate the polymer disentanglement concentration of HPMC hydrogel, and HPMC dissolution rate could be estimated using a mathematical model in Chapter IV. It will be beneficial to apply such methodology in other polymer systems and to study how the disentanglement concentration changes with polymer characteristics such as monomer type, molecular weight, molecular weight distribution and hydrophobicity.

2. Interaction between HPMC and Starch 1500®

In the thesis, it was shown that Starch 1500® increased gel strength and decreased the disentanglement concentration of HPMC, as a result, HPMC dissolution rate decreased with the increase of Starch 1500® content in the tablet. However, it is not fundamentally clear how Starch 1500® interacts with HPMC. Starch 1500® is partially soluble in aqueous solution. It contains 5% of free amylose and 15% of free amylopectin. It will be beneficial to separate the soluble fraction from the nonsoluble fraction and study their impact on HPMC gel strength separately.

The interaction can be studied at dilute solution using traditional IR, NMR or other appropriate spectroscopic techniques. In relatively high concentration, the interaction can be studied using cloud point measurement described in Chapter V. If there is synergetic interaction between HPMC and starch, the cloud point of HPMC solution will be expected to drop.

3. Interaction of HPMC and SDS in solution of high SDS concentration

At low concentration of SDS solution, the interaction of HPMC and SDS was very clear thanks to the work done by Stephen (Nilsson 1995). However, at high SDS concentration such as 75mM used in Chapter V, we demonstrated that HPMC dissolution rate increased significantly. The authors (Nilsson 1995) suggested that SDS micelles in solution dissolves the HPMC network, but the detailed mechanism was lacking.

There are two possible scenarios with the further addition of SDS when HPMC solution viscosity or gel strength reaches the maximum: 1) SDS micelles adsorption to HPMC chain reaches saturation, and the added SDS becomes free SDS micelles in the solution, which compete the HPMC chains in disentanglement state and finally dissolves HPMC completely. 2) The added SDS continues to adsorb onto HPMC chains and collapses HPMC network.

For the first scenario, one can imagine that polymer chains are well dispersed in the cluster of SDS micelles; while one might find several polymer chains are associated with a bigger cluster of SDS micelles in second scenario. Therefore, it is possible to obtain more details of interactions between HPMC and SDS at high SDS concentration by studying the cluster structure of SDS micelles with HPMC chains. The size of the cluster resulted from the first scenario should be in the order of the size of free SDS micelles, and

the cluster from the second scenario might have significantly larger size. Time-resolved fluorescence anisotropy and quasi-elastic light scattering method could be used for the measurement of the size of mixed cluster of SDS micelles and HPMC.

Another approach to study this interaction is to study the transition kinetics from gel strength increasing to decreasing with SDS concentration. In this regard, binary mixture of HPMC and SDS hydrogels are prepared first, and the concentration of SDS is chosen to get the strongest gel strength. Then such hydrogels are placed at swelling medium with SDS at concentration higher than critical adsorption concentration, and the gel strength is measured using TA at predetermined time. According to the first scenario, SDS concentration in the gel will be constant since SDS is already saturated with HPMC chains, and gel strength change with time due to the swelling will be independent on SDS concentration in the swelling medium. On the other hand, such transition is expected to depend on SDS concentration in the medium in the second scenario.

REFERENCE

Ferrari F., Bertoni M., Caramella C. and La Manna A. (1994). "Description and validation of an apparatus for gel strength measurements." International Journal of Pharmaceutics **109**(2): 115-124.

Nilsson S. (1995). "Interactions between water-soluble cellulose derivatives and surfactants. 1. The HPMC/SDS/Water system." Macromolecules **28**: 7837-7844.

Talukdar M. M., Vinckier I., Moldenaers P. and Kinget R. (1996). "Rheological characterization of xanthan gum and hydroxypropylmethyl cellulose with respect to controlled-release drug delivery." Journal of Pharmaceutical Sciences **85**(5): 537-540.